CSPAR-UAH

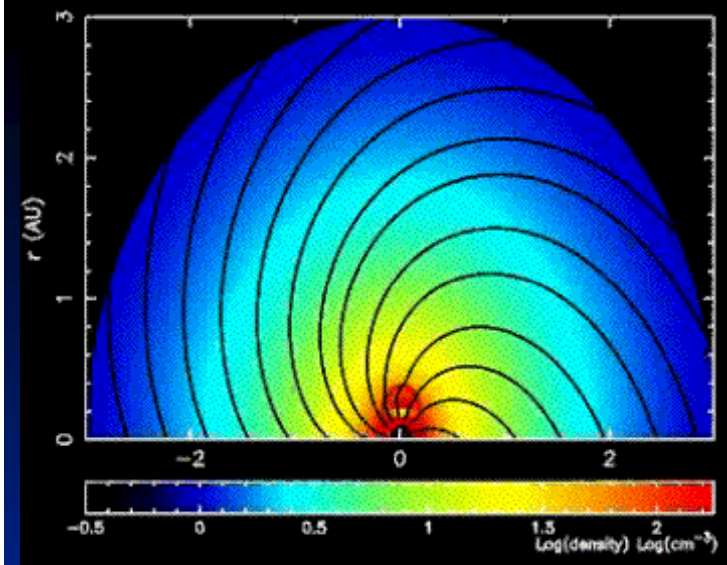

Shocks in the Heliosphere

G.P. Zank

Center for Space and Aeronomic Research (CSPAR)
University of Alabama in Huntsville

Three topics of discussion:

1) Particle acceleration at interplanetary shocks
2) Large-scale structure of the heliospheric termination shock (HTS)
3) Structure and dissipation at the HTS

CSPAR-UAH

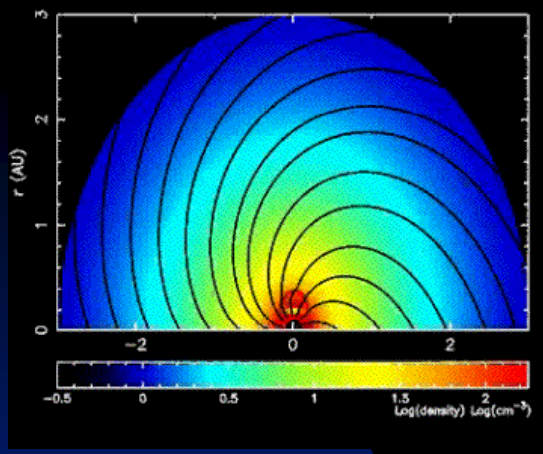

Particle Acceleration at Interplanetary Shocks

Review particle acceleration by interplanetary shocks:

1. *Time scales for the interplanetary shock acceleration problem.*
2. *Unsteady diffusive shock acceleration at a quasi-parallel shock.*
   - *Protons*
   - *Heavy ions*
3. *Particle acceleration at a quasi-perpendicular shock.*
4. *Modeling specific events*

CSPAR-UAH

Two Classes of Solar Energetic Particle Events

CME-Associated (Gradual Event)

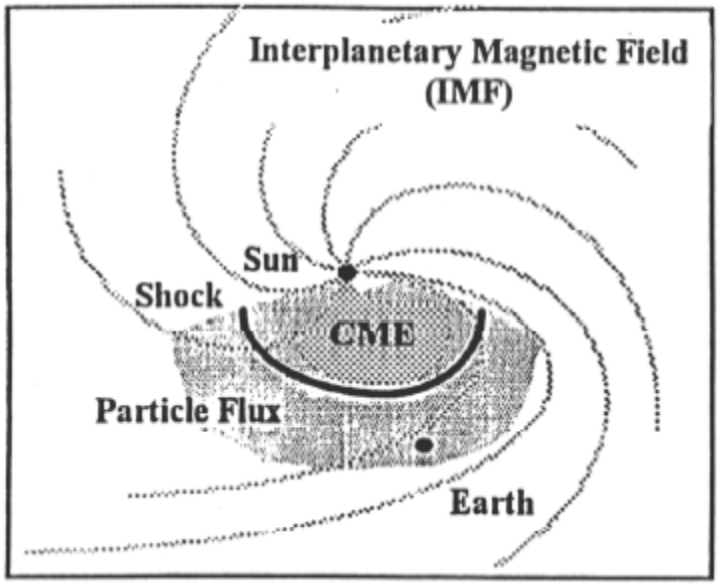

Proton-Rich
Long-Lived (Days)
60-180 Degrees Solar Longitude

Fe/O ≈ 0.1 - 0.2
$^3He/^4He \approx .0004$
Q(Fe) ≈ 14
Shocks accelerate solar wind

Impulsive Flare-Associated (Impulsive Event)

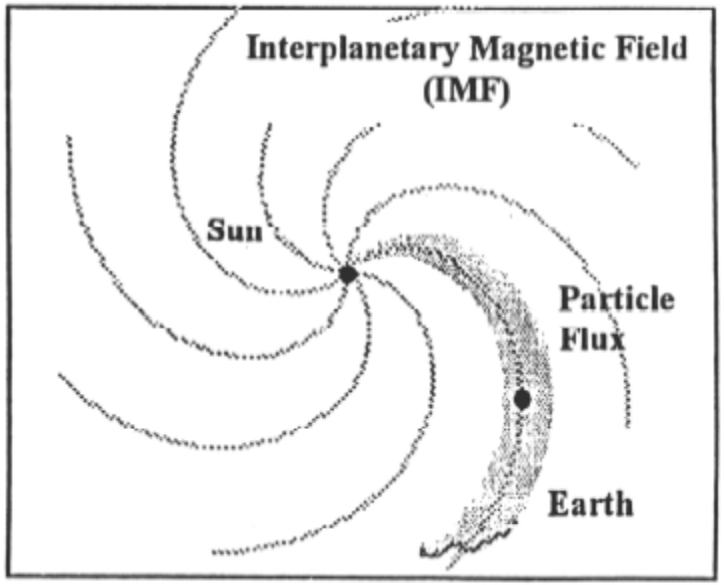

Electron-Rich
Short-Lived (Hours)
30-45 Degrees Solar Longitude

Fe/O ≈ 1
$^3He/^4He \approx$ 0.1 - 10
Q(Fe) ≈ 20
Heated flare material accelerated

Criteria summarized by Reames (1995)

CSPAR-UAH

Time scales for the SEP/ESP problem

- Shock propagation in an inhomogeneous solar wind – expanding, decelerating, decreasing magnetic field strength, in situ turbulence convection, decay, driving, variability of shock normal
- Particle acceleration time scales; maximum energy, shock obliquity
- Variability in generation of shock turbulence by streaming energetic particles; particle trapping and escape
- Diffusive time scales (diffusive mfp)
- Transport time scales/length scales (transport mfp)

The shock itself introduces a multiplicity of time scales, ranging from shock propagation time scales to particle acceleration time scales at parallel and perpendicular shocks, and many of these time scales feed into other time scales (such as determining maximum particle energy scalings, escape time scales, etc.).

CSPAR-UAH

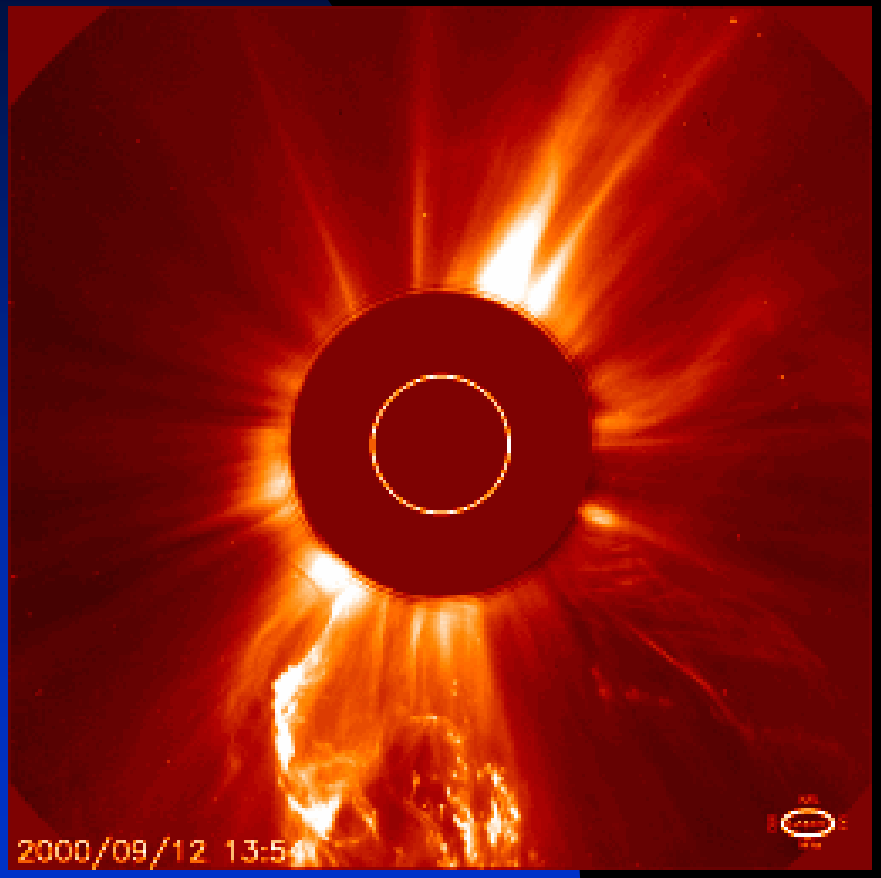

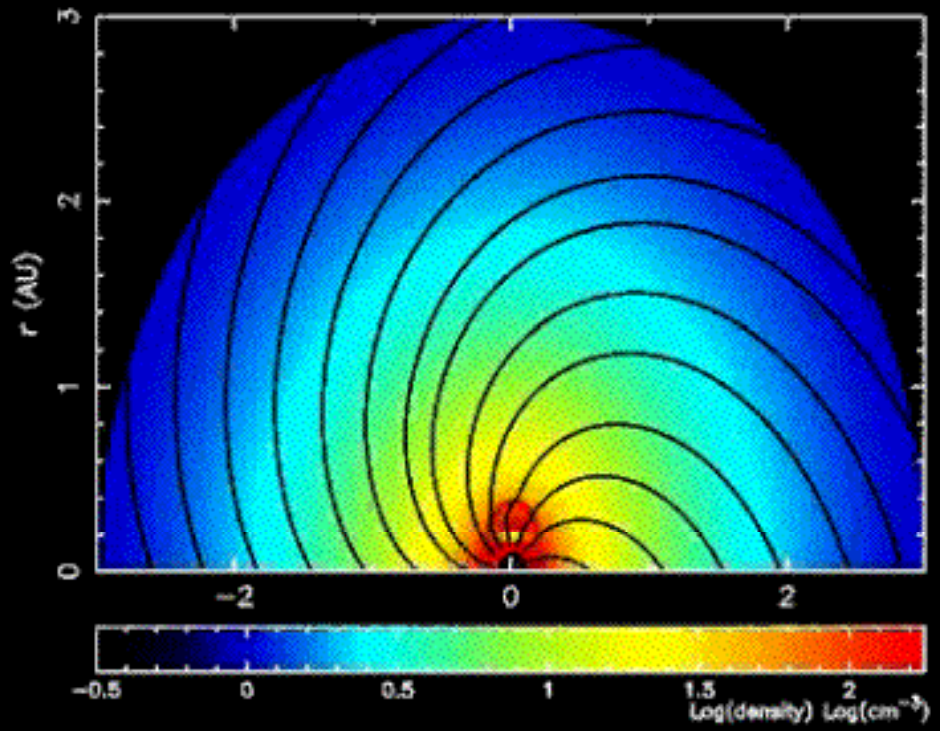

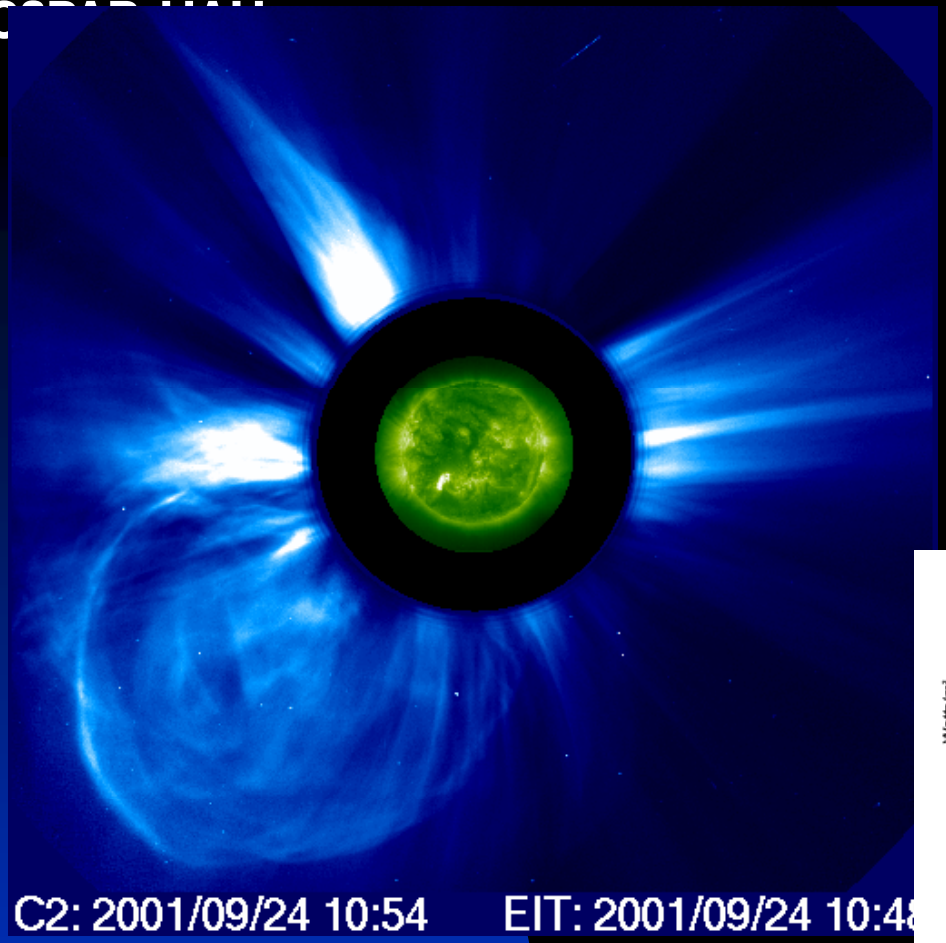

Halo CME: Sept. 24, 2001: 10:30 linear speed: 2400km/sec (from the SOHO/LASCO CME Catalog, courtesy of the CDAW Data Center, GSFC).

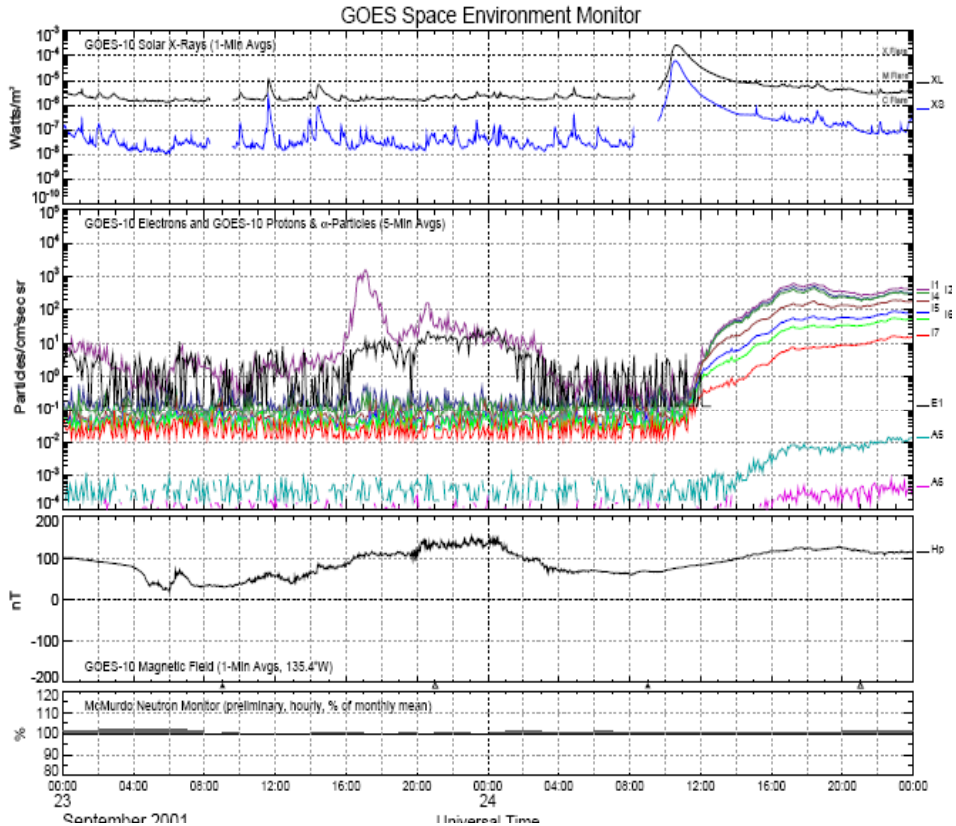

SEP Event # 215 (shock arrival at ACE: Sept. 29, 2001, 09:06 UT)

CSPAR-UAH

Shock position, velocity and compression ratio are computed from 0.1 AU to up to several AU.

Simulation results of the shock velocity dependence on radial distance from the Sun. The decaying shock propagates from 0.1 AU, reaching a compression ratio of about 1.8 at 1AU. The modeling was performed for 61 shells.

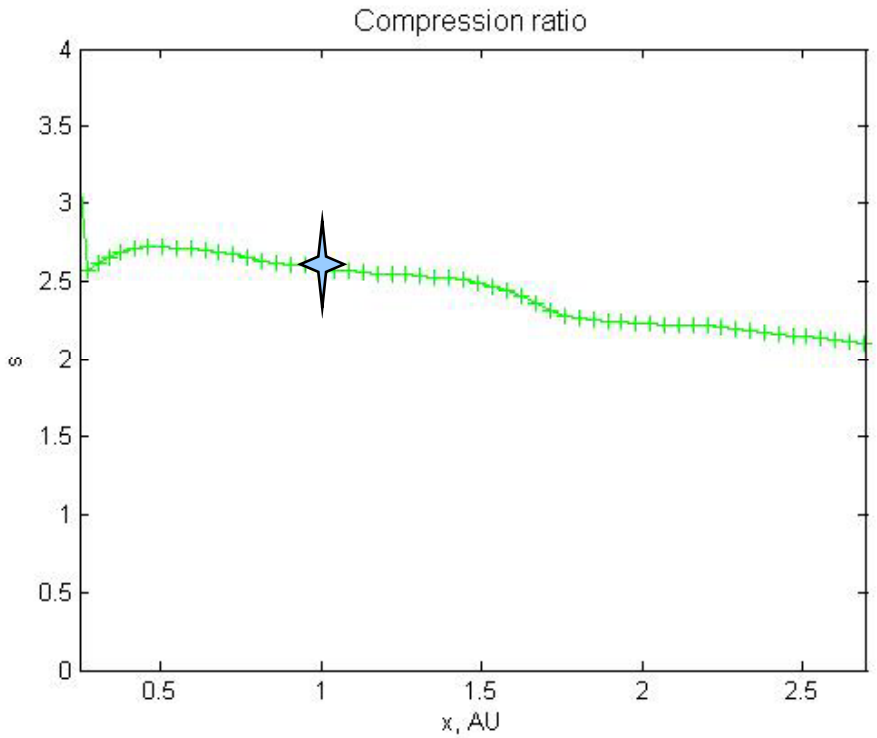

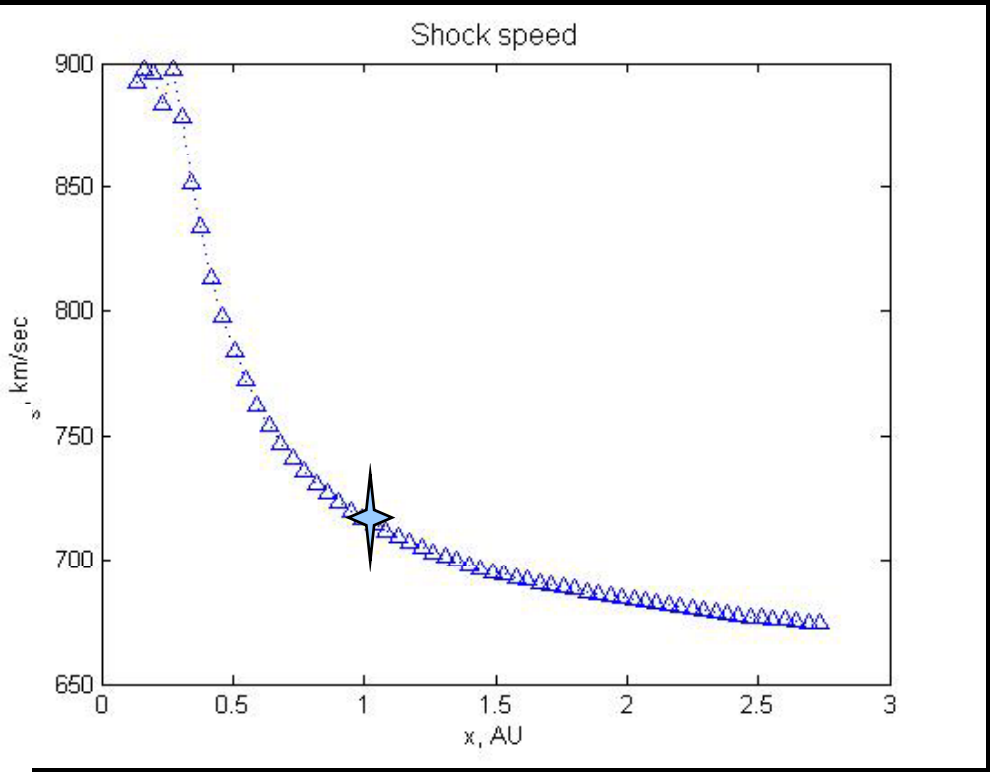

SEP Event # 215 (shock arrival at ACE: Sept. 29, 2001, 09:06 UT)

- Post-shock complex time scales: Convection, adiabatic expansion, growth of post shock region and weakening of shock front.

$$\delta v(t) = \frac{\delta v_i}{\sqrt{1+(\alpha_v \delta v_i)t}} \qquad \alpha_v \equiv \frac{C_{f0}^2 + \gamma C_{sd0}^2 + 2C_{A0}^2}{2C_{f0}^2}$$

$$t = t_i$$

$$t = t_{i+1} = t_i + \Delta t$$

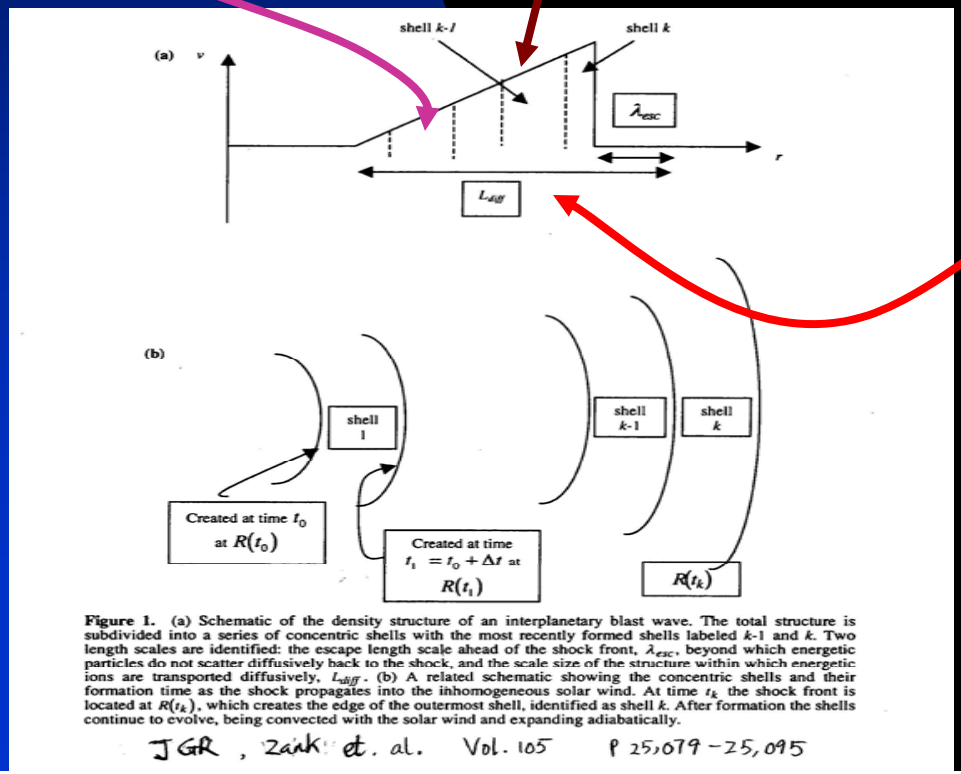

Figure 1. (a) Schematic of the density structure of an interplanetary blast wave. The total structure is subdivided into a series of concentric shells with the most recently formed shells labeled k-1 and k. Two length scales are identified: the escape length scale ahead of the shock front, λ_{esc}, beyond which energetic particles do not scatter diffusively back to the shock, and the scale size of the structure within which energetic ions are transported diffusively, L_{diff}. (b) A related schematic showing the concentric shells and their formation time as the shock propagates into the inhomogeneous solar wind. At time t_k the shock front is located at $R(t_k)$, which creates the edge of the outermost shell, identified as shell k. After formation the shells continue to evolve, being convected with the solar wind and expanding adiabatically.

JGR, Zank et. al. Vol. 105 P 25,079-25,095

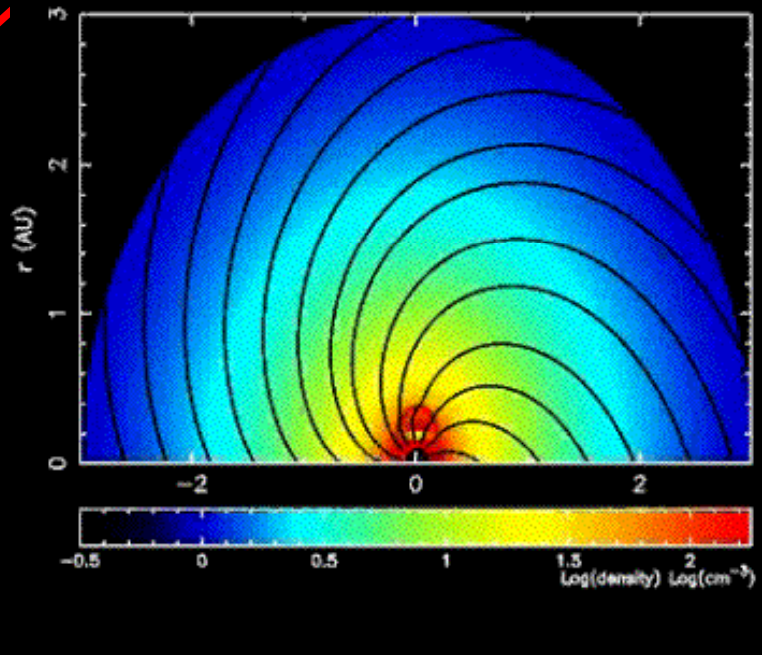

$$\frac{\partial f}{\partial t} = -U_i \frac{\partial f}{\partial x_i} + \nabla \bullet U \frac{p}{3} \frac{\partial f}{\partial p} + \nabla \bullet \left(\mathrm{K} \bullet \nabla f \right) + Q$$

convection energy change diffusion source

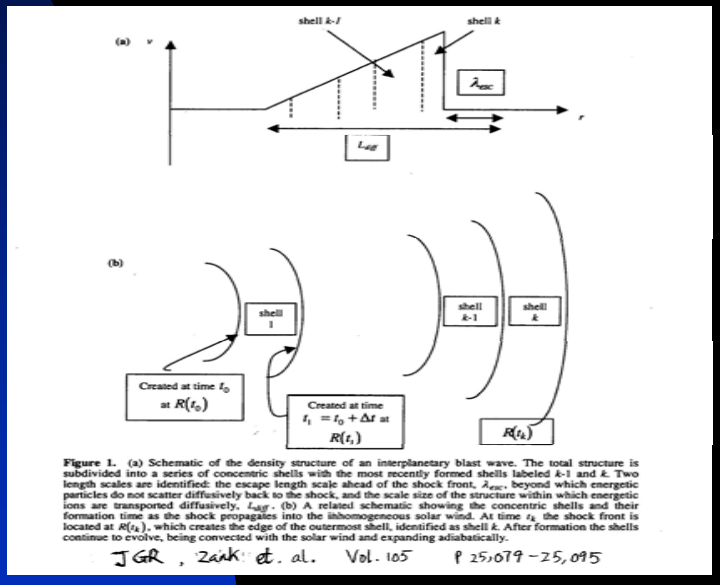

Figure 1. (a) Schematic of the density structure of an interplanetary blast wave. The total structure is subdivided into a series of concentric shells with the most recently formed shells labeled k-1 and k. Two length scales are identified: the escape length scale ahead of the shock front, λ_{esc}, beyond which energetic particles do not scatter diffusively back to the shock, and the scale size of the structure within which energetic ions are transported diffusively, L_{diff}. (b) A related schematic showing the concentric shells and their formation time as the shock propagates into the inhomogeneous solar wind. At time t_k the shock front is located at $R(t_k)$, which creates the edge of the outermost shell, identified as shell k. After formation the shells continue to evolve, being convected with the solar wind and expanding adiabatically.

JGR, Zank et. al. Vol. 105 p 25,079-25,095

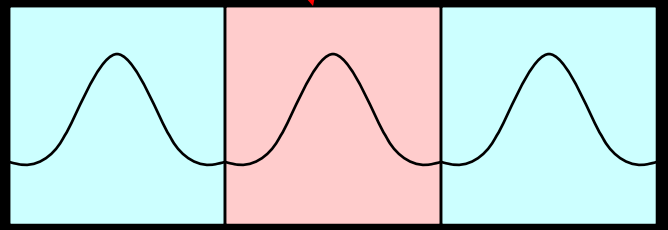

$$\frac{\partial f}{\partial t} = \frac{1}{r^2} \frac{\partial}{\partial r} \left(r^2 \kappa \frac{\partial f}{\partial r} \right)$$

$$f_i\left(t_k, p, r\right) = \frac{1}{\sqrt{\pi}} \frac{f_i^n\left(t_{k-1}, p\right)}{4\pi r_i^2\left(t_k\right)} \frac{1}{\sqrt{4\kappa\left(t_k - t_{k-1}\right) + \left(\kappa / U_1\right)^2}} \exp\left[\frac{\left(r - r_i\left(t_k\right)\right)^2}{4\kappa\left(t_k - t_{k-1}\right) + \left(\kappa / U_1\right)^2} \right]$$

CSPAR-UAH

Shock geometry

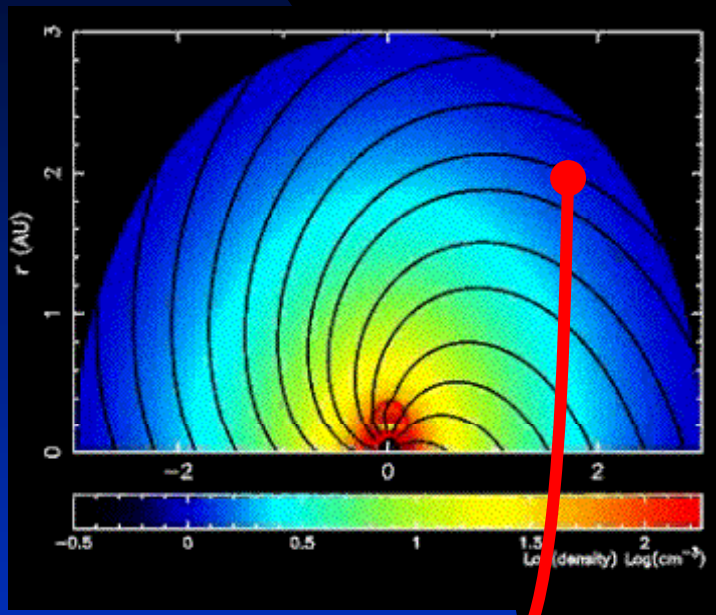

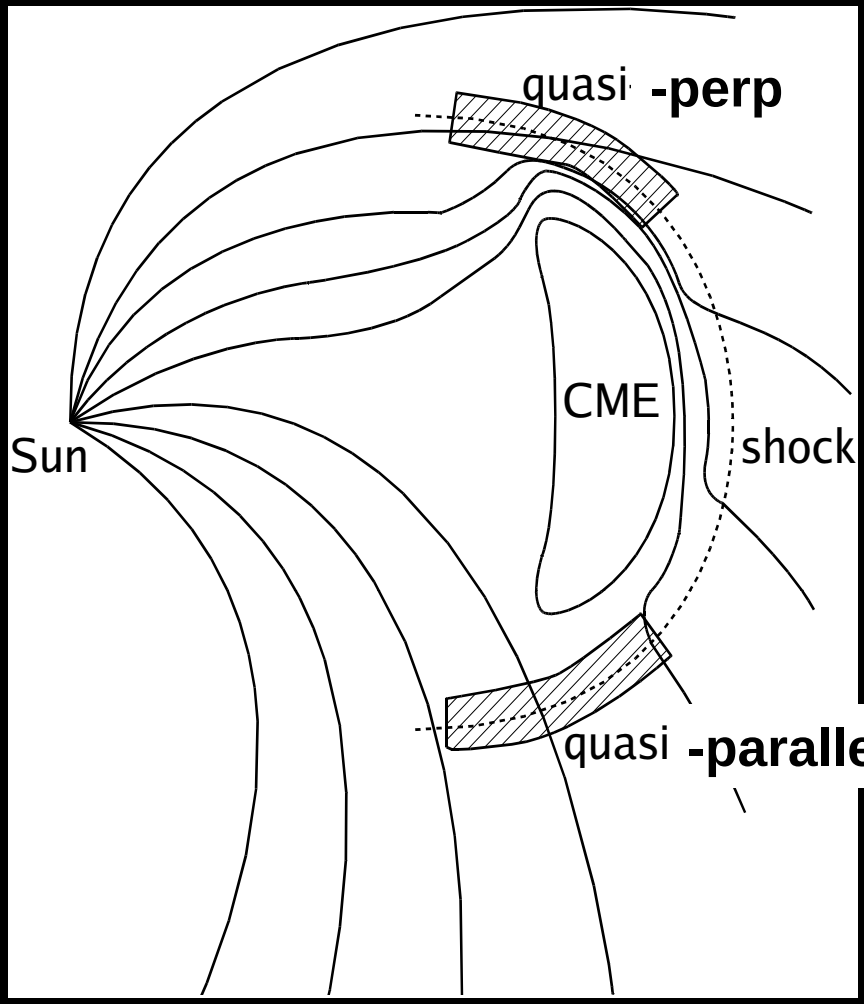

Red dot (spacecraft) connected to quasi-perpendicular shock initially and the connection gradually evolves to much more quasi-parallel configuration.

$$\tau_{convect} \sim L/U$$

$$\tau_{DYN} \sim R/dR/dt \quad \Rightarrow \tau_\theta \sim \sqrt{\frac{L}{U} R/dR/dt}$$

Maximum particle energy

- The maximum particle energy can be determined by equating the dynamic timescale of the shock with the acceleration timescale (Drury, 1983; Zank et al., 2000).

$$R(t) \Big/ \left(dR/dt\right) = \frac{3s}{s-1} \int_{p_{inj}}^{p_{\max}} \frac{\kappa\left(t, p', r\right)}{U_1^2} d\left(\ln p'\right)$$

CSPAR-UAH

Diffusion coefficient at parallel shock

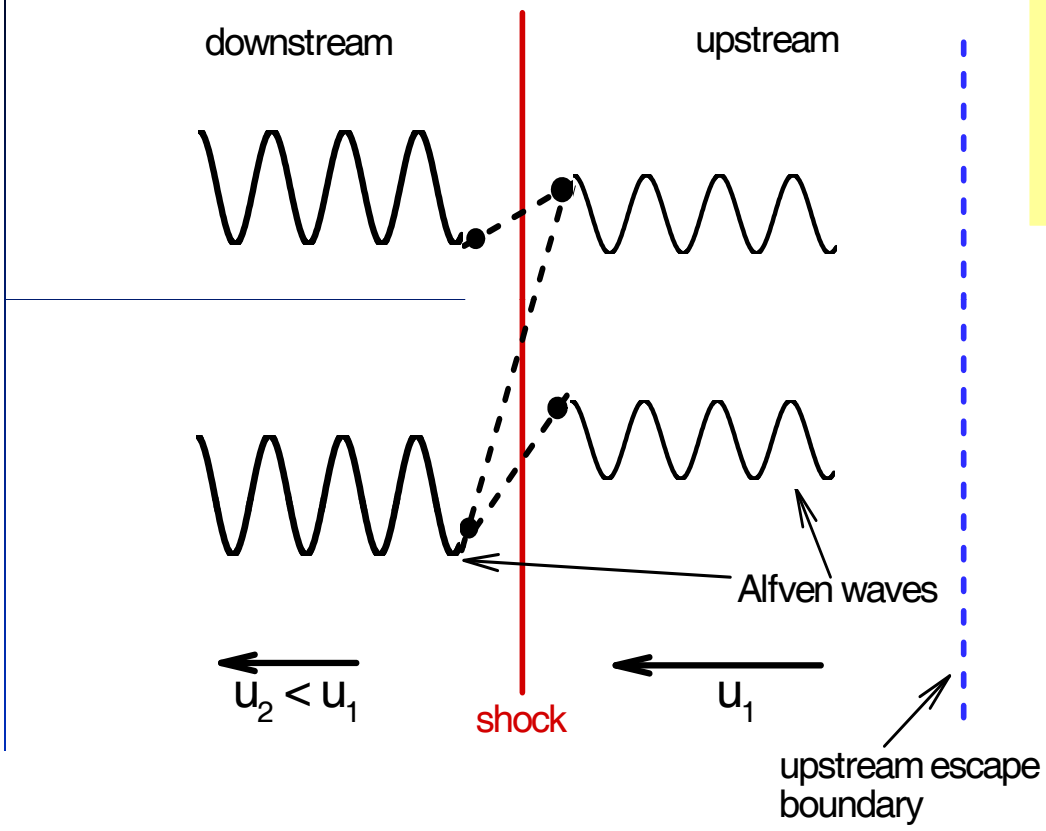

Near the shock front, Alfven waves are responsible for particle scattering. The particle distribution f, and wave energy density A are coupled together through:

$$\frac{\partial A}{\partial t} + u\frac{\partial A}{\partial r} = \Gamma A - \gamma A,$$

$$\frac{\partial f}{\partial t} + u\frac{\partial f}{\partial r} - \frac{p}{3}\frac{\partial u}{\partial r}\frac{\partial f}{\partial p} = \frac{\partial}{\partial r}\left(\kappa\frac{\partial f}{\partial r}\right),$$

$$\kappa(p) = \frac{\kappa_0}{A(k)}\frac{B_0}{B}\frac{(p/p_0)^2}{\sqrt{(m_p c/p_0)^2 + (p/p_0)^2}},$$

$$\kappa_0 = \frac{4}{3\pi}r_{g0}c = \frac{4}{3\pi}\frac{p_0 c}{eB_0},$$

Gordon et al., 1999 used to evaluate wave intensity. P_max, N_inj, p_inj, s, etc. Bohm limited applied when wave energy density per log bandwidth exceeds local solar wind magnetic energy density.

CSPAR-UAH

Maximum particle energy at quasi-parallel shock:

$$\frac{R(t)}{\dot{R}(t)} \approx \frac{q(t)}{u_1^2}\int_{p_{inj}}^{p_{\max}} \kappa(p')\,d\left(\ln(p')\right) = \frac{q(t)}{\dot{R}^2(t)}\left(\frac{5M^2(t)+3}{M^2(t)+3}\right)\int_{p_{inj}}^{p_{\max}} \kappa(p')\,d\left(\ln(p')\right)$$

Age Strength Magnetic field heliocentric dependence

$$p_{\max} = \left\{\left[\frac{M^2(t)+3}{5M^2(t)+3}\frac{R(t)\dot{R}(t)}{q(t)\kappa_0}\frac{B}{B_0} + \sqrt{\left(\frac{m_p c}{p_0}\right)^2 + \left(\frac{p_{inj}}{p_0}\right)^2}\right]^2 - \left(\frac{m_p c}{p_0}\right)^2\right\}^{1/2}$$

$$\frac{B}{B_0} = \left(\frac{R_0}{r}\right)^2\left[1+\left(\frac{\Omega_0 R_0}{u}\right)^2\left(\frac{r}{R_0}-1\right)^2 \sin^2\theta\right]^{1/2}$$

CSPAR-UAH

Maximum energies for protons

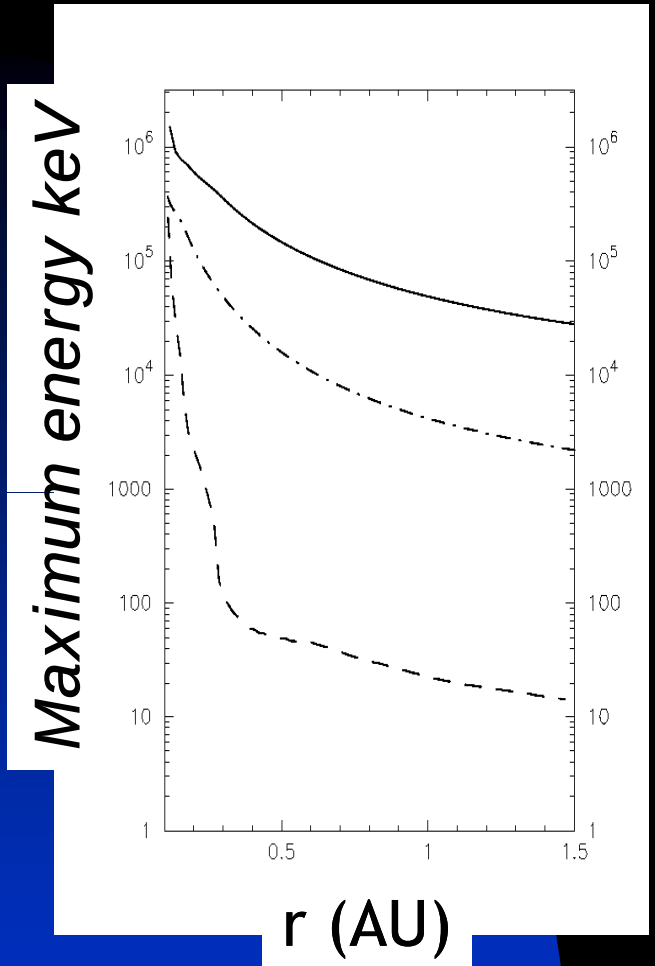

Strong, medium, weak shock examples

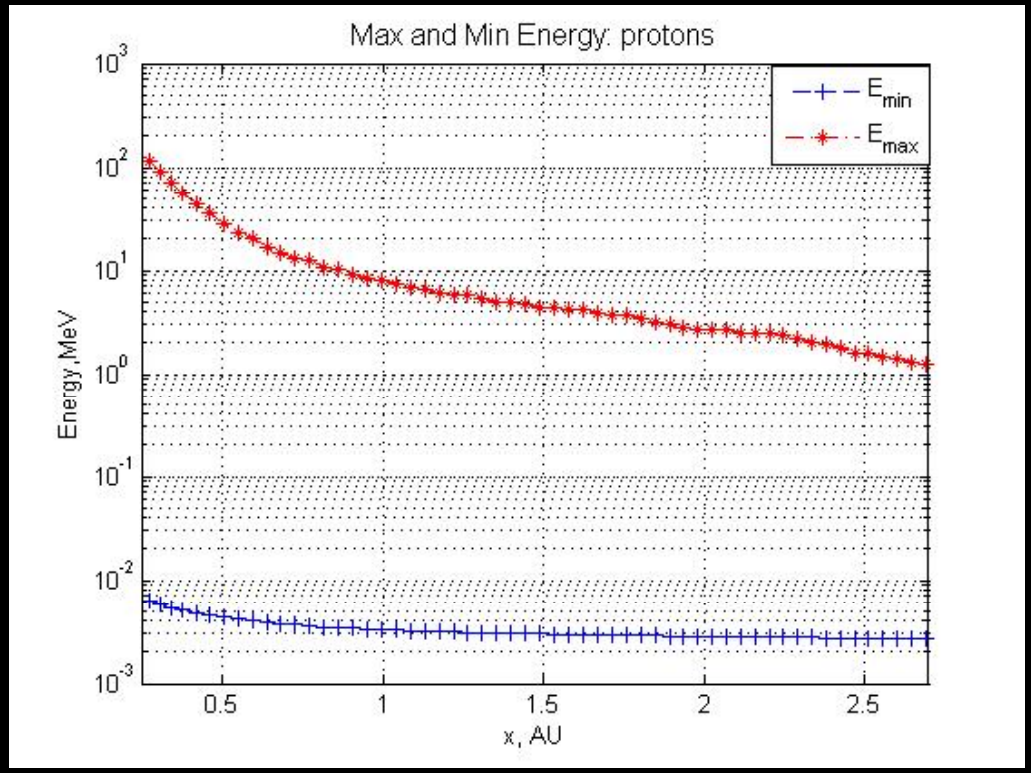

SEP Event # 215 (shock arrival at ACE: Sept. 29, 2001, 09:06 UT)

The maximum particle momentum obtained for a strong shock at early times can be as high as a few GeV – consistent with observations by Kahler [1994].

- What happens to the turbulence excited by the streaming protons?
- For quasi-|| shocks, turbulence excited by usual streaming instability; amplified on shock transmission
- Shell picture nice for describing the evolution of turbulence in downstream region – simplest is to assume WKB description as shell is convected outward and expands or to include turbulent dissipation.

Particle Transport

Particle transport obeys Boltzmann(Vlasov) equation:

$$\frac{df(x,p,t)}{dt} + q[E + \mathrm{v} \times B] \bullet \frac{\partial f(x,p,t)}{\partial p} = \left.\frac{df(x,p,t)}{dt}\right|_{coll}$$

The LHS contains the material derivative and the RHS describes various "collision" processes.

- Collision in this context is pitch angle scattering caused by the irregularities of IMF and in quasi-linear theory

$$\frac{df}{dt} = \frac{\partial}{\partial \mu}\left(D_{\mu\mu}\frac{\partial f}{\partial \mu}\right)$$

- The result of the parallel mean free path $\lambda_{//}$, from a simple QLT is off by an order of magnitude from that inferred from observations, leading to a 2-D slab model.

$$\frac{\lambda}{10^6\,\mathrm{km}} = 8.30\,\frac{(B/B_0)^2}{\delta B_x^2/\delta B_{x0}^2}\left(\frac{l}{l_0}\right)^{2/3}\left(\frac{p/M_n}{B/B_0}\right)^{1/3}$$

Allows a Monte-Carlo technique.

Particle Acceleration – Diffusion Coefficient

Near the shock front, Alfven waves are responsible for particle scattering. The particle distribution function and wave energy density are coupled together.

SEP Event # 215 (shock arrival at ACE: Sept. 29, 2001, 09:06 UT)

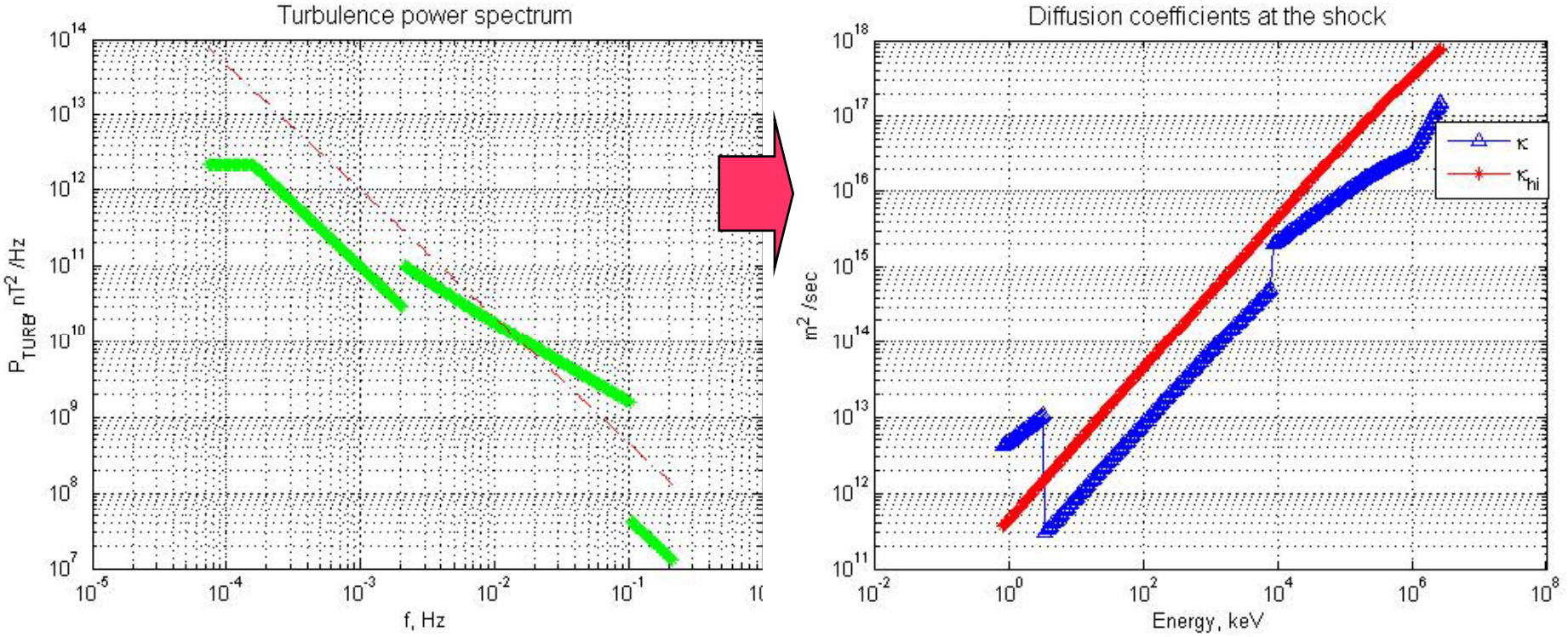

CSPAR-UAH

Wave spectra and diffusion coefficient at shock

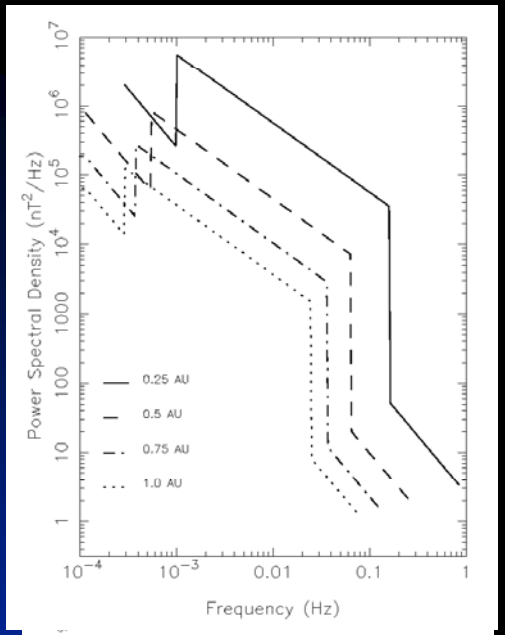

Wave intensity

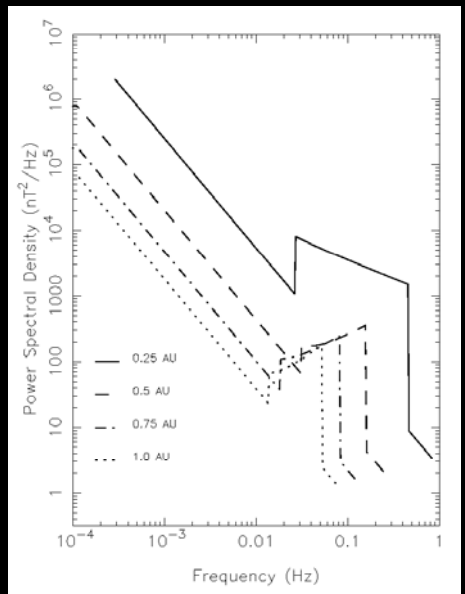

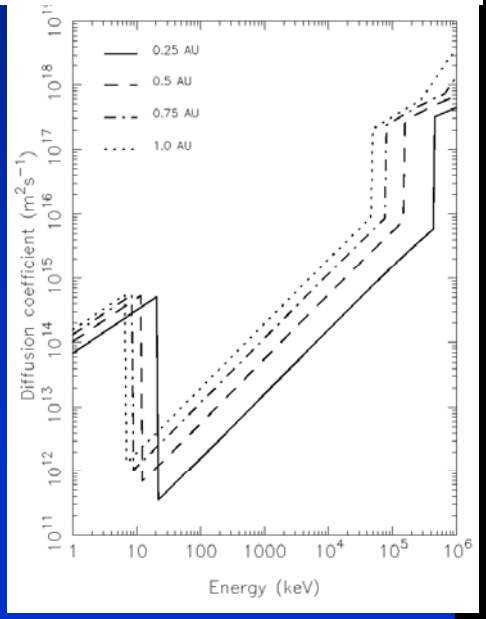

Diffusion coefficient

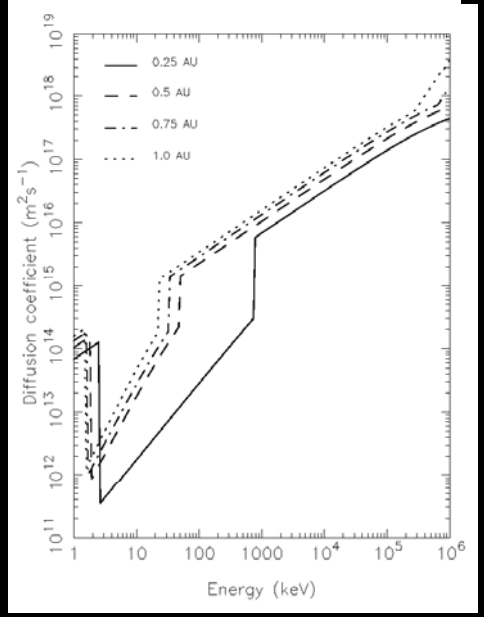

Strong shock

Weak shock

Upstream particle spectrum(strong shock)

Early time

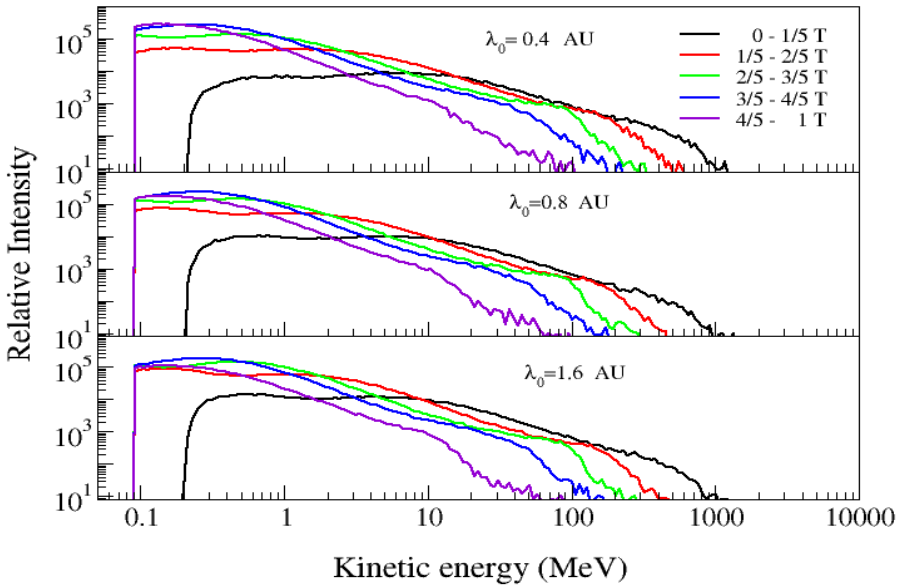

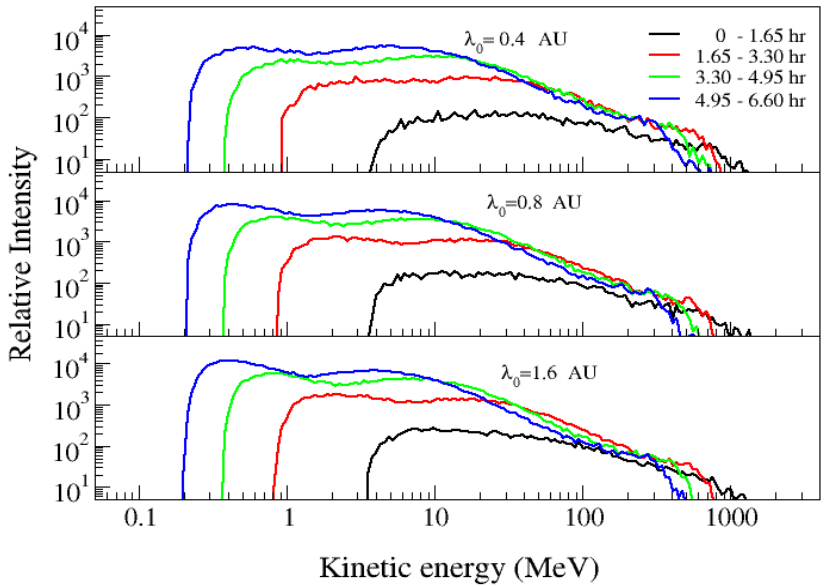

- Cumulative spectra at 1 AU for five time intervals are shown, T=1.3 days.
- Spectra exhibit a power law feature.
- Broken power law at later times, especially for larger mfp (λ_0 = 1.6AU). E.g., K=20 MeV for the time interval t = 4/5-1 T - particle acceleration no longer to these energies.

Event Integrated spectra

Total or cumulative spectrum at 1AU, integrated over the time from shock initiation to the arrival of the shock at 1AU.

Strong shock case

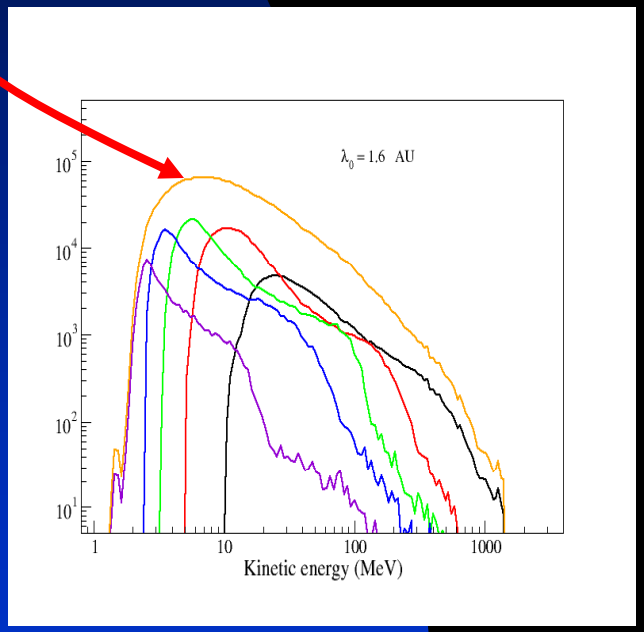

Weak shock case

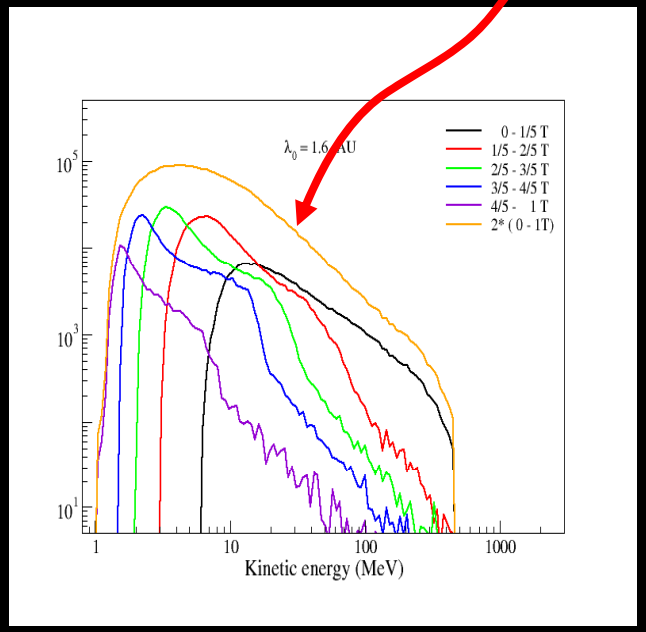

Note the relatively pronounced roll-over in the cumulative strong shock spectrum and the rather flat power-law spectrum in the weak shock case.

Intensity profile (strong shock)

Early time

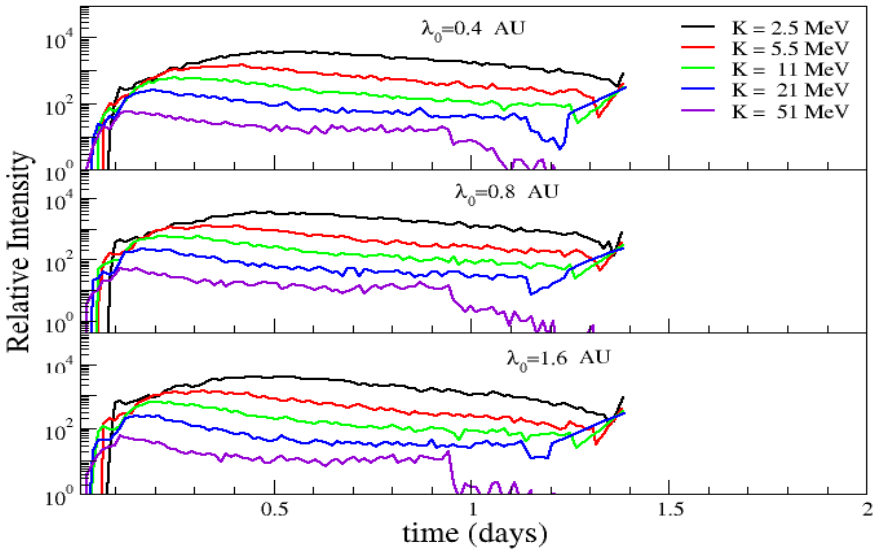

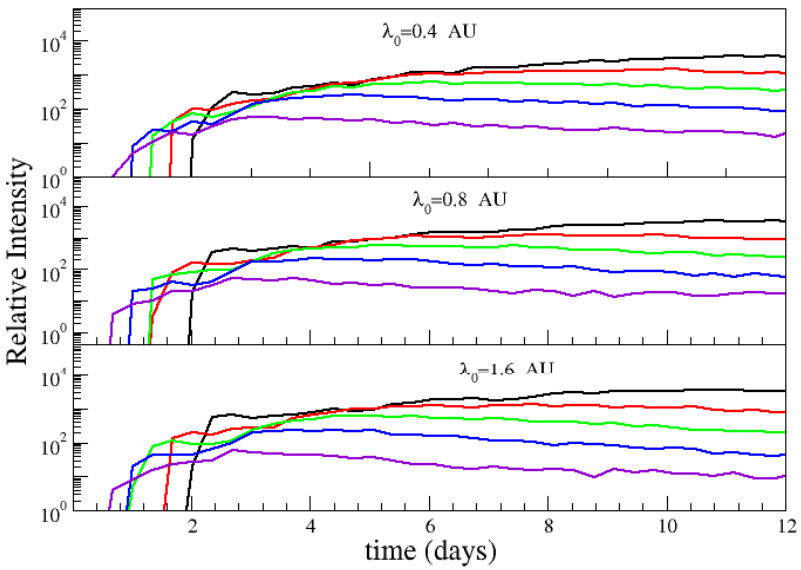

- Shock arrives 1.3 days after initiation
- No ~ 50 MeV particles at shock by 1 AU since shock weakens and unable to accelerate particles to this energy and trapped particles have now escaped.
- A slowly decreasing plateau feature present – result of both pitch angle scattering and shock propagation.
- Early time profile shows the brief free streaming phase.

CSPAR-UAH

Multiple particle crossings at 1AU

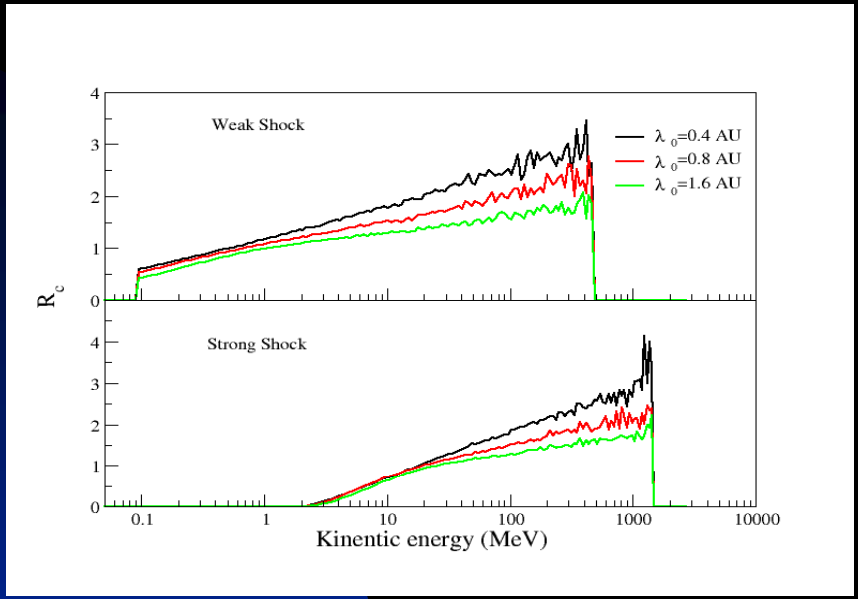

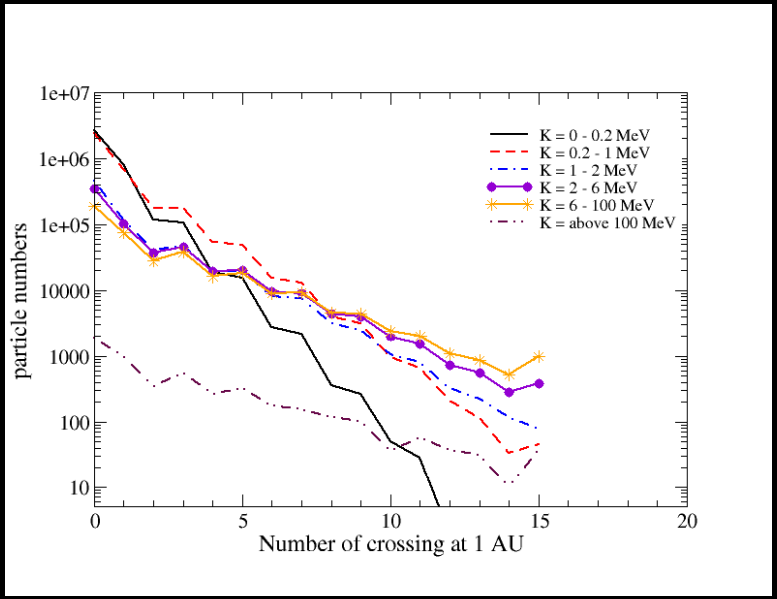

$$R_c(K) \equiv \frac{\text{number of particles of energy K that cross 1 AU}}{\text{number of particles of energy K that leave the shock}}$$

Due to pitch angle scattering, particles, especially of high energies, may cross 1 AU more than once, and thus from both sides. In an average sense, a 100 MeV particle has Rc ~ 2, or on average, two crossings. Histogram shows that some particles may cross as many as 15 times. A smaller mfp leads to a larger Rc since particles with smaller mfp will experience more pitch angle scatterings.

Anisotropy at 1 AU (weak shock)

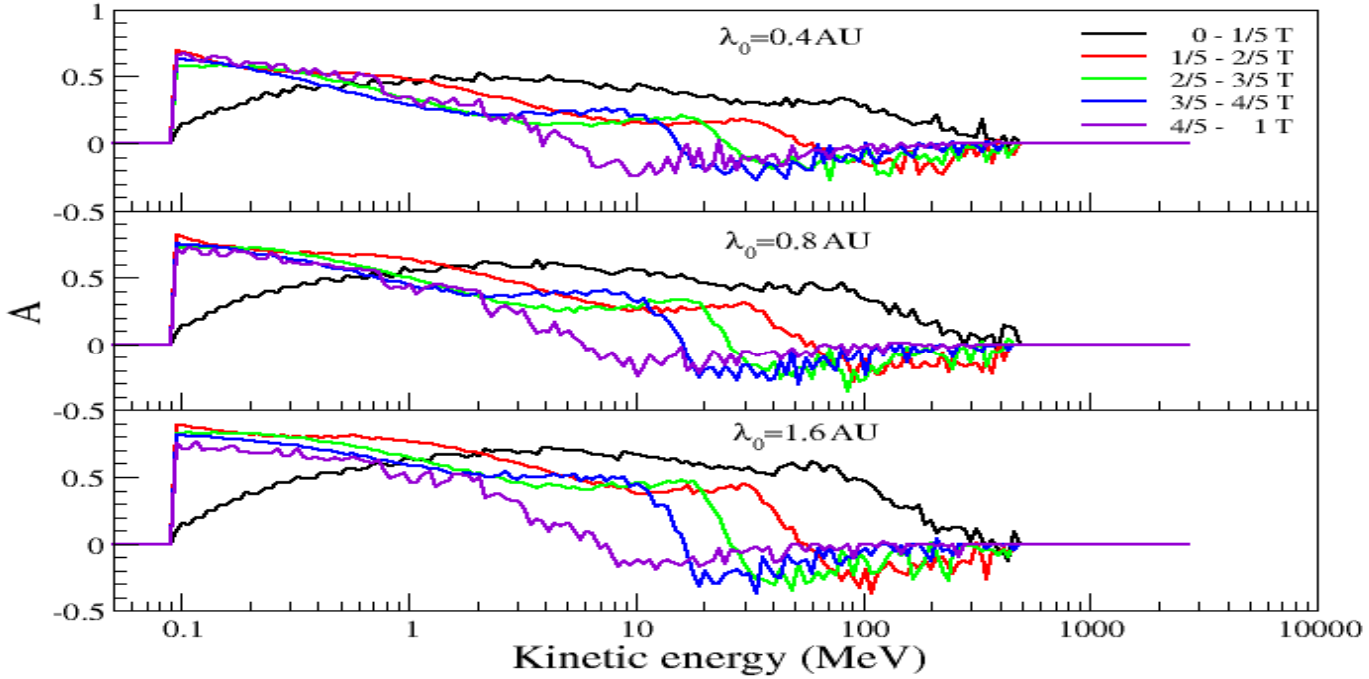

- Similar to the strong shock case.

- The value of asymmetry for larger λ_0 is consistently larger than that of a smaller λ_0 because fewer particles will propagate backward for a larger λ _0.

Time evolution of number density in phase space

- Snap shots of the number density observed at 1 AU prior to the shock arrival at t = 1/20, 2/20, …. T, with a time interval of 1/20 T in (v_par, v_perp)-space.
- Coordinates:

$$Z_x = cos(\theta_{\hat{\mathbf{B}},\hat{\mathbf{p}}})(log(p/\mathrm{MeV}) - 4.25);$$
$$Z_y = sin(\theta_{\hat{\mathbf{B}},\hat{\mathbf{p}}})(log(p/\mathrm{MeV}) - 4.25).$$

- B field along positive Zx direction
- Particle energies from innermost to outermost circle are K = 4.88, 8.12, 10.47, 15.35, 21.06, 30.75, 50.80, 100.13 MeV respectively.

The next figures exhibit the following characteristics:

- At early times, more high energy particles cross 1 AU along +B direction, followed by lower energies later.

- Number density of higher energy particles at later times exhibits a “reverse propagation” feature corresponding to A < 0.

- The gap at Θ = 90 degree reflects that particles must have a component along B to be observed.

CSPAR-UAH

Phase space evolution – time sequence

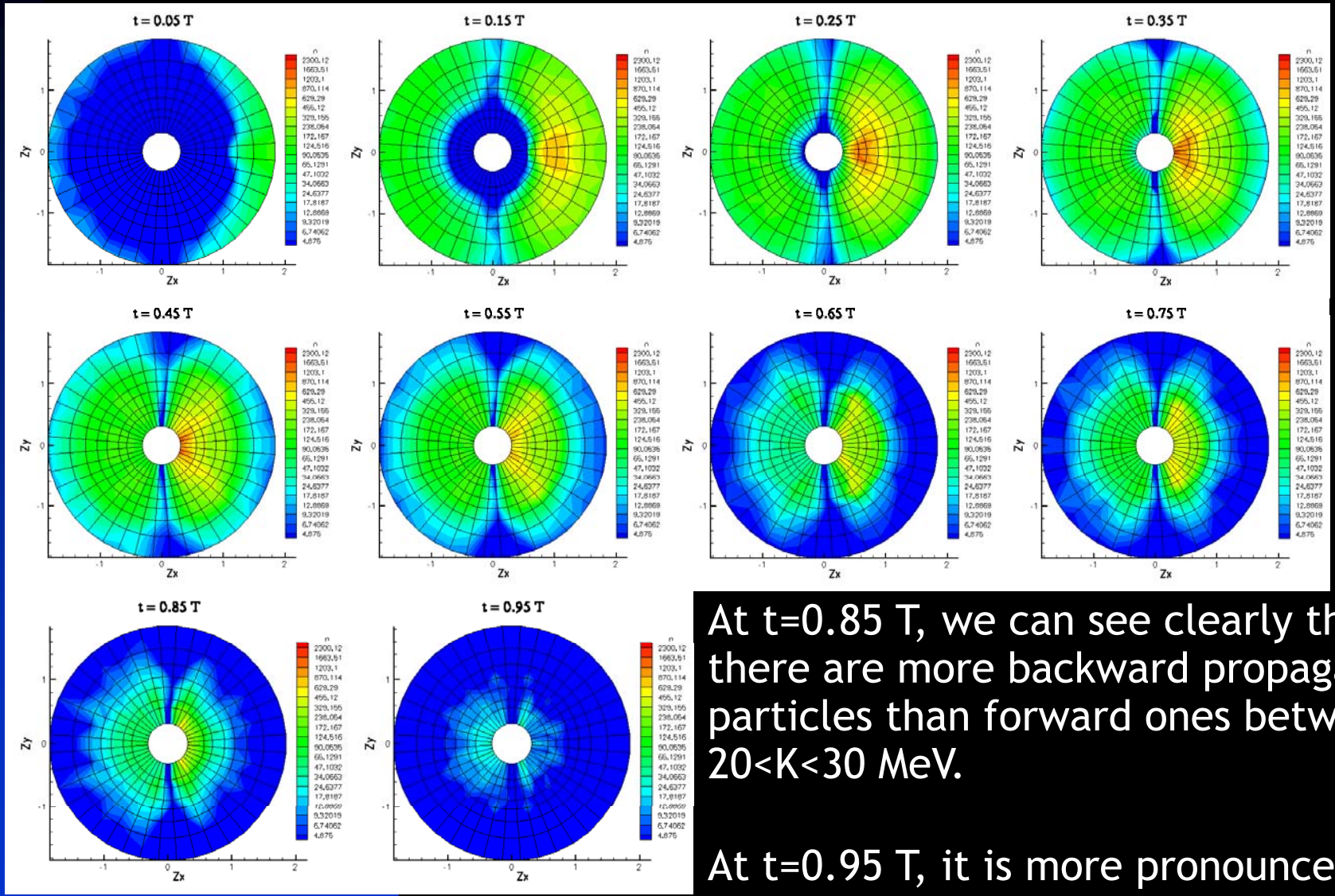

At t=0.85 T, we can see clearly that there are more backward propagating particles than forward ones between 20<K<30 MeV.

At t=0.95 T, it is more pronounced for K~10 MeV.

HEAVY IONS (CNO and Fe)

CNO: Q = 6, A = 14
Fe: Q = 16, A = 54

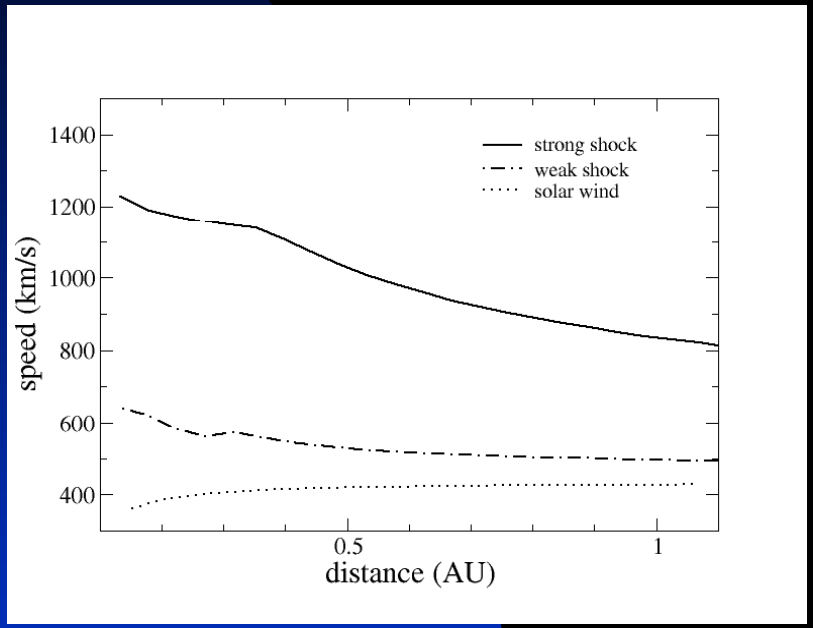

Shock speeds for strong and a weak shock.

Effect of heavy ions is manifested through the resonance condition, which then determines maximum energies for different mass ions and it determines particle transport - both factors that distinguish heavy ion acceleration and transport from the proton counterpart.

$$k = \frac{\gamma m_p \Omega}{\mu p}$$

$$\Omega = \frac{(Q/A)eB}{\gamma m_p c}$$

$$\lambda_{\parallel} = \lambda_0 \left(\frac{\tilde{p}c}{1GeV}\right)^{1/3} \left(\frac{A}{Q}\right)^{1/3} \left(\frac{r}{1AU}\right)^{2/3}$$

CSPAR-UAH

Deciding the maximum energy

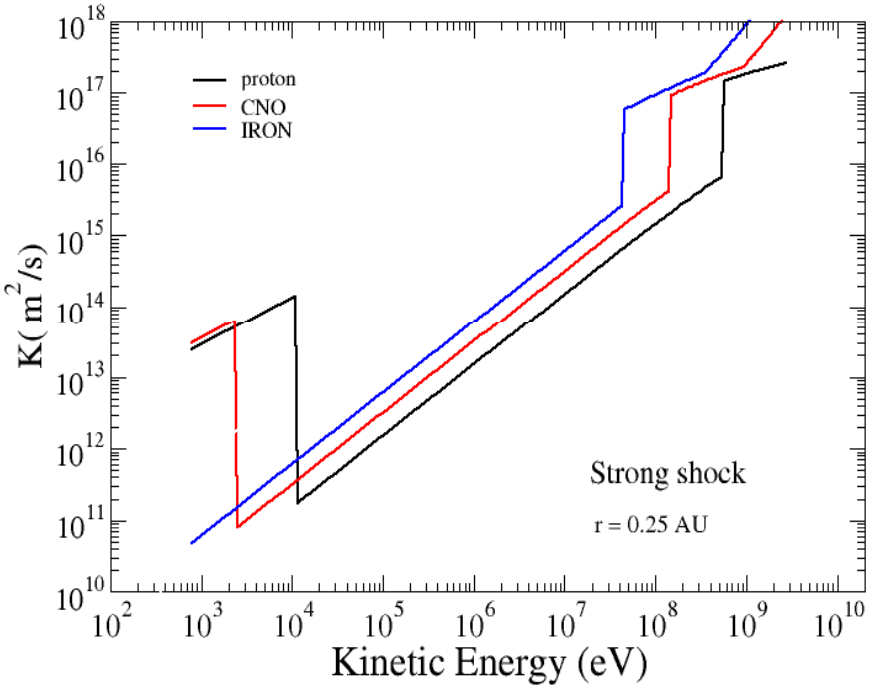

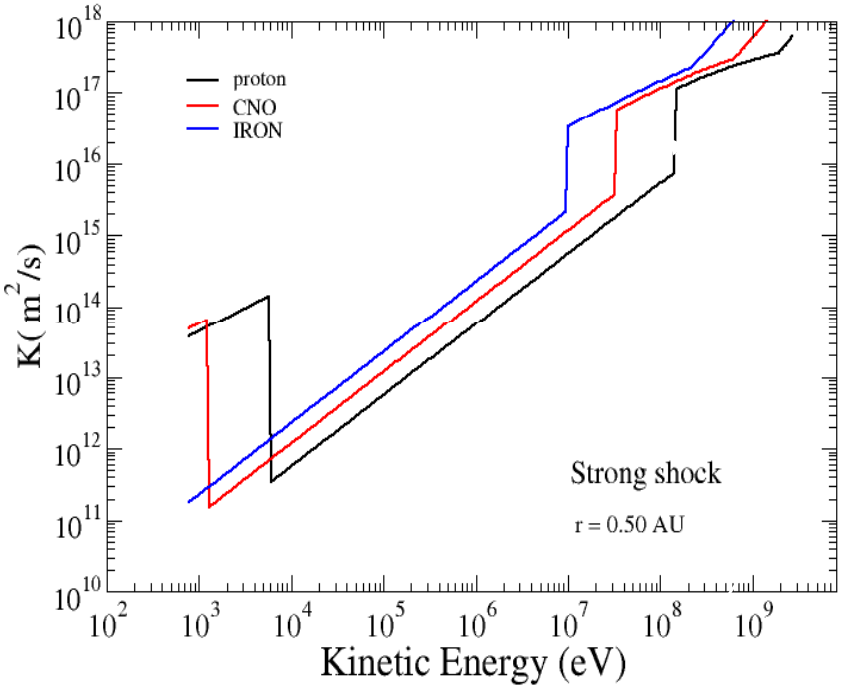

Evaluate the injection energy by assuming it is a half of the down stream thermal energy per particle.

Then evaluate the maximum energy via

$$\frac{R(t)}{\dot{R}(t)} \approx \frac{q(t)}{u_1^{\,2}} \int_{p_{inj}}^{p_{max}} \kappa(p') d\left(\ln(p')\right)$$

Maximum accelerated particle energy

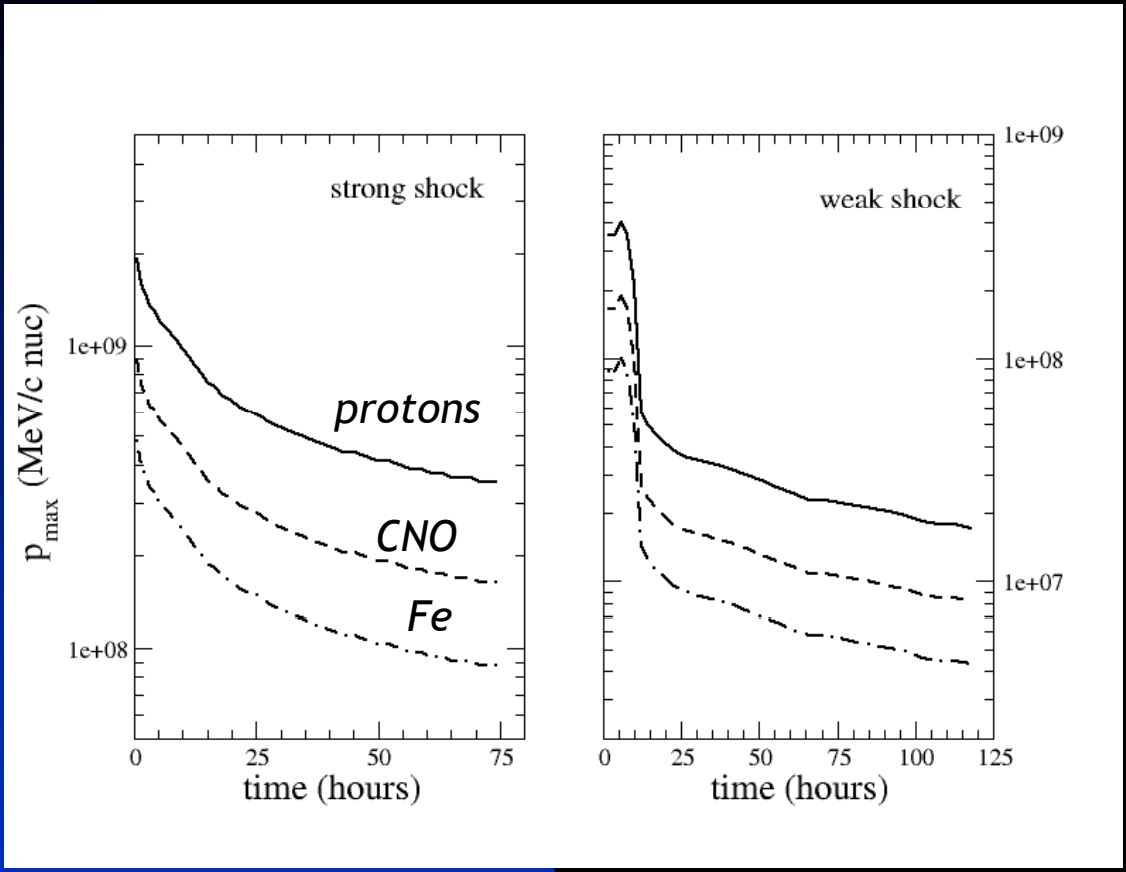

The maximum energy accelerated at the shock front. Particles having higher energies, which are accelerated at earlier times but previously trapped in the shock complex, will "see" a sudden change of κ. The maximum energy/nucleon for CNO is higher than iron since the former has a larger Q/A, thus a smaller κ.

Bohm approximation used throughout strong shock simulation but only initially in weak shock case.

Verkhoglyadova et al. 2007 results

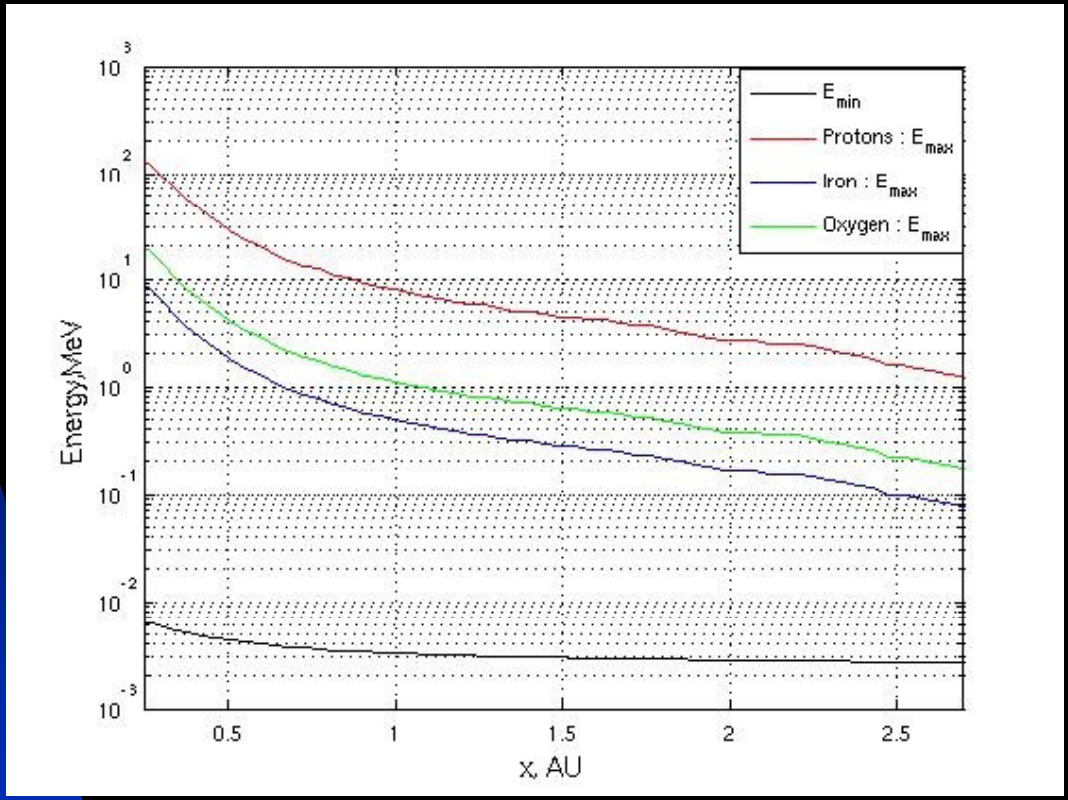

Dynamical evolution of the maximum energies for protons (red), oxygen (green) and iron (blue) ions as the quasi-parallel shock propagates from ~0.1 AU. The minimum energy (shown in black) is the same for all species.

SEP Event # 215 (shock arrival at ACE: Sept. 29, 2001, 09:06 UT)

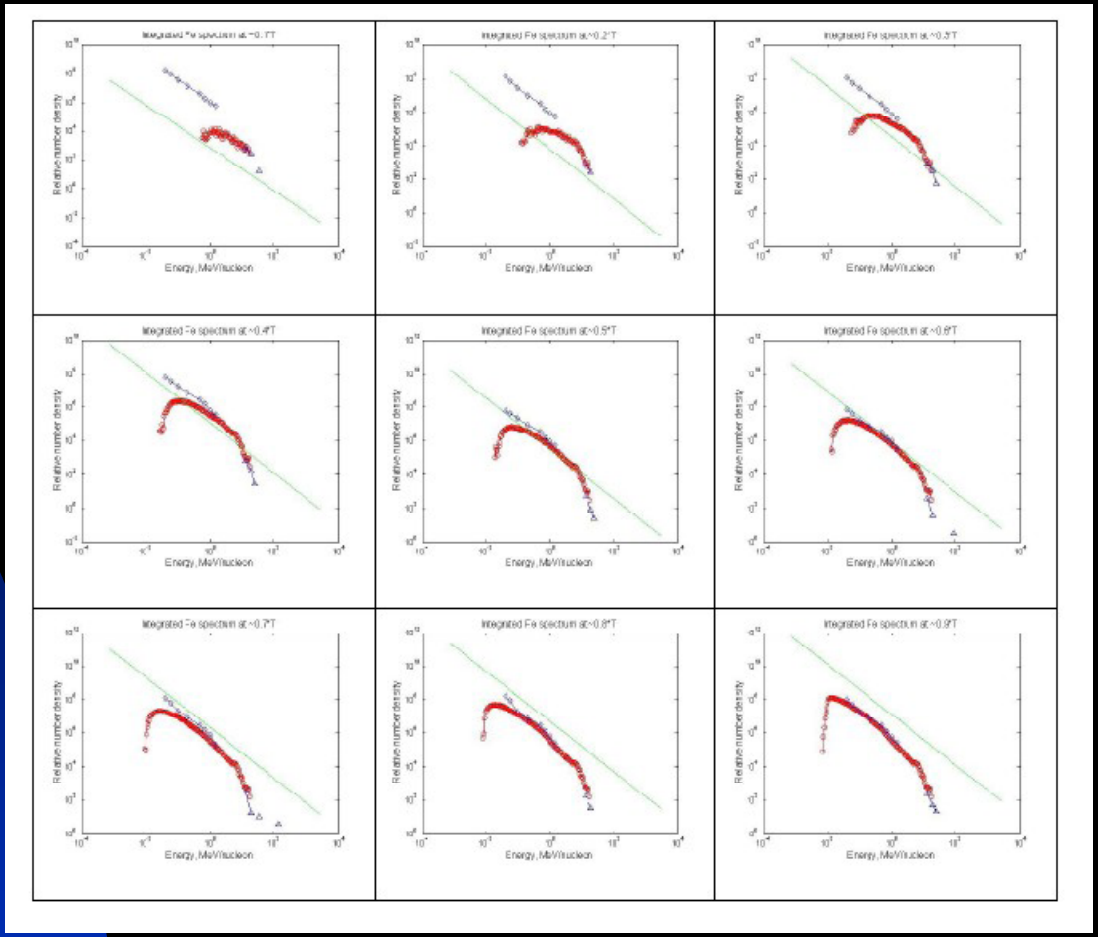

Dynamical spectra of iron ions averaged over consecutive ~5hrs time intervals until shock arrival at 1AU. ULEIS and SIS measurements are shown by blue diamonds and triangles, respectively. The straight line shows the theoretical limit for a power-law spectrum corresponding to shock parameters at 1 AU. Note the enhanced background at early times prior to the shock arrival at ~ 1AU.

SEP Event # 215 (shock arrival at ACE: Sept. 29, 2001, 09:06 UT)

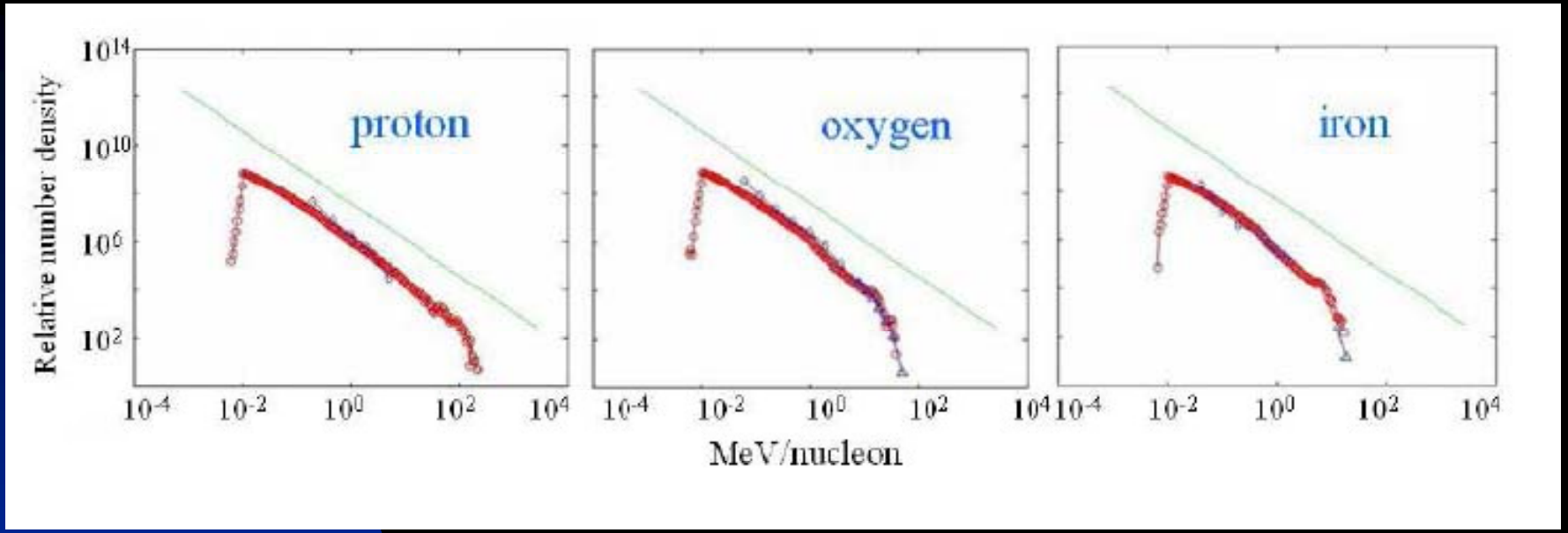

Event-integrated spectra for (a) protons, (b) oxygen and (c) iron ions. Modeling results are shown in red. ULEIS and SIS measurements integrated over the same time interval are shown by blue diamonds and triangles, respectively. The straight line shows the theoretical limit for a power-law spectrum corresponding to shock parameters at 1 AU. (Zank et al 2007).

SEP Event # 215 (shock arrival at ACE: Sept. 29, 2001, 09:06 UT)

Event integrated spectra

NOTE change in Fe/O ratio at about 10 MeV/nuc

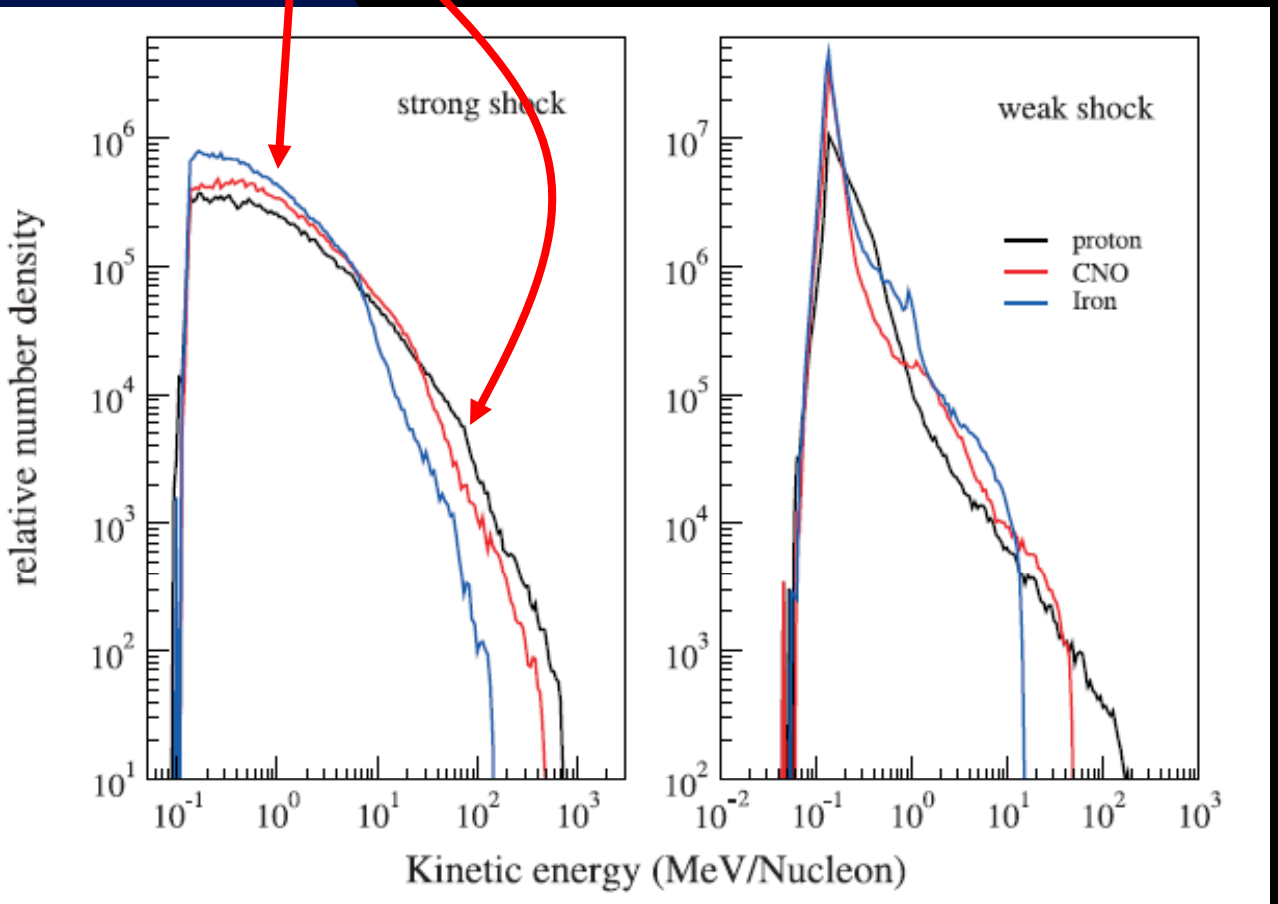

Iron Q = 14, A =56

CNO Q = 6. A = 14

Similar spectral indices at low energies, with Iron slightly softer.

Roll-over feature at high energy end with approximately $(Q/A)^2$ dependence.

Count only those particles before the shock arrival.

CSPAR-UAH

Time intensity profiles

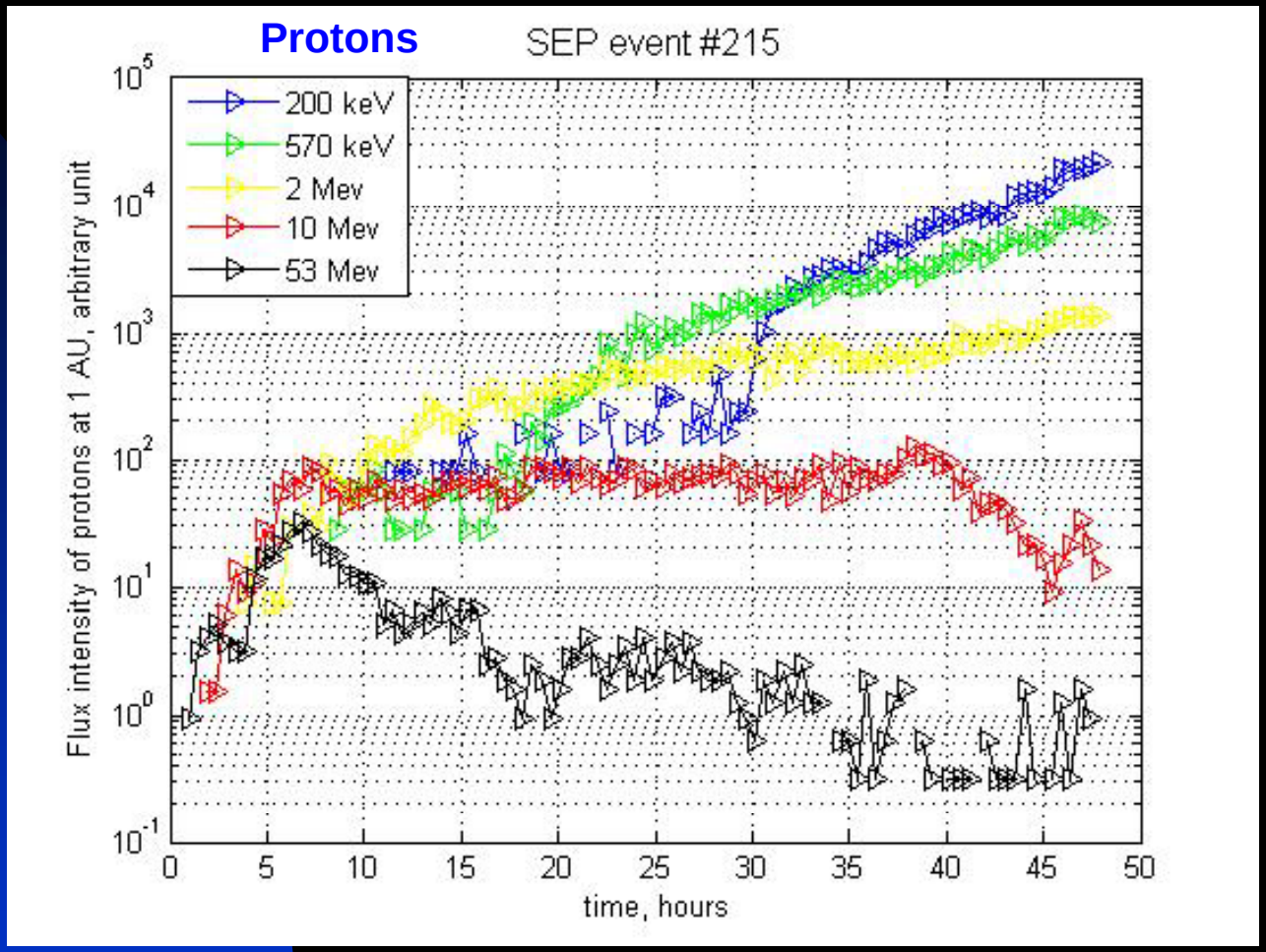

SEP Event # 215 (shock arrival at ACE: Sept. 29, 2001, 09:06 UT)

s=2.5

CSPAR-UAH

Time intensity profiles

Time intensity profiles of iron and oxygen ions. Representative energies are (from top to bottom): 0.2, 0.57, 2 and 10 MeV/nucleon. Time is in hours starting from the shock launch at 0.1 AU until the shock arrival at 1 AU

NOTE change in Fe/O ratio after 40 hours

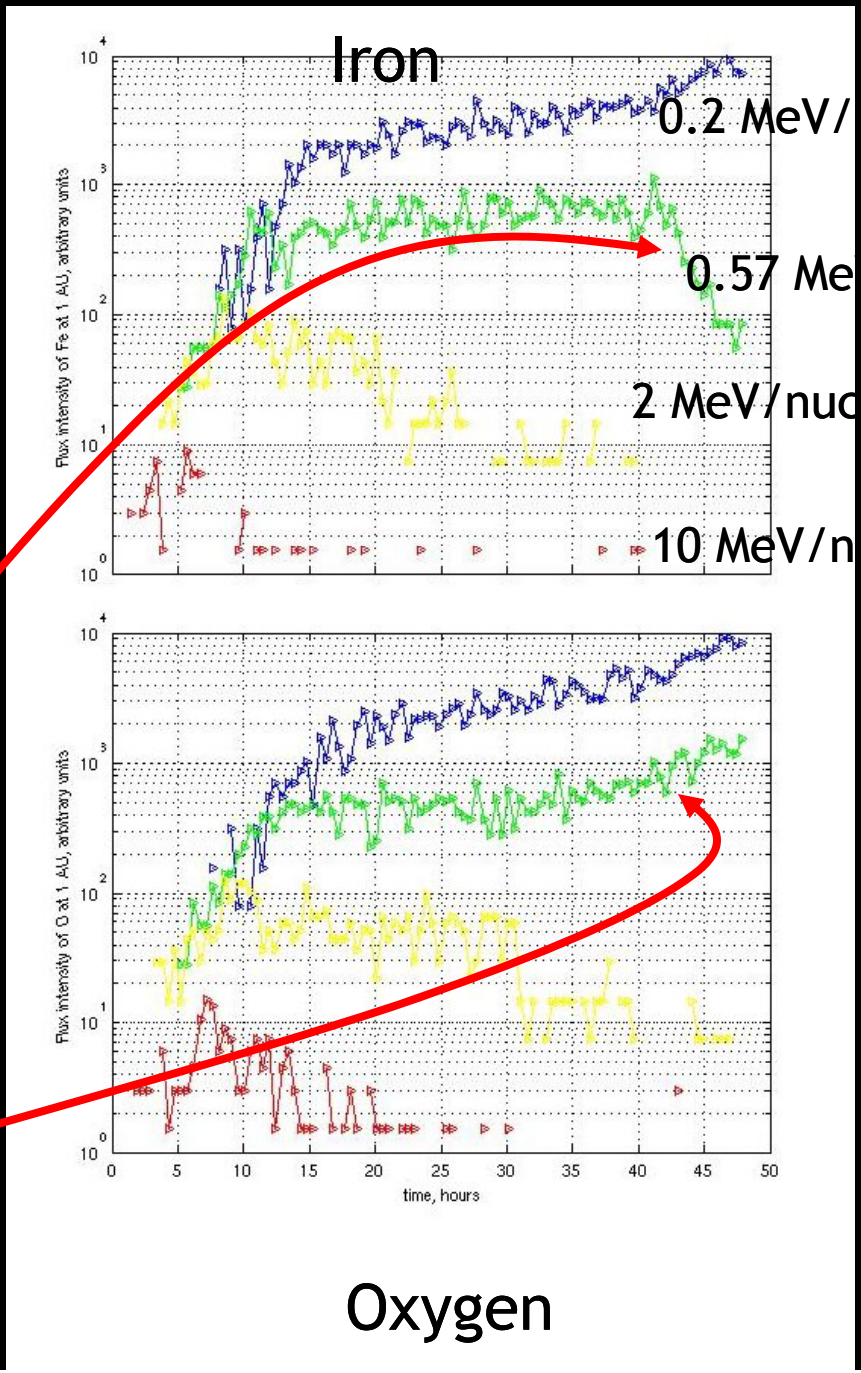

Summary of modeling – quasi-parallel shocks

- A time-dependent model of shock wave propagation (1- and 2-D), local particle injection, Fermi acceleration at the shock, and non-diffusive transport in the IP medium has been developed to describe observed SEP events: This includes spectra, intensity profiles, anisotropies.
- We can similarly model heavy ion acceleration and transport in gradual events, even understanding differences in Fe / O ratios, for example.
- We have begun to model mixed events to explore the consequences of a pre-accelerated particle population (from flares, for example) and have also related this to the timing of flare – CME events.

Perpendicular shocks

Particle acceleration at perpendicular shocks

The problems: 1) Injection threshold?
2) No self-excited waves

$$\frac{\partial f}{\partial t}+u\frac{\partial f}{\partial r}-\frac{p}{3}\frac{\partial u}{\partial r}\frac{\partial f}{\partial r}=\frac{\partial}{\partial r}\left(\kappa\frac{\partial f}{\partial r}\right);\qquad \frac{\partial A}{\partial t}+u\frac{\partial A}{\partial r}=\Gamma A-\gamma A;$$

$$\kappa(p)=\frac{\kappa_0}{A(k)}\frac{B_0}{B}\frac{(p/p_0)^2}{\sqrt{(m_pc/p_0)^2+(p/p_0)^2}};\qquad \kappa_0=\frac{4}{3\pi}r_{g0}c=\frac{4}{3\pi}\frac{p_0c}{eB_0},$$

TRANSVERSE COMPLEXITY

Qin et al. [2002a,b] - perpendicular diffusion can occur only in the presence of a transverse complex magnetic field. Flux surfaces with high transverse complexity are characterized by the rapid separation of nearby magnetic field lines.

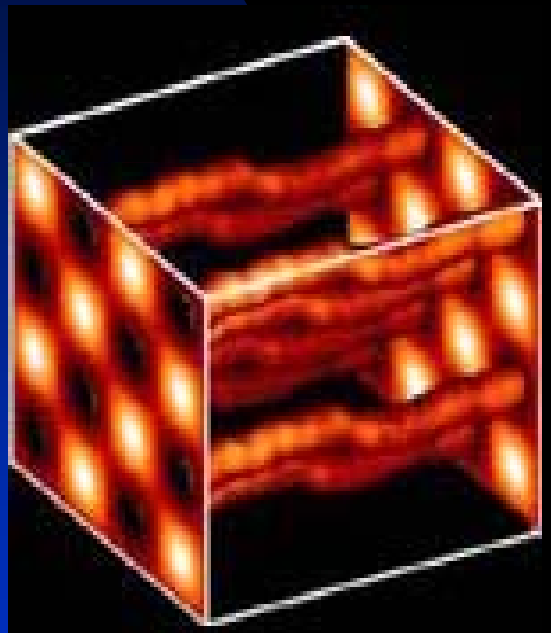

Slab turbulence only – no development of transversely complex magnetic field.

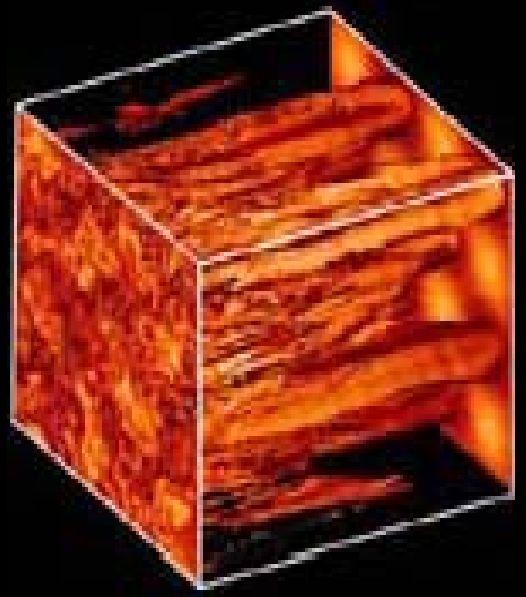

Superposition of 80% 2D and 20% slab turbulence, with the consequent development of a transversely complex magnetic field.

CSPAR-UAH

INTEGRAL FORM OF THE NONLINEAR GUIDING CENTER THEORY

Matthaeus, Qin, Bieber, Zank [2003] derived a nonlinear theory for the perpendicular diffusion coefficient, which corresponds to a solution of the integral equation

$$\kappa_{xx} = \frac{a^2 v^2}{3B_0^2} \int_0^\infty \frac{S_{xx}(\mathbf{k})\, d^3\mathbf{k}}{v/\lambda_{\|} + k_\perp^2 \kappa_{xx} + k_z^2 \kappa_{zz}}$$

Superposition model: 2D plus slab

$$S_{xx}(\mathbf{k}) = S_{xx}^{2D}\delta(k_\perp)\delta(k_z) + S_{xx}^{slab}\delta(k_\perp)$$

Solve the integral equation approximately (Zank, Li, Florinski, et al, 2004):

$$\lambda_{xx} \simeq \left(\sqrt{3}\pi a^2 C\right)^{2/3} \left(\frac{\left\langle b_{2D}^2 \right\rangle}{B_0^2}\right)^{2/3} \lambda_{2D}^{2/3} \lambda_{\|}^{1/3} \left[1 + \frac{\left(a^2 C\right)^{1/3}}{\left(\sqrt{3}\pi\right)^{2/3}} \frac{\left\langle b_{slab}^2 \right\rangle}{\left\langle b_{2D}^2 \right\rangle^{2/3} \left(B_0^2\right)^{1/3}} \frac{\min\left(\lambda_{slab}, \lambda_{\|}/\sqrt{3}\right)}{\lambda_{slab}^{2/3} \lambda_{\|}^{1/3}} \left(4.33 H\left(\lambda_{slab} - \lambda_{\|}/\sqrt{3}\right) + 3.091 H\left(\lambda_{\|}/\sqrt{3} - \lambda_{slab}\right)\right)\right]^{2/3}$$

$\lambda_{\|}$ modeled according to QLT.

CSPAR-UAH

WHAT ABOUT WAVE EXCITATION UPSTREAM?

Quasi-linear theory (Lee, 1983; Gordon et al, 1999): wave excitation proportional to cos ψ i.e.,

$$\frac{\partial I}{\partial t} \approx 0$$

at a highly perpendicular shock.

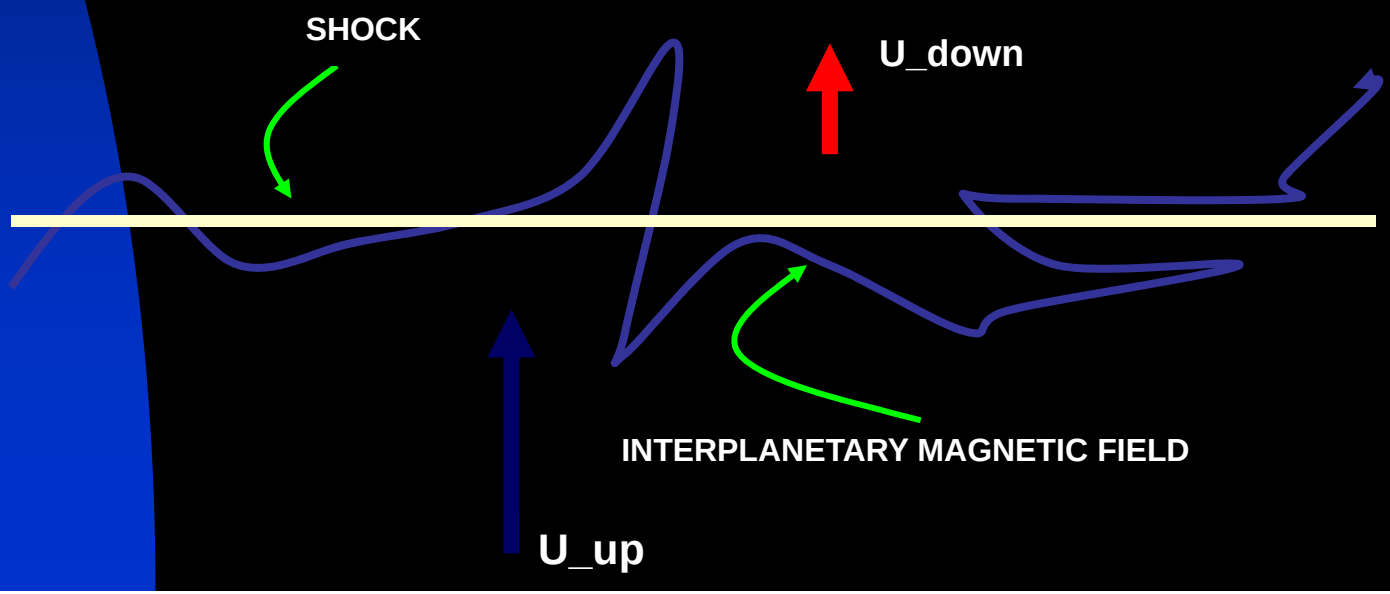

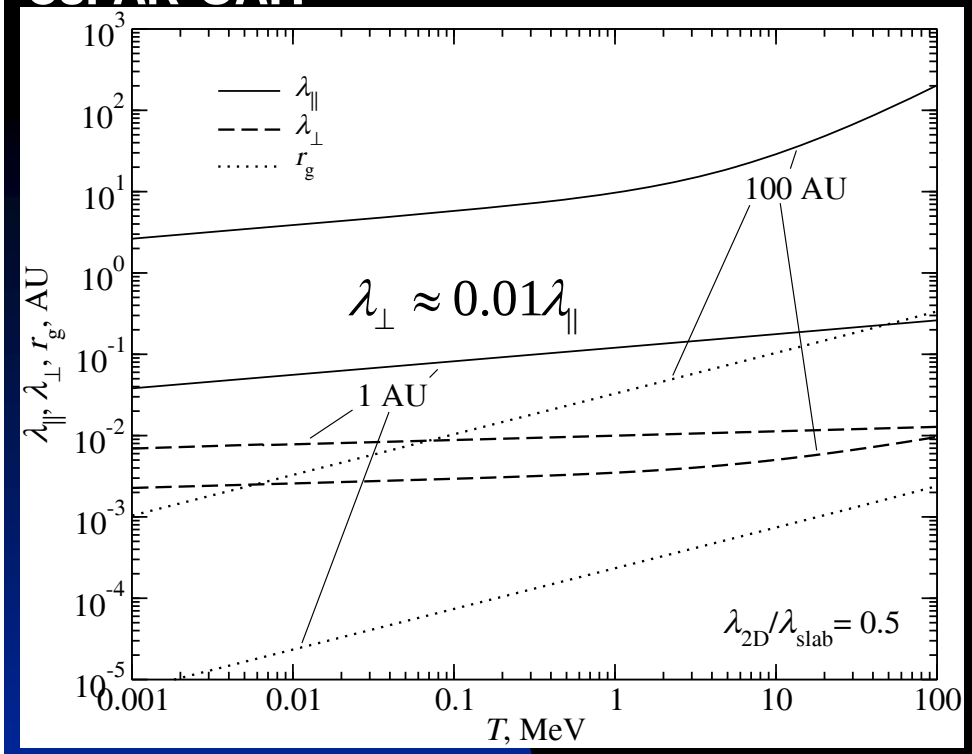

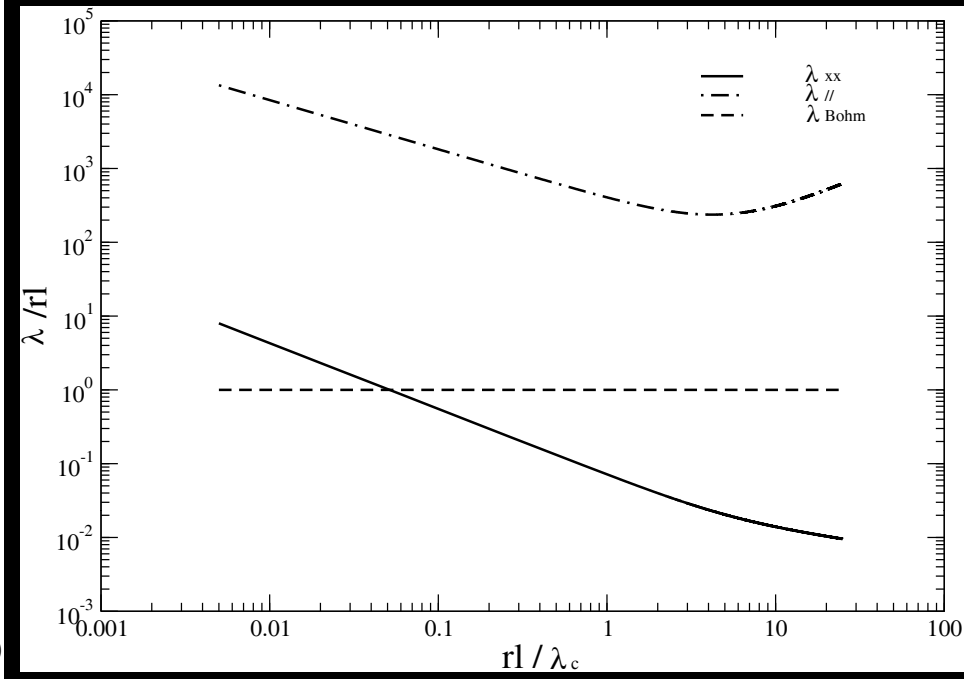

Left: Plot of the parallel (solid curve) and perpendicular mfp (dashed curve) and the particle gyroradius (dotted) as a function of energy for 100 AU (the termination shock) and 1 AU (an interplanetary shock).

Right: Different format - plots of the mean free paths at 1 AU as a function of particle gyroradius and now normalized to the correlation length. *The graphs are equivalent to the ratio of the diffusive acceleration time to the Bohm acceleration time, and each is normalized to gyroradius*. Solid line corresponds to normalized (to the Bohm acceleration time scale) perpendicular diffusive acceleration time scale, the dashed-dotted to parallel acceleration time scale, and the dashed to Bohm acceleration time scale (obviously 1).

CSPAR-UAH

PARTICLE ACCELERATION AT PERPENDICULAR SHOCKS

- STEP 1: Evaluate K_perp at shock using NLGC theory instead of wave growth expression.

$$\kappa_{xx} \simeq \frac{v}{3}\left(\sqrt{3}\pi a^2 C\right)^{2/3}\left(\frac{\left\langle b_{2D}^2\right\rangle}{B_0^2}\right)^{2/3}\lambda_{2D}^{2/3}\lambda_{\parallel}^{1/3}$$

$$\times\left[1+\frac{\left(a^2C\right)^{1/3}}{\left(\sqrt{3}\pi\right)^{2/3}}\frac{\left\langle b_{slab}^2\right\rangle}{\left\langle b_{2D}^2\right\rangle^{2/3}\left(B_0^2\right)^{1/3}}\frac{\min\left(\lambda_{slab},\lambda_{\parallel}/\sqrt{3}\right)}{\lambda_{slab}^{2/3}\lambda_{\parallel}^{1/3}}\left(4.33H\left(\lambda_{slab}-\lambda_{\parallel}/\sqrt{3}\right)\right)+3.091H\left(\lambda_{\parallel}/\sqrt{3}-\lambda_{slab}\right)\right]^{2/3}$$

$$\left\langle b^2\right\rangle = \left\langle b_{slab}^2\right\rangle + \left\langle b_{2D}^2\right\rangle \quad 20\%:80\%$$

$$\left\langle b^2\right\rangle \propto R^{-3}$$

Parallel mfp evaluated on basis of QLT (Zank et al. 1998.

PARTICLE ACCELERATION AT PERPENDICULAR SHOCKS

- STEP 2: Evaluate injection momentum p_min by requiring the particle anisotropy to be small.

$$v_{inj} \approx 3u\left[\frac{1}{(r-1)^2}+\frac{r_g^2+\lambda_{\parallel}^2\cos^2\theta_{bn}}{(\lambda_{\perp}+\lambda_{\parallel}\cos^2\theta_{bn})^2}\right]^{1/2}$$

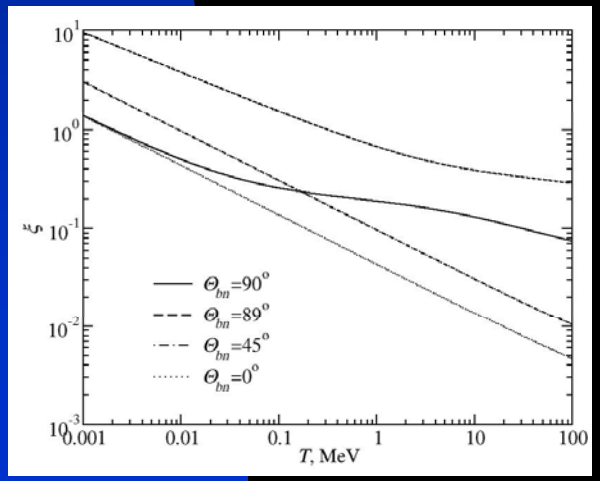

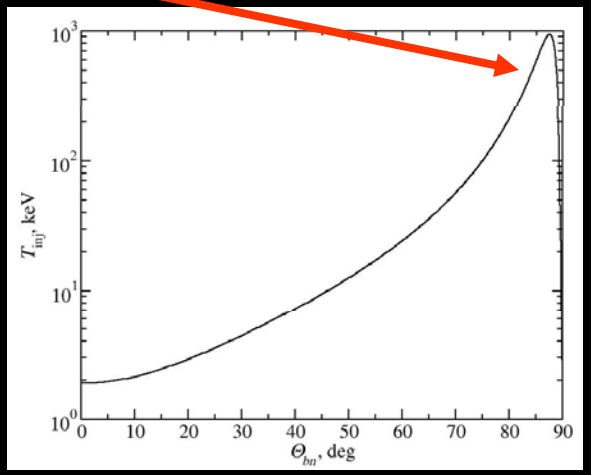

PARTICLE ACCELERATION AT PERPENDICULAR SHOCKS

- STEP 3: Determine maximum energy by equating dynamical timescale and acceleration timescale – complicated in NLGC framework. In inner heliosphere, particles resonate with inertial range (unlike outer heliosphere).

$$\frac{\dot{R}(t)}{R(t)} \approx \frac{q(t)}{u_1^2} \int_{p_{\mathrm{inj}}}^{p_{\max}} f(p) p^2 d(\ln(p))$$

$$\frac{p_{\max}}{m_p} \approx \left(\frac{Q}{A}\right)^{1/4} \left(\frac{e}{m_p}\right)^{1/4} \left(\lambda_c^{slab}\right)^{-1/2} \left[0.148 \frac{V_{sh}^2 (r-1)}{\alpha r} \frac{R}{\dot{R}}\right]^{1/4} \frac{\left\langle b_{slab}^2 \right\rangle^{3/4}}{B^{5/4}}$$

Remarks:

$$\frac{\left\langle b_{slab}^2 \right\rangle}{B^2} \sim R^{-1}$$

$$\frac{V_{sh}^2 R}{\dot{R}} \sim t^{2\beta-3}$$

$$\kappa_\perp \sim \alpha \kappa_\parallel^{1/3} \qquad \alpha = 0.1 - 0.001$$

Like quasi-parallel case, p_max decreases with increasing heliocentric distance.

Remarks re maximum energies

- Fundamental difference between the perpendicular and quasi-parallel expressions is that the former is derived from a quasi-linear theory based on pre-existing turbulence in the solar wind, whereas the latter results from solving the coupled wave energy and cosmic ray streaming equation explicitly, i.e., in the perpendicular case, the energy density in slab turbulence corresponds to that in the ambient solar wind whereas in the case of quasi-parallel shocks, it is determined instead by the self-consistent excitation of waves by the accelerated particles themselves.

- From another perspective, unlike the quasi-parallel case, the resonance condition does not enter into the evaluation of p_max. The diffusion coefficient is fundamentally different in each case, and hence the maximum attainable energy is different for a parallel or perpendicular shock.

- In the inner heliosphere where the mean magnetic field is strong, the maximum momentum decreases with increasing field strength, this reflecting the increased "tension" in the mean field.

Remarks re maximum energies – different shock configurations and ionic species

Three approaches have been identified for determining p_max [Zank et al 2000; Li et al 2003].

- 1. For protons accelerated at quasi-parallel shock, p_max determined solely on basis of balancing the particle acceleration time resulting from resonant scattering with the dynamical timescale of the shock. The wave/turbulence spectrum excited by the streaming energized protons extends in wave number as far as the available dynamical time allows.

- 2. For heavy ions at a quasi-parallel shock, the maximum energy is also computed on the basis of a resonance condition but only up to the minimum k excited by the energetic streaming ions, which control the development of the wave spectrum. Thus, maximum energies for heavy ions are controlled by the accelerated protons and their self-excited wave spectrum. This implies a *(Q/A)^2* dependence of the maximum attainable particle energy for heavy ions.

Remarks re maximum energies – different shock configurations and ionic species

- 3. For protons at a highly perpendicular shock, the maximum energy is independent of the resonance condition, depending only on the shock parameters and upstream turbulence levels. For heavy ions, this implies either a *(Q/A)^{1/2}* or a (Q/A)^{4/3} dependence of the maximum attainable particle energy, depending on the relationship of the maximum energy particle gyroradius compared to turbulence correlation length scale.

- It is possible to extract observational signatures related to the spectral break point that distinguishes between particle acceleration at quasi-parallel or highly perpendicular shocks (Li et al., 2009).

CSPAR-UAH

Observations

Perpendicular shock

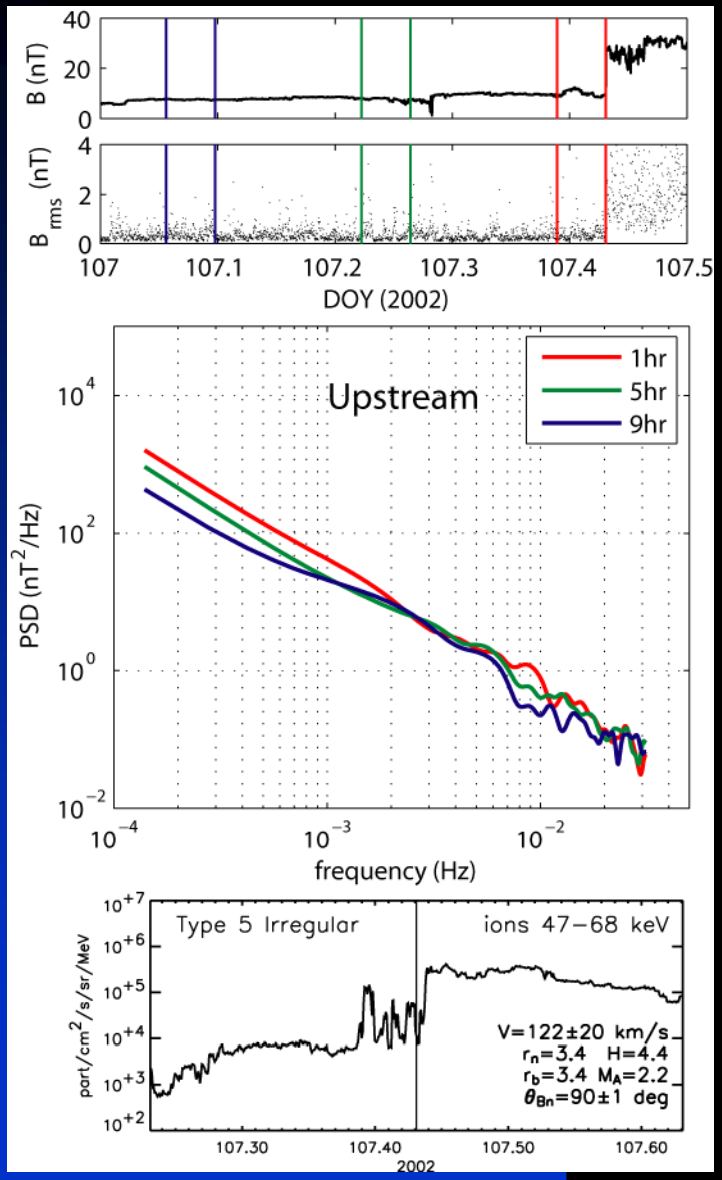

Quasi-perp shock

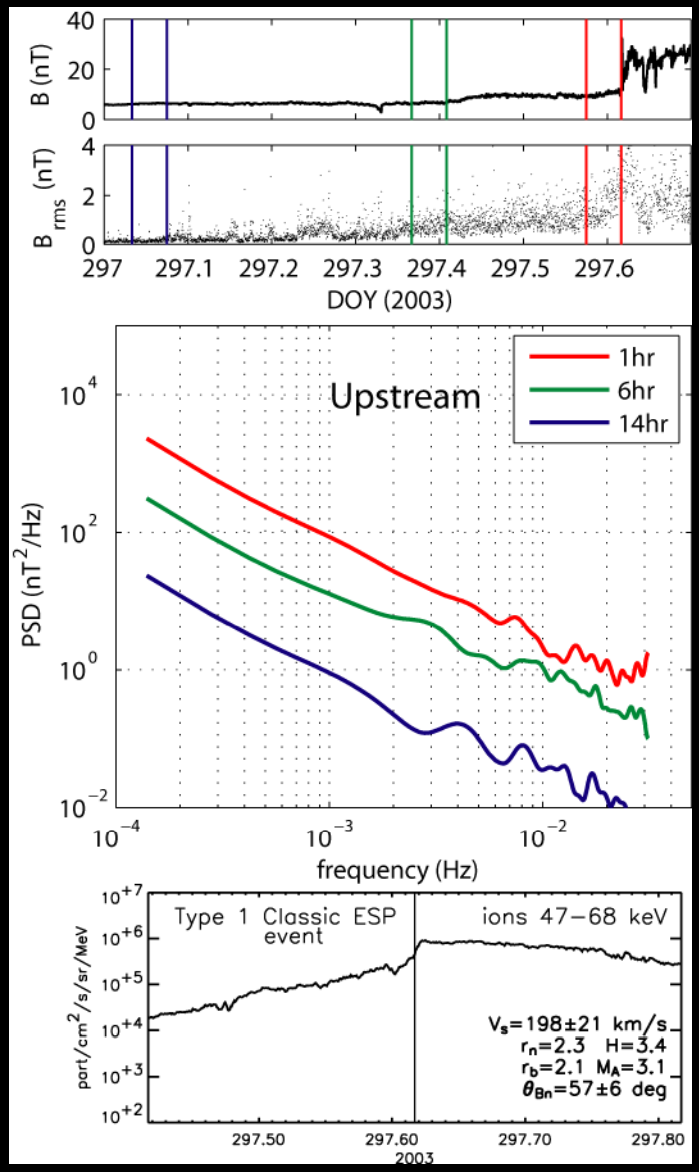

CONCLUDING REMARKS FOR PERPENDICULAR SHOCKS

- Developed basic theory for particle acceleration at highly perpendicular shocks based on convection of in situ solar wind turbulence into shock.
- Highest injection energies needed for quasi-perp shocks and not for pure perpendicular shock. 90 degree shock “singular” example.
- Determination of K_perp based on Nonlinear Guiding Center Theory
- Maximum energies at quasi-perp shocks less than at quasi-par shocks near sun. Further from sun, reverse is true.
- Injection energy threshold much higher for quasi-perp shocks than for quasi-parallel shocks and therefore can expect distinctive compositional signatures for two cases.
- Observations support notion of particle acceleration at shocks in absence of stimulated wave activity.

SEP event of December 13, 2006 is among large SEP events of the Solar Cycle 23:

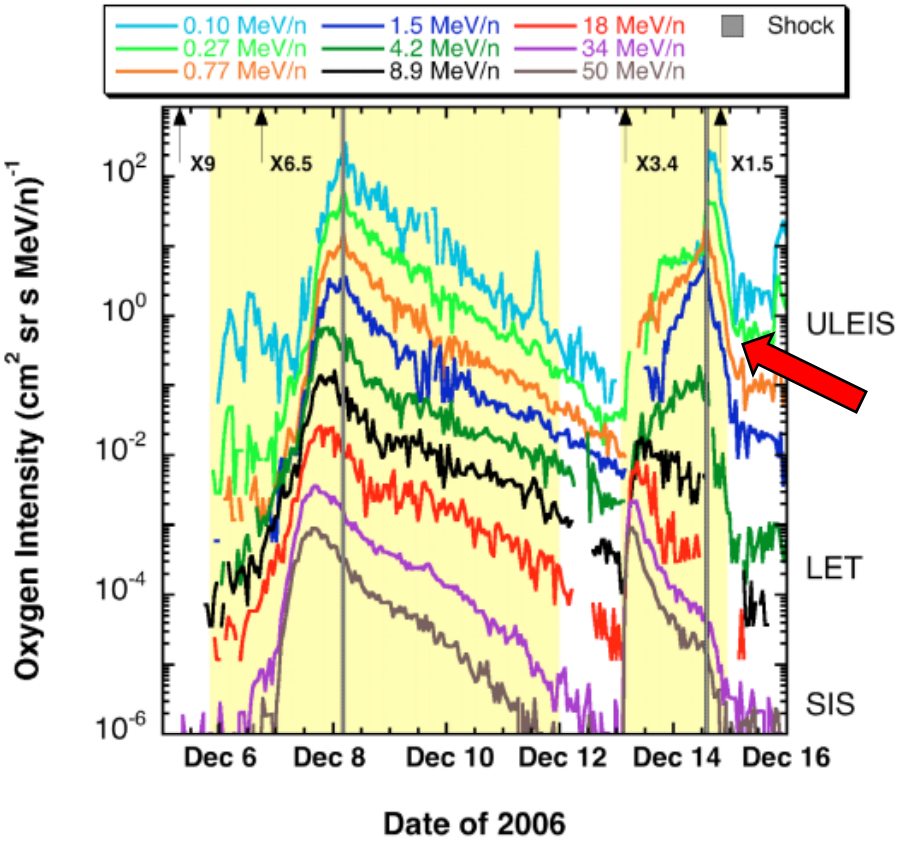

FIGURE 1. Hourly oxygen intensities as a function of time from the ACE/ULEIS, STEREO-B/LET, and ACE/SIS instruments. Interplanetary shock passages are marked by vertical lines and the times of X-class flares are indicated at the top. The shaded regions indicate averaging intervals for abundances.

ACE at 1 AU

From Cohen et al., AIP Proc. (2008); see also Mulligan et al. (2008).

Particle acceleration spectra and abundances observed in the mixed events are due to:

- Scenario 1: (Quasi-perpendicular) shock geometry change *(Tylka et al., 2005);*
- Scenario 2: Presence of both flare and shock-accelerated particles *(Cane et al., 2003), (Li and Zank,2005);*

Modelling the 3 possible cases:

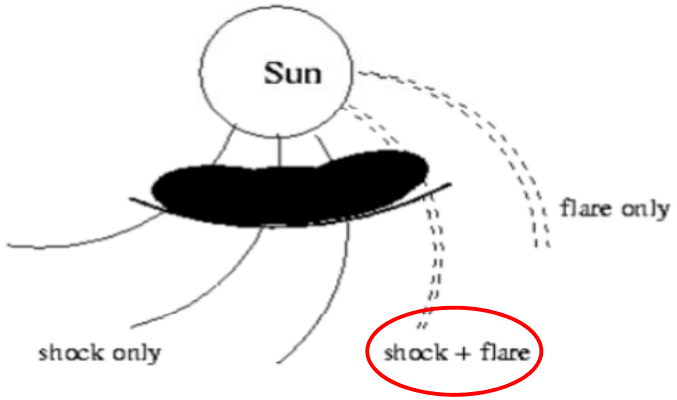

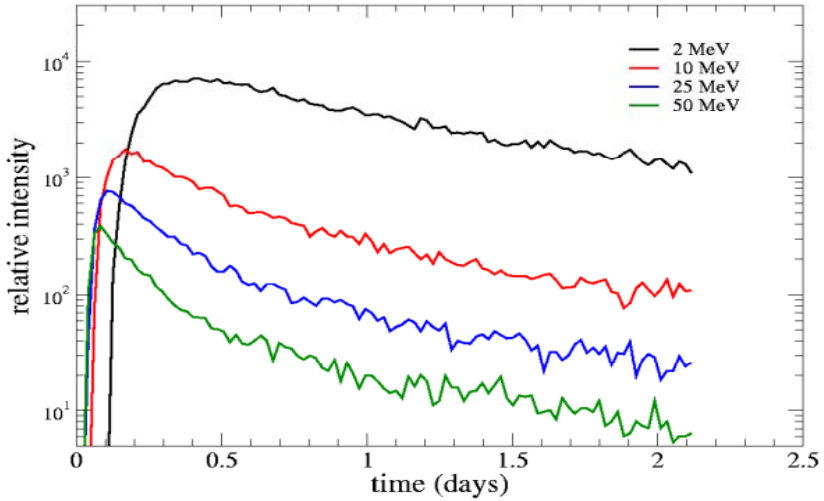

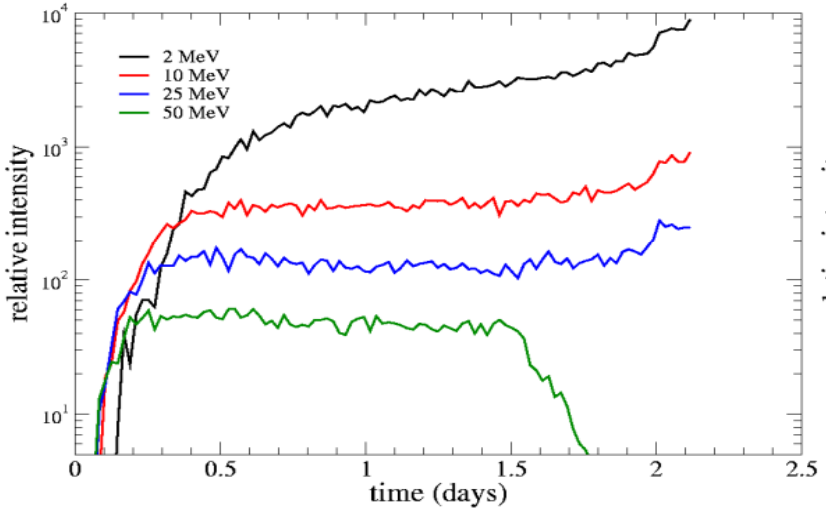

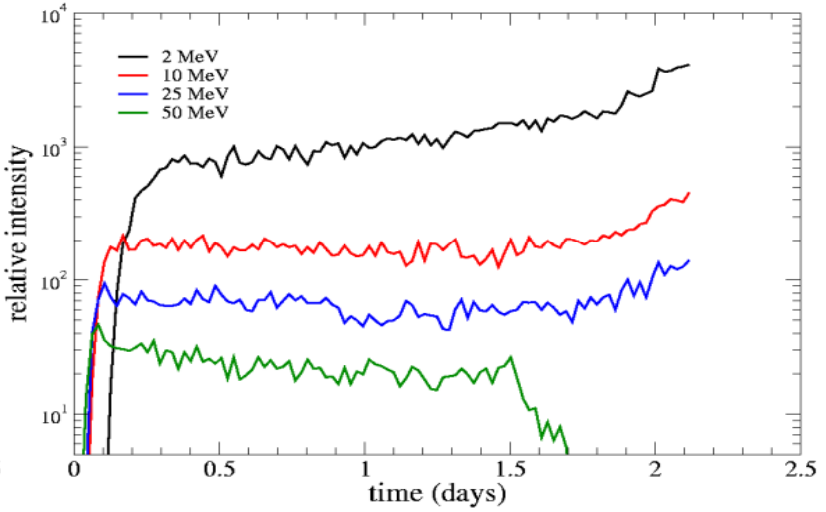

From Li and Zank, GRL, 2005

Control parameters for the PATH model

- *Shock obliquity Θ_{Bn}=30˚*
- *Ratio of Q/M for seed particles (ACE observations): Q[Fe]=16; Q[O]=6*
- *Injection with energy (10 keV) and efficiency (1% flux density)*
- *Flare parameters*
- *Ratio of flare to SW particles*

(Zank et al., 2007; Verkhoglyadova et al., 2008)

CSPAR-UAH

Event-integrated spectra (~ 50 hrs): protons

* ACE, STEREO, GOES and SAMPEX data

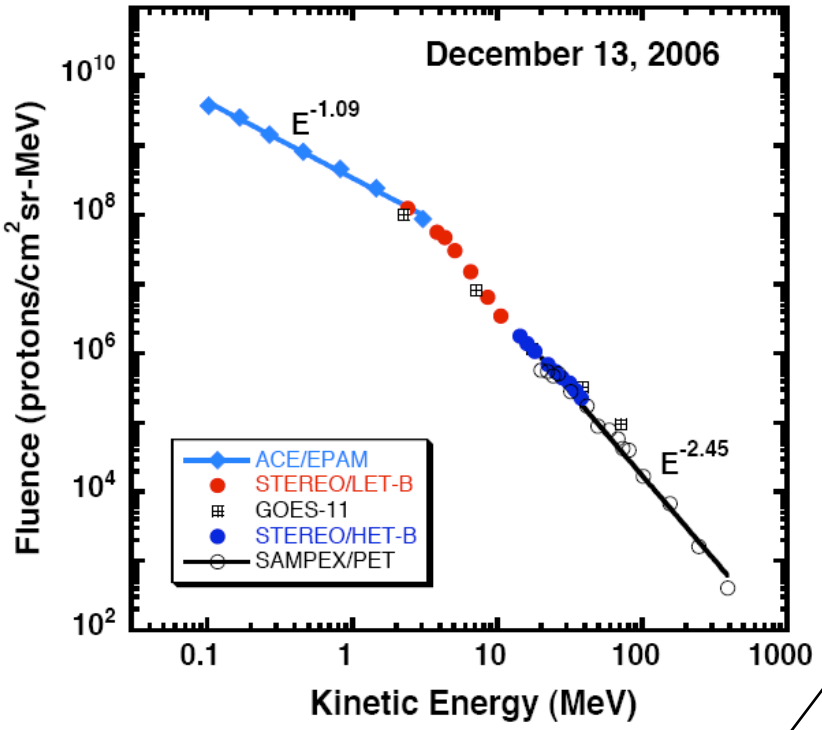

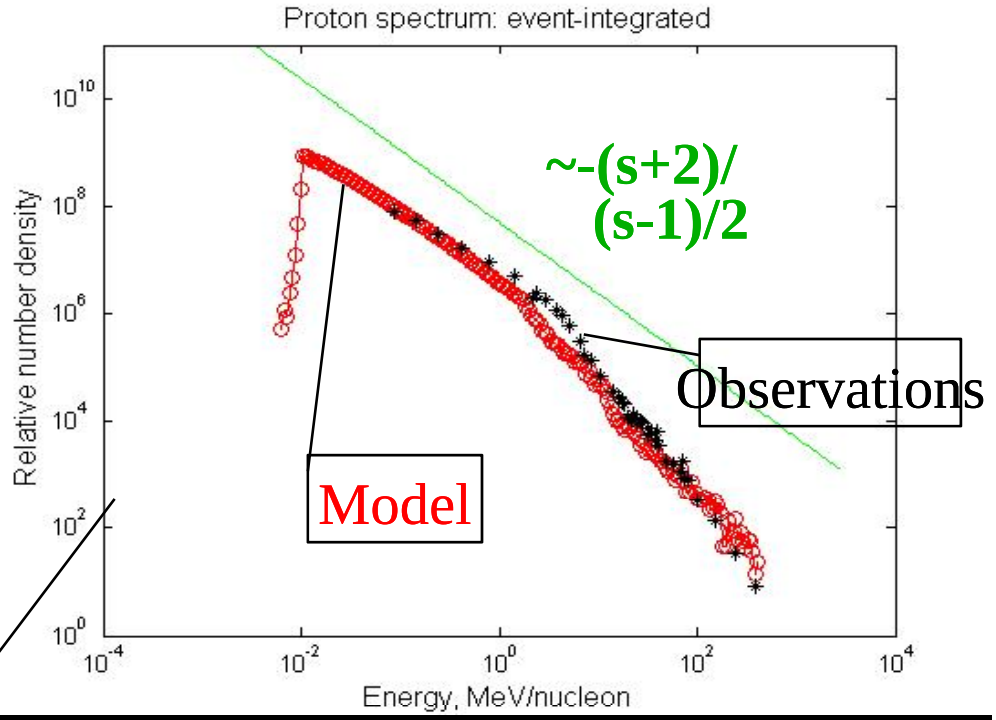

(Mewaldt, 2007; Cohen, 2007, 2008)

Arbitrary units

25% flare particles in this mixed event

CSPAR-UAH

Event-integrated spectra of Fe ions (~ 50 hrs):

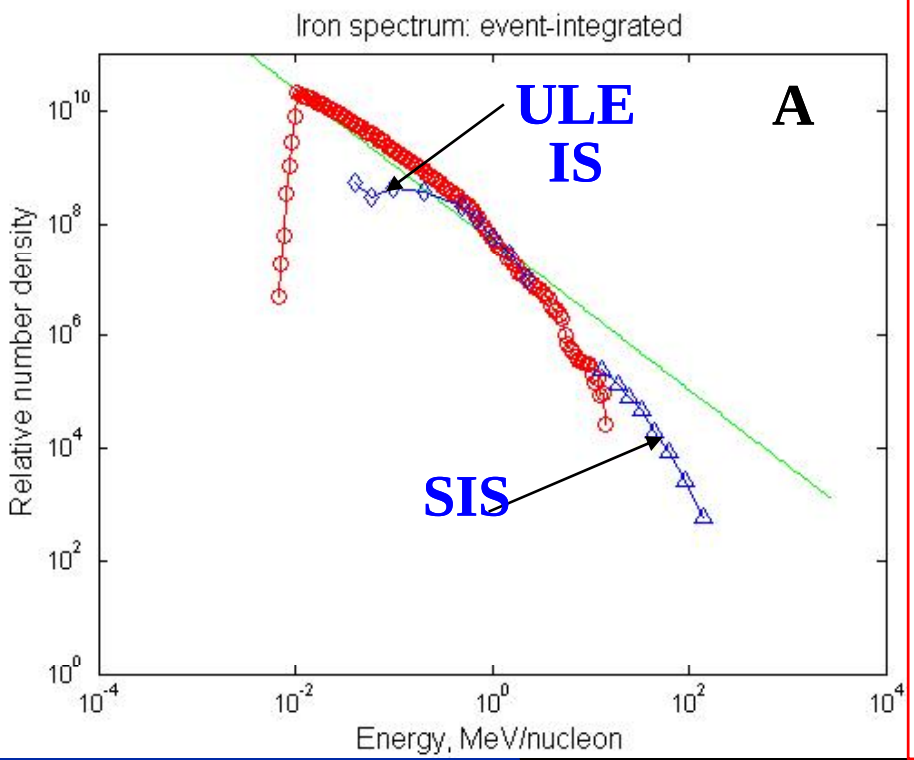

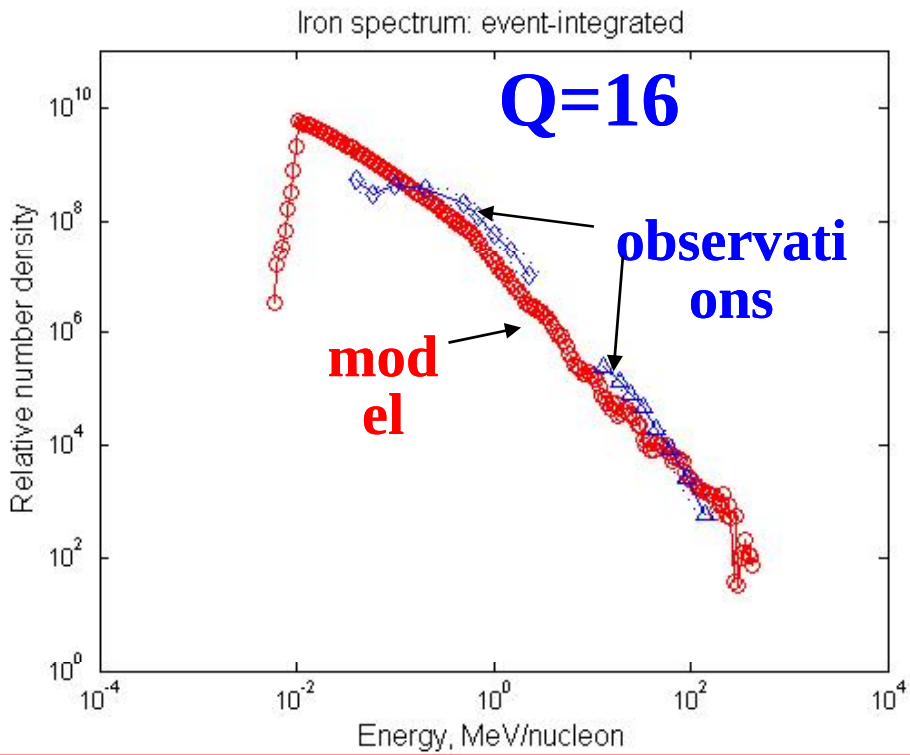

Seed population:

A – shock only
flare particles

B – 25%

(high-energy spectrum is missing)

CSPAR-UAH

Event-integrated spectra of O ions (~ 50 hrs)**:**

ACE

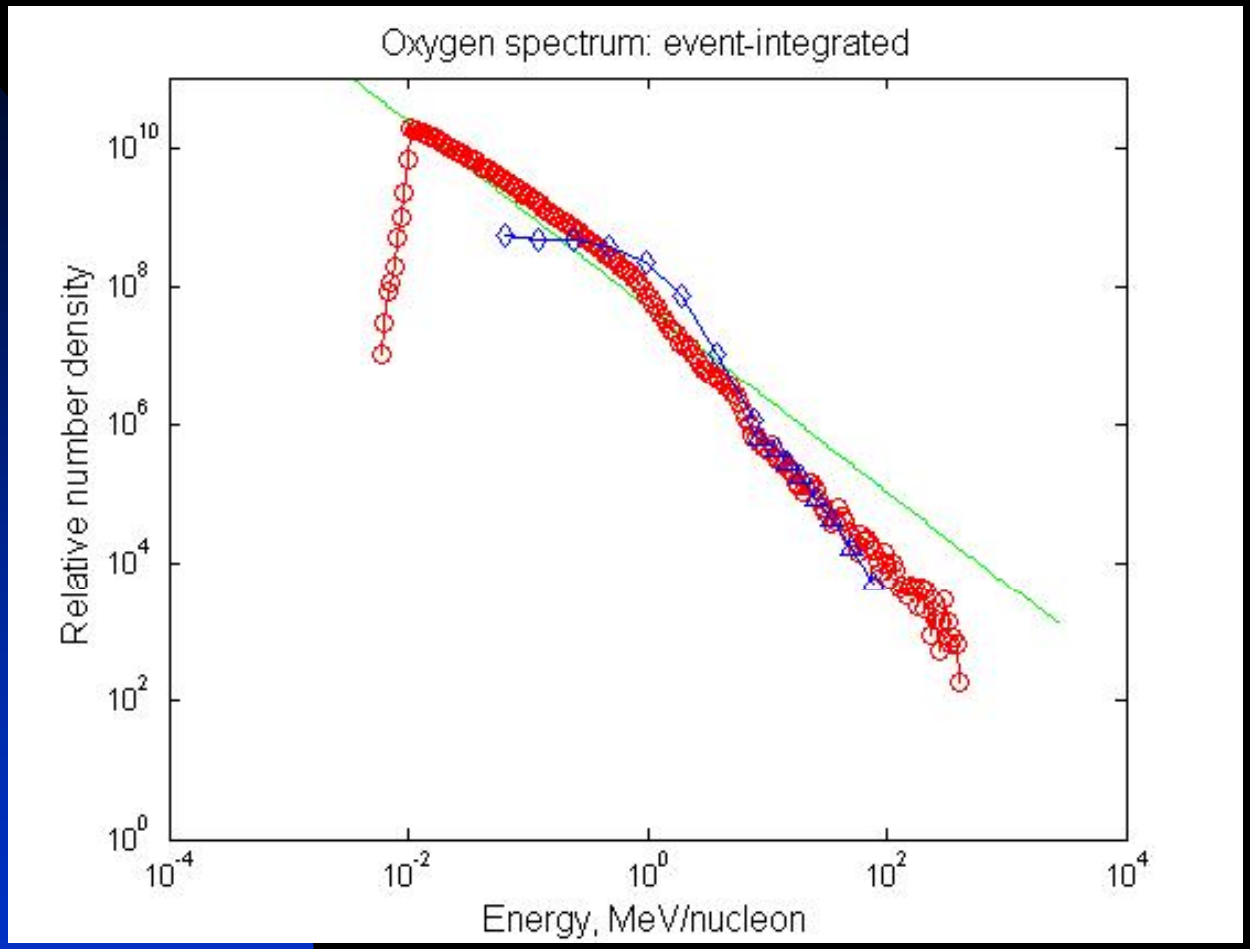

OXYGEN

25% flare particles in this mixed event

Free parameters of the model

- Escape length (p)
- MFP scaling and dependence on *r* and *p*
- *Injection energy (10 keV) and efficiency (1% flux density)*
- *Flare parameters: duration, max/min p, spectra;*
- *Ratio of flare to shock-accelerated particles*
  (Zank et al., 2000; Li et al., 2003; 2005; Zank et al., 2007)

CSPAR-UAH

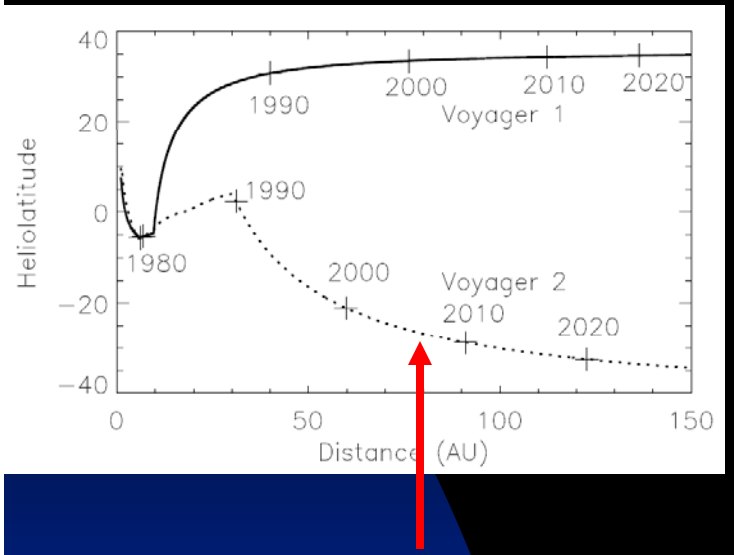

An energetic-particle-mediated termination shock observed by Voyager 2

8/30/07 – 83.7 AU

Vladimir Florinski, G.P. Zank, and Rob Decker

1) Center for Space and Aeronomic Science (CSPAR) and Department of Physics University of Alabama, Huntsville
2) APL, Johns Hopkins University

Voyager 2 termination shock crossing on days 242--244 of 2007 was quite different from Voyager 1

- Broad precursor structure extending 0.7 AU upstream (using V2 speed of 14.8 km/s)
- Solar wind decelerated from ~370 km/s far upstream to ~300 km/s just upstream of the shock
- Decreases may be associated with two magnetic structures

Richardson et al., 2008

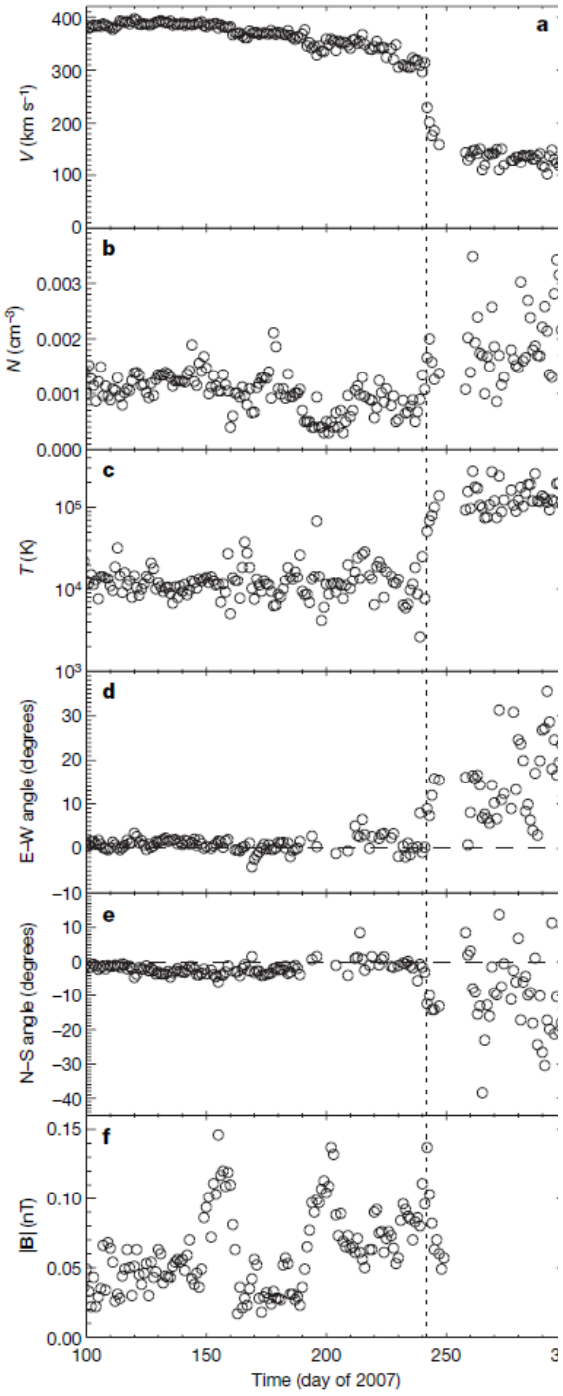

C

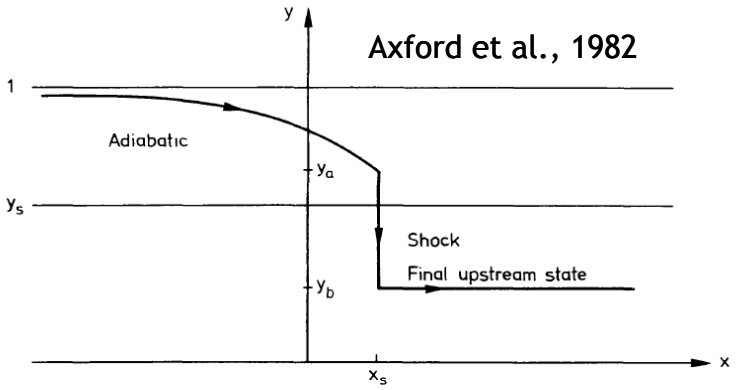

Fig. 5. In the intermediate Mach number regime the structure consists of a smooth adiabatic (gas) portion ($1 < y < y_a$) followed by a gas shock at $x = x_s$

We know that energetic charged particles affect the background plasma flow via their pressure gradients.

Theory of particle-mediated shocks is well developed: Drury & Volk (1981); Axford et al. (1982), Donohue & Zank (1993), le Roux & Fichtner (1997), Chalov & Fahr (1997), Florinski et al. (2004).

- *A particle-modified shock consists of two regions: an extended particle mediated precursor, and a gas-dynamic subshock.*

- Amount of deceleration (in terms of dynamic pressure) in the precursor is ~ the difference between pressures of energetic particles at the shock and far upstream

- *The length scale of the precursor is the same as the diffusive length of the particles, K/u, where K is the radial diffusion coefficient, and u is the solar wind speed.*

- The subshock properties are still governed by Rankine-Hugoniot conditions, without a contribution of energetic particles (in the diffusive approximation their intensity is conserved across the subshock).

And now - some theory

Simple one-dimensional conservation laws - apply to the region of precursor. *Energetic particles are considered massless, and contribute only to the energy of the mixture gas+particles*. gamma=5/3 is the adiabatic index (ions are non-relativistic), and K (with the overbar) is the AVERAGE diffusion coefficient (more on this later).

$$\frac{d(\rho u)}{dx} = 0,$$

$$\rho u \frac{du}{dx} + \frac{dp_g}{dx} + \frac{dp_c}{dx} = 0,$$

$$u \frac{dp_g}{dx} + \gamma p_g \frac{du}{dx} = 0,$$

$$u \frac{dp_c}{dx} + \gamma p_c \frac{du}{dx} - \frac{d}{dx}\left(\bar{\kappa} \frac{dp_c}{dx}\right) = 0.$$

We can obtain an ODE for the plasma velocity in the precursor:

$$\frac{du}{dx} = -\frac{(\gamma - 1)(Au^2/2 - C) + \gamma u(B - Au)}{\bar{\kappa}(A - \gamma D u^{-\gamma - 1})}$$

A, B, C, and D are the four integrals of the system, fixed by the measurements made just upstream at the shock.

CSPAR-UAH

To apply this theory to Voyager 2 observations we must answer:

1. Is energetic particle pressure gradient sufficient to cause the observed plasma speed decrease?
2. Are particle anisotropies upstream small enough to use diffusive theory?
3. What is the value of the average diffusion coefficient?

Partial pressure of energetic particles:

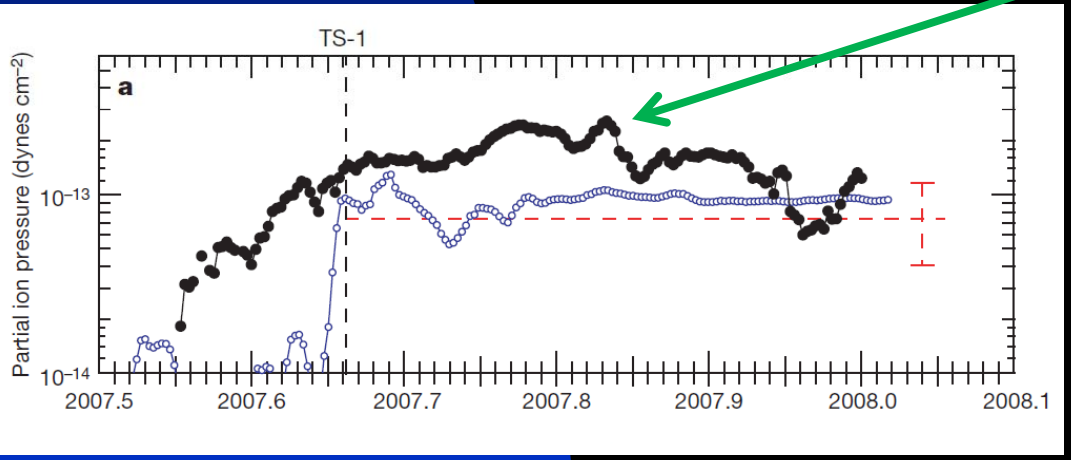

Black: partial pressure of ions 28 keV to 3.5 MeV, Voyager 2/LECP Blue: same for V1 shock encounter,ime-shifted to superimpose the two shock crossings on the same plot. Note the smooth increase upstream at Voyager 2 vs. abrupt rise at Voyager 2 Red line shows magnetic pressure (smaller than particle pressure).

Cf: a typical upstream SW dynamic pressure rho u^2 ~ 10^-12 dynes/cm^2 Energetic particles carry ~10% - non-negligible! Based on this estimate, we expect a precursor. But on what spatial scale?

V2/LECP ion spectra were strongly modulated upstream of the shock. Concentrate on spectrum plotted with filled triangles

Most of the pressure is at the high end of the energy range, 1-3.5 MeV. Therefore, this energy range should determine \bar{K.} Use the upper LECP channels

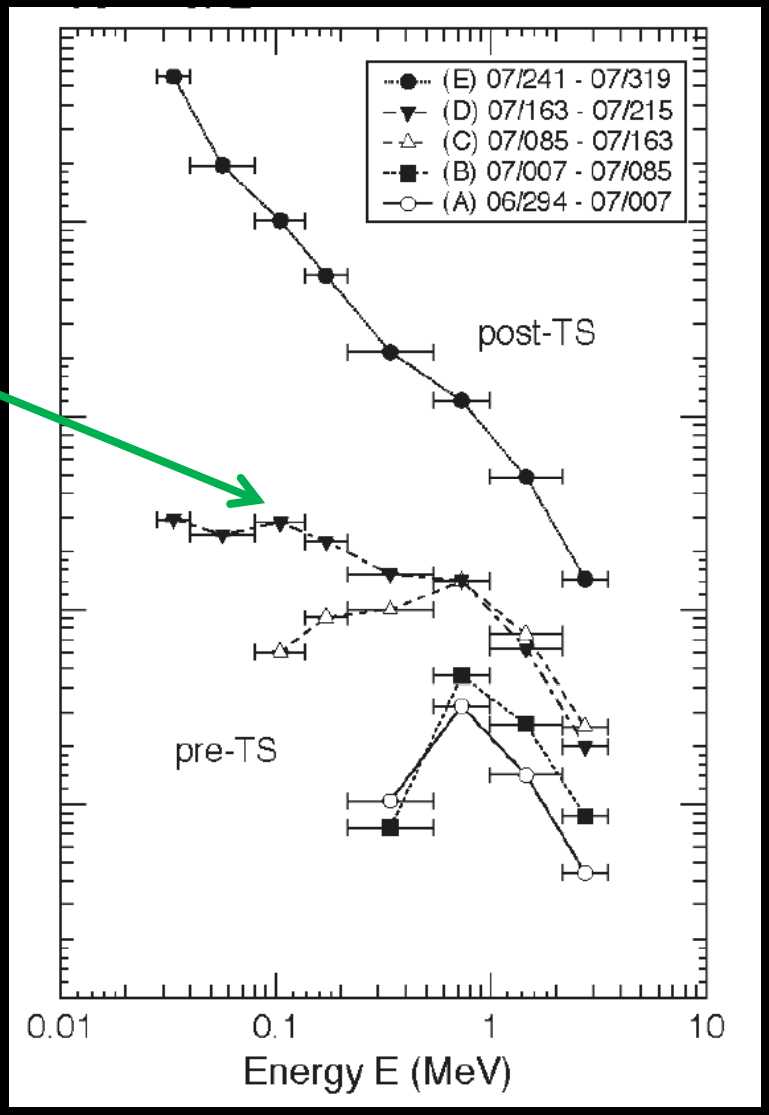

Decker et al., 2008b

CSPAR-UAH V2 LECP PL07 and PL08 fluxes in two opposite azimuthal sectors (red and black lines). Circles show sector-averaged intensities. Notice that anisotropies (normalized intensity difference in the two opposite sectors) during V2's last 40 days in the solar wind are small: 10-20% most of the time. Can use diffusive theory!

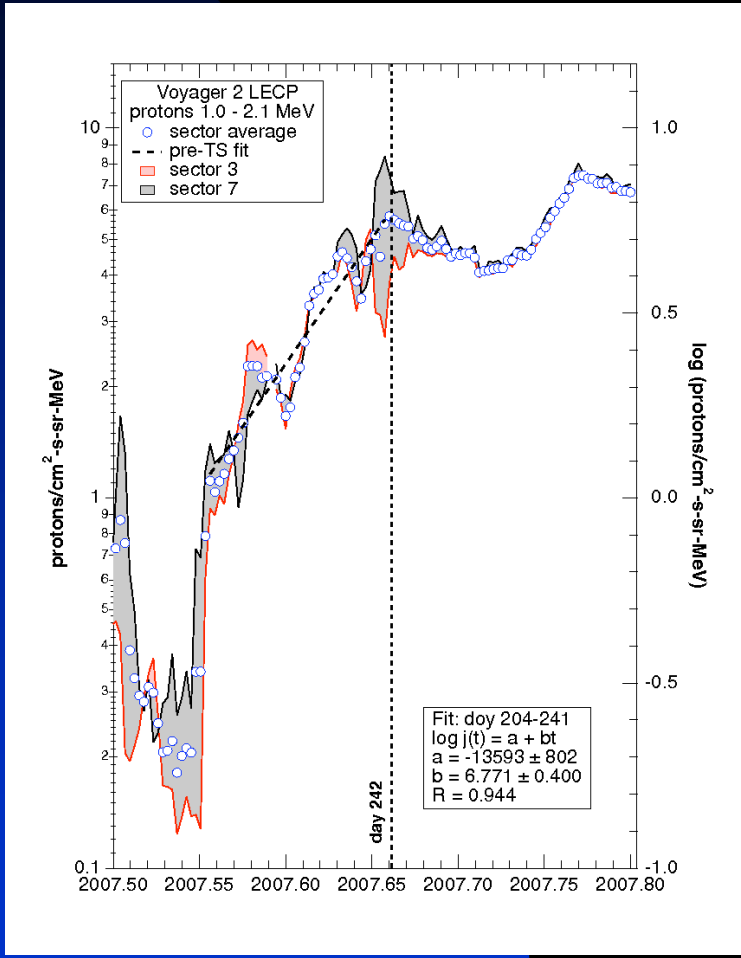

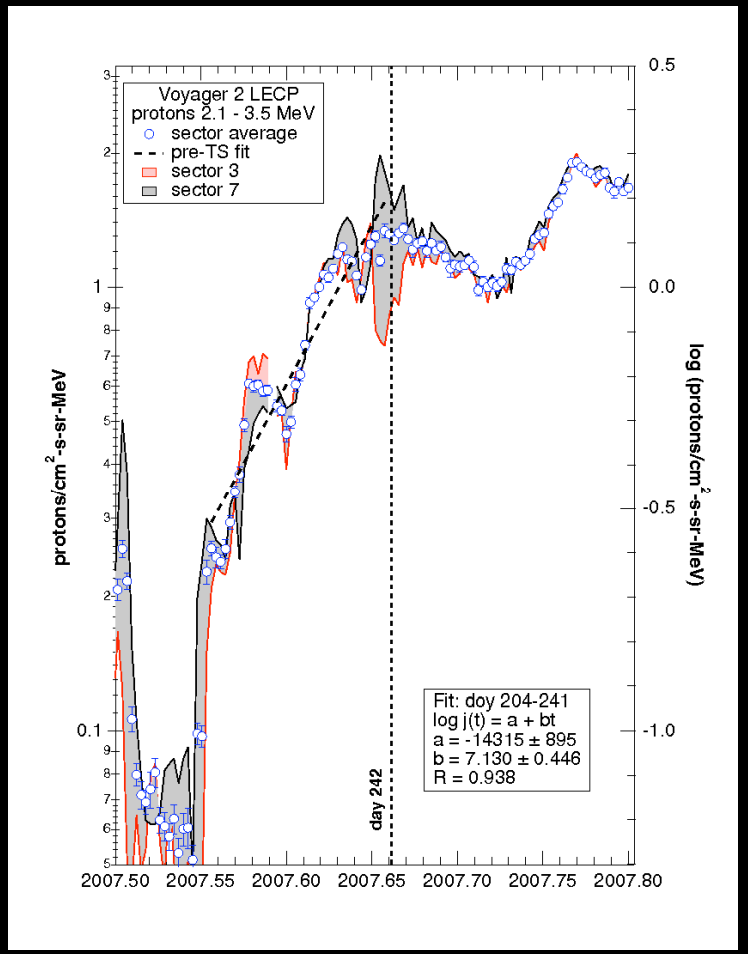

Dashed lines show fits to the intensity rise. Linear increase on a Log plot is exponential increase on a linear plot - the precursor is indeed exponential!

CSPAR-UAH

Calculate diffusion coefficients from on e-folding lengths in PL07 and PL08 channels:

$$\kappa = \frac{V_{V2} u}{b \ln(10)}$$

where V_v2 is the speed of Voyager 2 (14.8 km/s), u is solar wind speed, b is the measured logarithmic gradient (in 1/s)

Results: K_(1-3.5)=10^20 cm^2/s (radial diffusion). This will be the average diffusion coefficient for the purpose of evaluating solar wind slowdown.

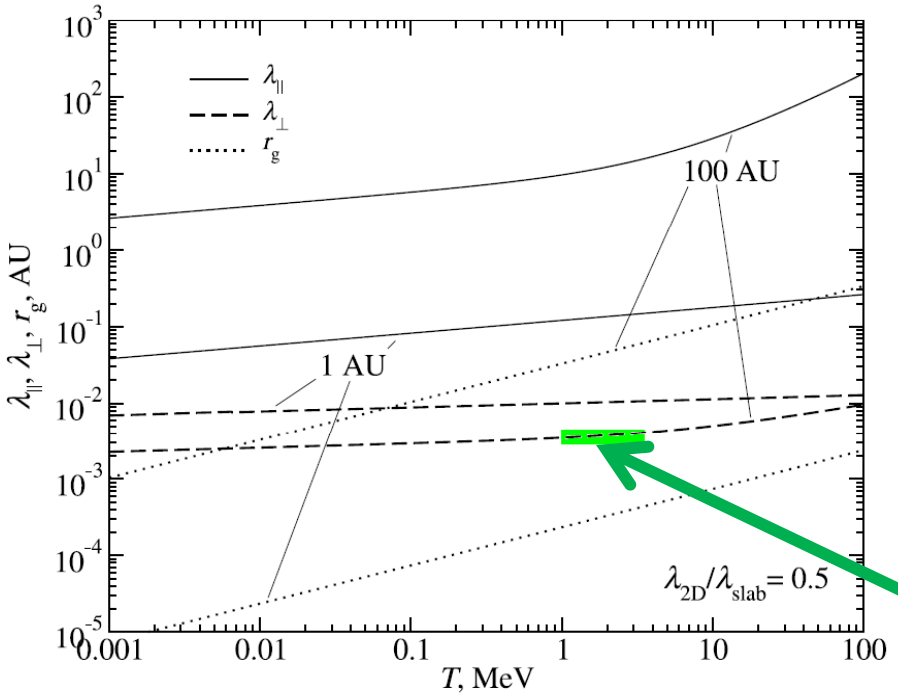

Zank et al., 2006

Compare this with diffusion theory

Parallel and perpendicular mean free paths based on quasi-linear and NLGC expression. This model predicts K_{perp} = 4X10^19 cm^2/s, very close to the estimate above! Parallel diffusion contributes ~ similar amount to K_rr (even better agreement).

Model input parameters immediately upstream of the shock (NOT far upstream!)

- u = 300 km/s
- n = 0.0007 cm^-3
- Plasma + PUI thermal pressure P_g = 0.09 eV/cm^3 PUI thermal pressure dominates, of course.
- Energetic particle pressure P_c = 0.1 eV/cm^3
- Calculation performed from x = -0.37 AU (x is negative upstream) to x=0 (the TS) using Voyager 2 speed to convert time into distance.

These parameters yield subshock compression ratio s=2.4, consistent with observed velocity drop downstream.

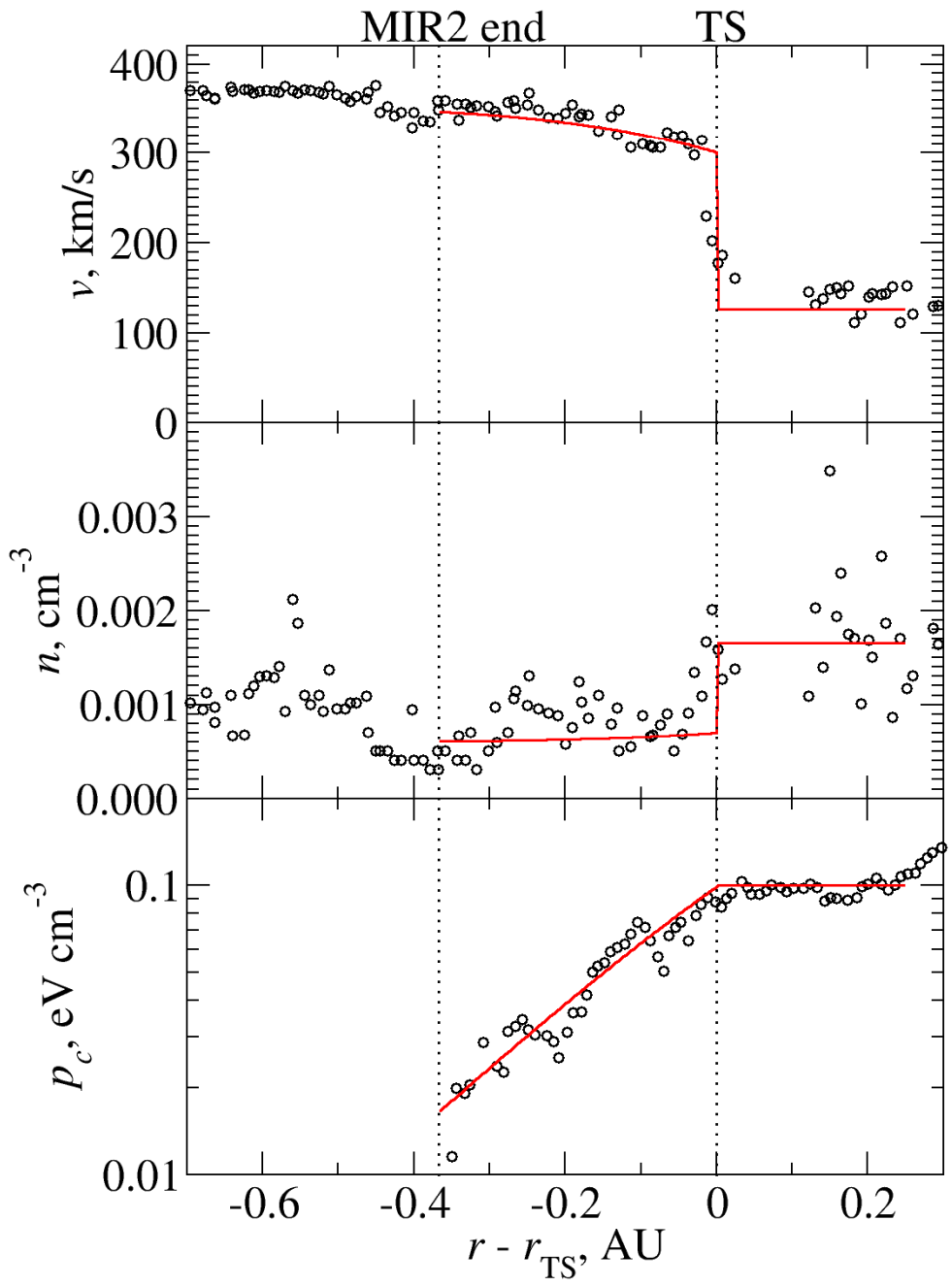

Principal results:

- *The velocity, the plasma density, and the energetic particle pressure are all a good fit to observations*
- *Solar wind slows down from 347 km/s to 300 km/s over a distance of 0.35 AU.*
- *Classical modified shock behavior!*

Conclusions:

1. *Solar wind slowdown from ~40 days (0.37 AU) upstream to the TS was likely caused by energetic particles between 1 and 3.5 MeV.*

2. *Partial pressure of energetic ions was enough to decelerate the flow by ~50 km/s*

3. *What about the entire 0.7 AU precursor? Could ions with T>3.5 MeV be responsible? Possibly - need to look in CRS data.*

4. *Could Voyager 1 have observed a mediated shock? Perhaps - but the shock was moving inward rapidly and steadily, so would appear 6-7 times shorter in time. Could have been masked by transients.*

CSPAR-UAH

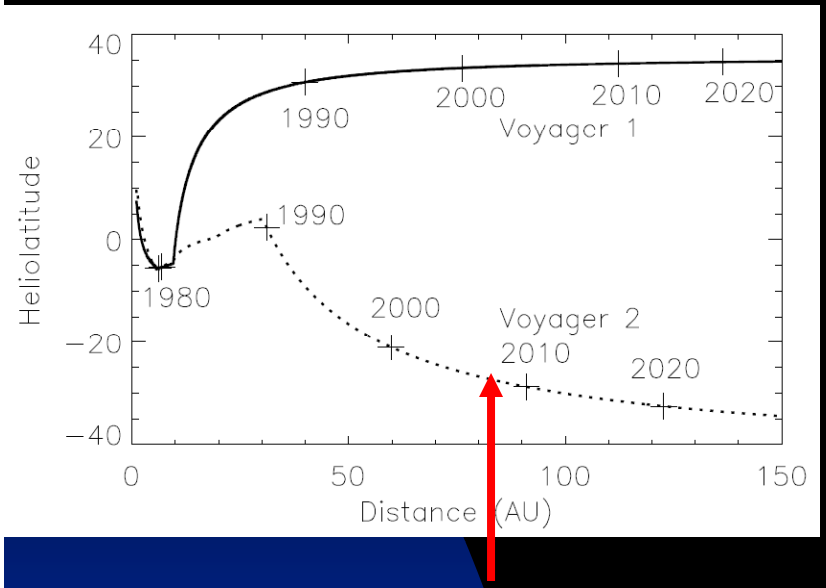

8/30/07 – 83.7 AU

The Interaction of Pickup Ions at the Termination Shock:

Implications for Energetic Neutral Atoms

G.P. Zank
Center for Space and Aeronomic Science (CSPAR)
and Department of Physics
University of Alabama, Huntsville

Jacob Heerikhusien, Ross Burrows, Mitsuo Oka, Nick Pogorelov

Three crossings of the termination shock

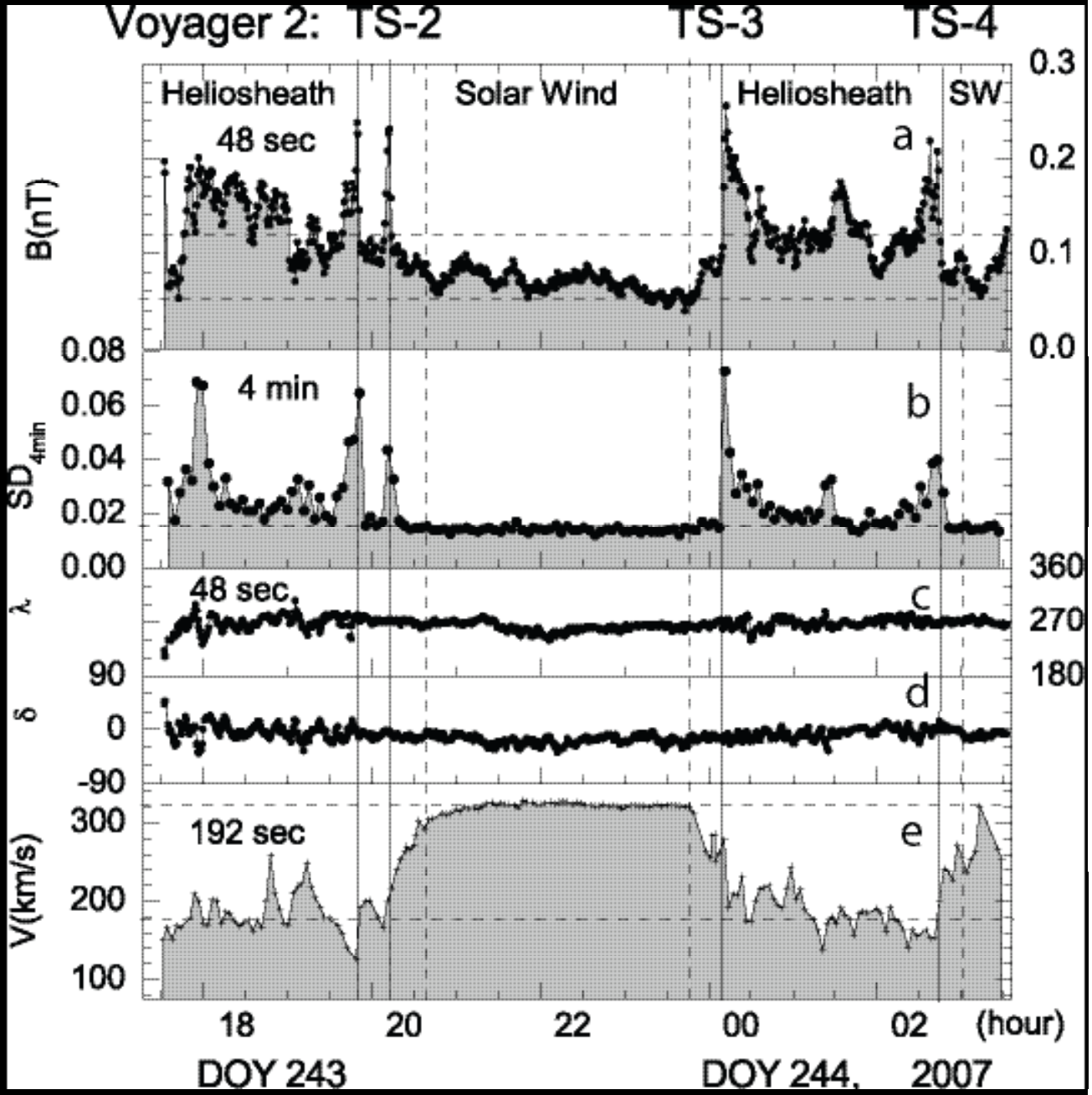

Voyager 2 observations of TS

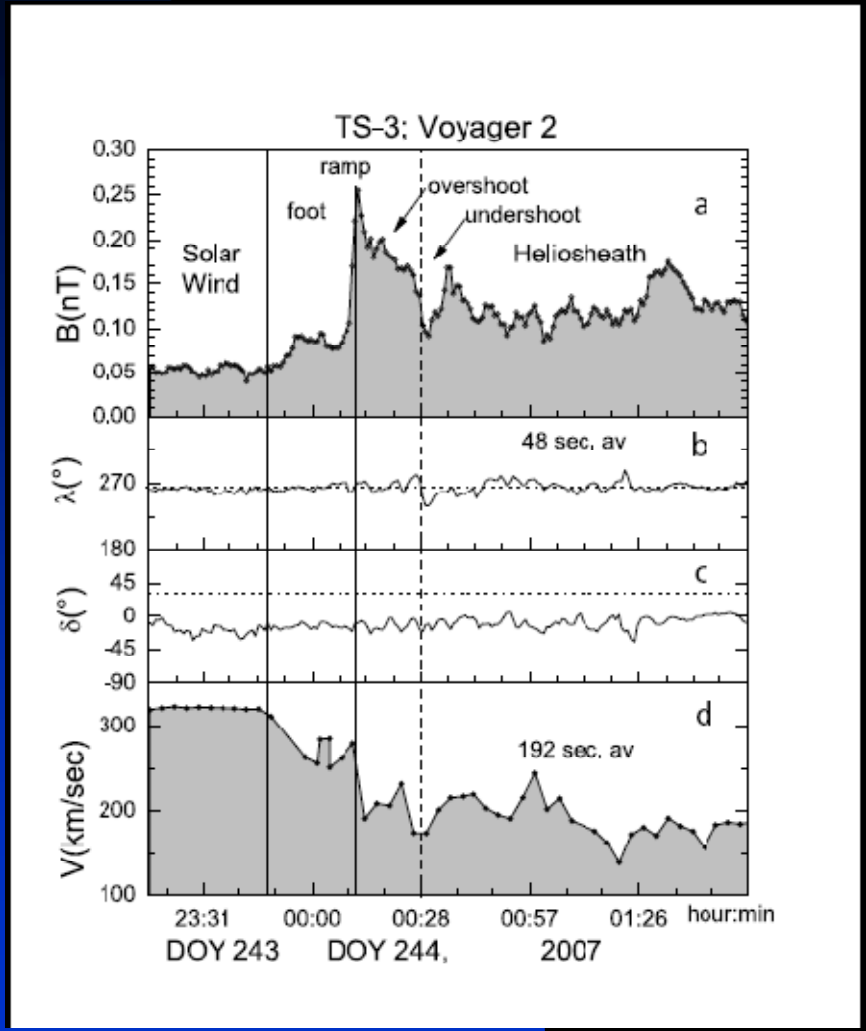

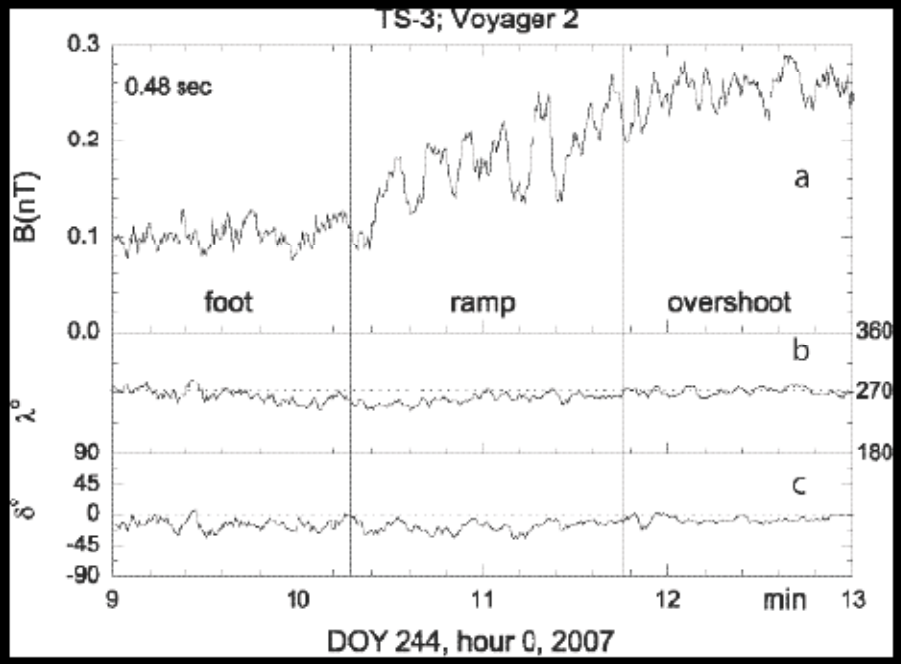

Burlaga et al. 2008

TS-3 is a supercritical quasi-perpendicular shock. The magnetic field strength profile shows the classical features of a supercritical quasi-perpendicular shock: a "foot", "ramp", "overshoot", "undershoot", and smaller oscillations. (Right) The internal structure of the ramp of TS-3. **Note highly oscillatory structure in the foot and ramp.**

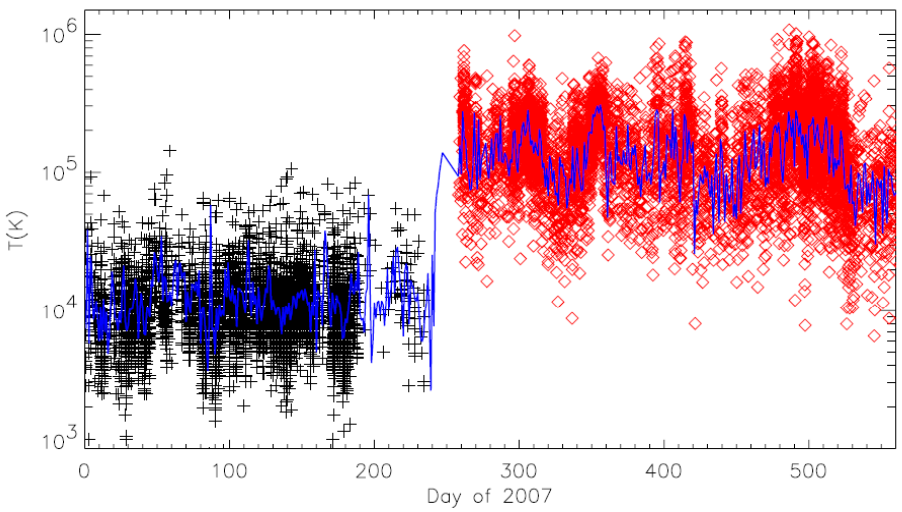

Richardson et al., 2008

The temperatures observed by V2 in the solar wind and heliosheath. The points show high-time-resolution data and the lines show daily averages.

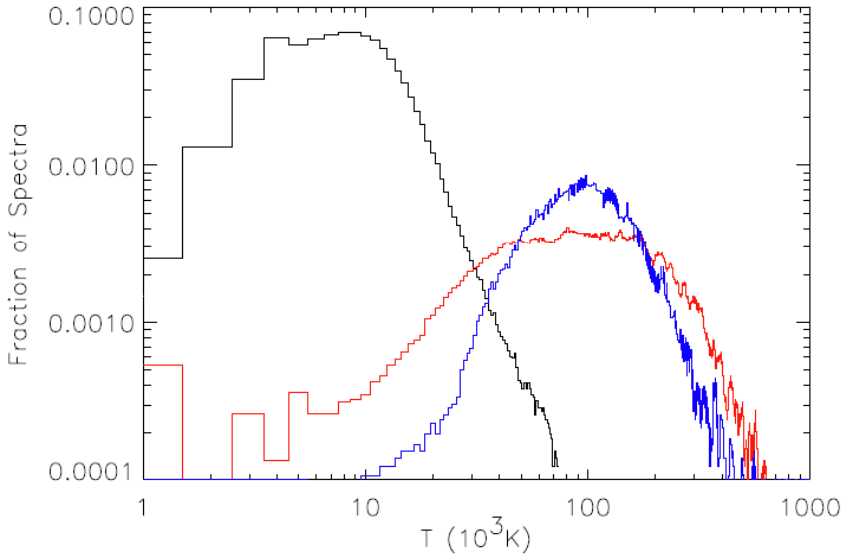

Histograms of the temperature distributions in the solar wind and the heliosheath. The black shows the solar wind distribution, the red shows the heliosheath distribution, and the blue shows the distribution of the solar wind temperature multiplied by 13, the ratio between the upstream solar wind and downstream heliosheath temperatures.

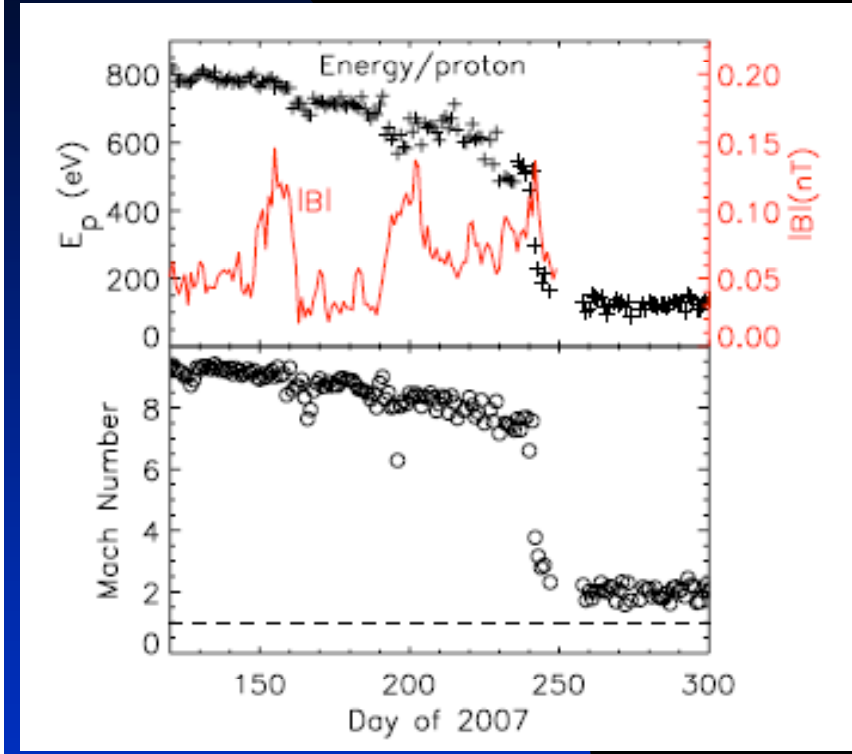

Most of the solar wind flow energy does not go into the solar wind plasma.

Top: Daily-averaged energy/proton (flow energy plus thermal energy) near the TS with the magnitude of B superposed.

Bottom: *The fast mode Mach number near the TS*. The dashed line shows a Mach number of 1. The Mach number (M) of the *thermal plasma*, is about nine before the shock and two after the shock.

CSPAR-UAH

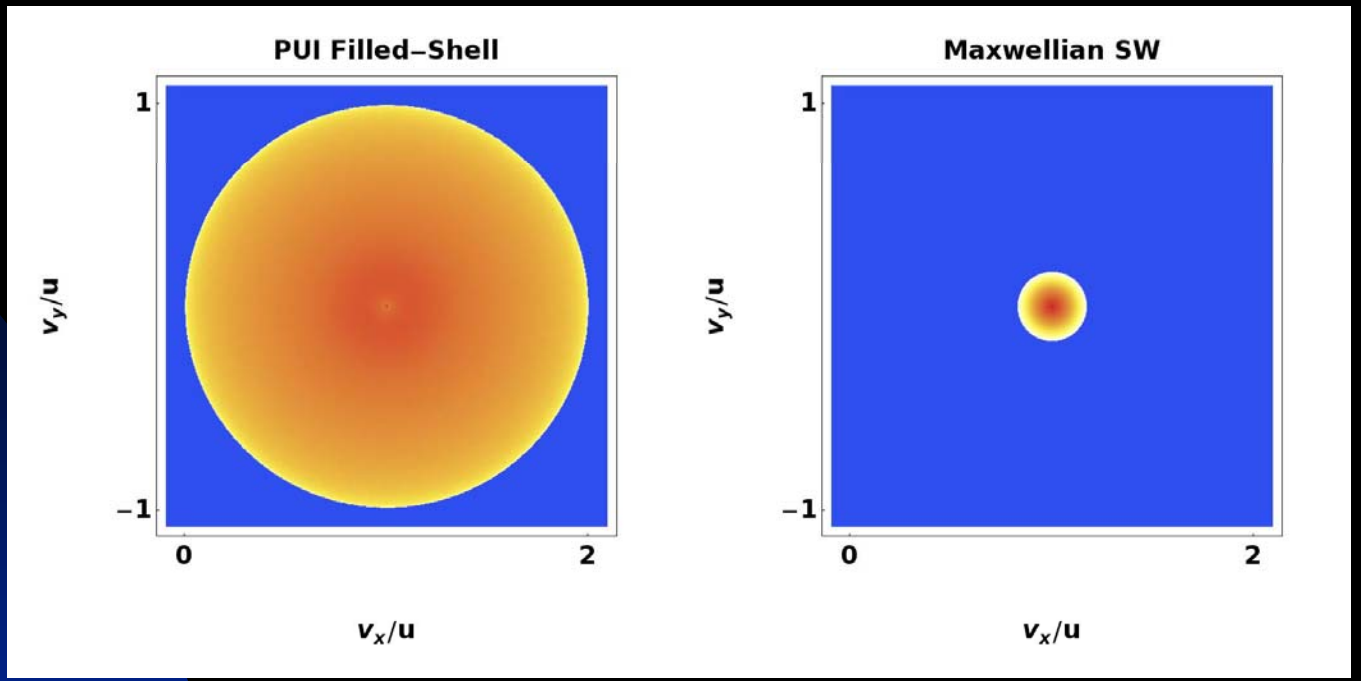
PUI Filled–Shell
Maxwellian SW
1
−1
0
2
v_y/u
v_x/u

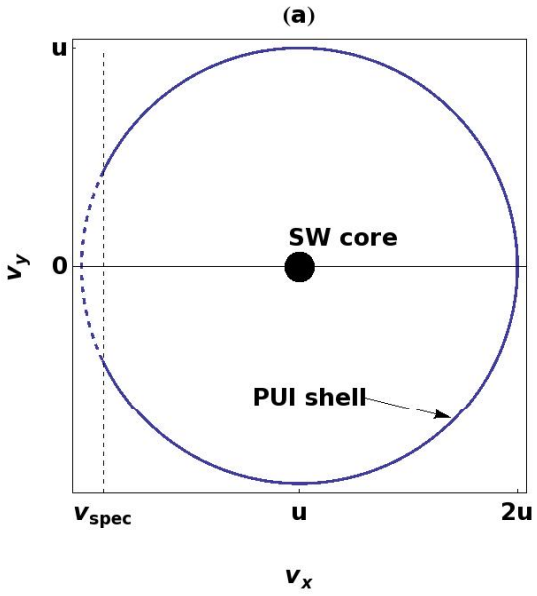
(a)
u
0
v_y
SW core
PUI shell
v_{spec}
u
2u
v_x

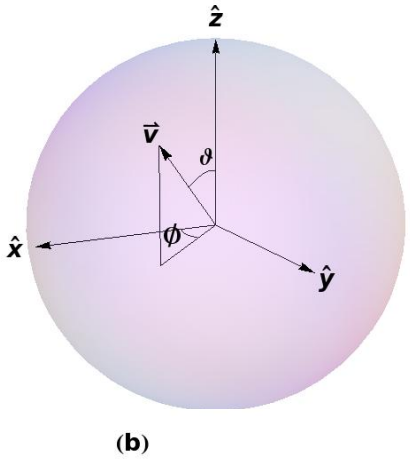
$\hat{z}$
$\vec{v}$
ϑ
ϕ
$\hat{x}$
$\hat{y}$
(b)

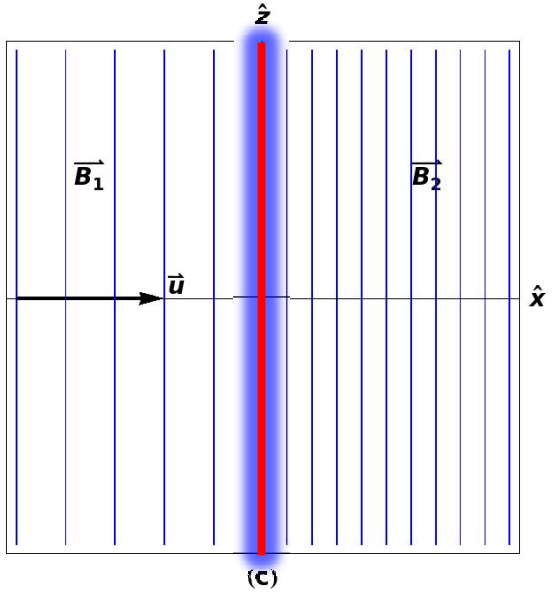
$\hat{z}$
$\vec{B}_1$
$\vec{B}_2$
$\vec{u}$
$\hat{x}$
(c)

CSPAR-UAH

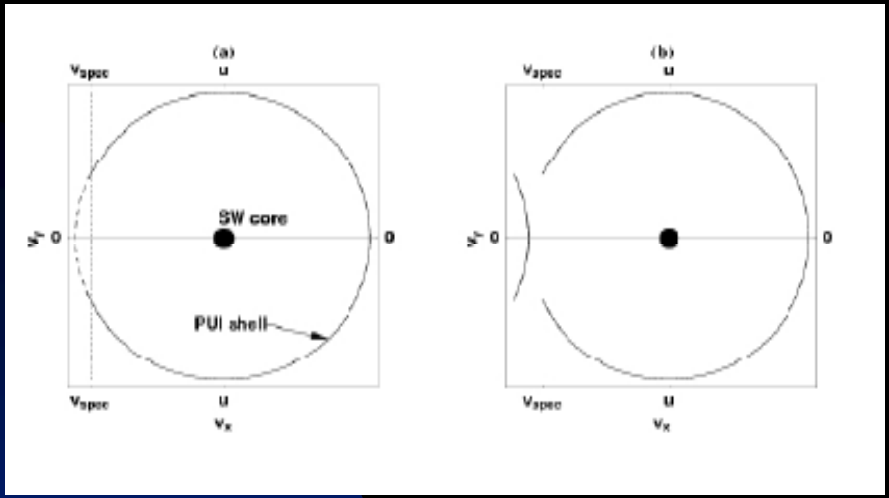

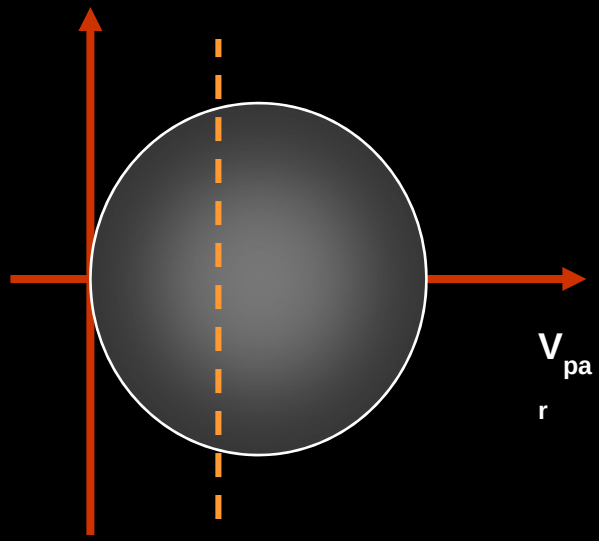

R. Burrows thesis, 2008

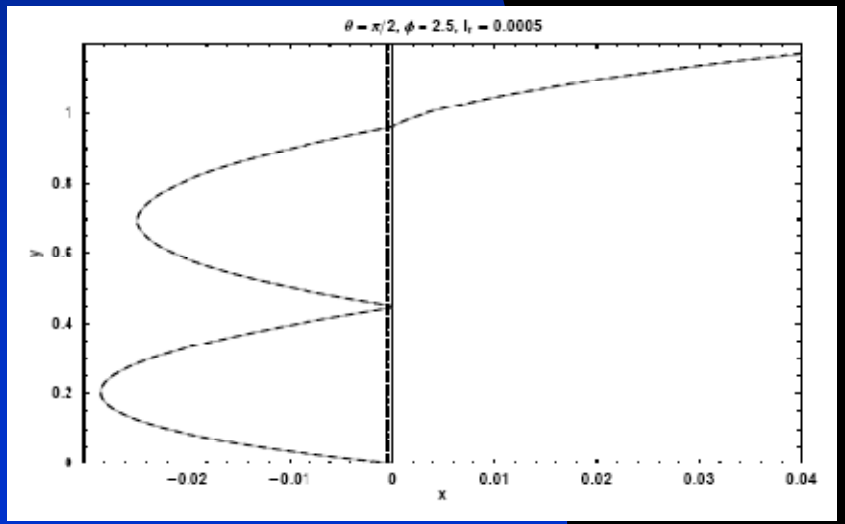

Once Specularly Reflected Shell Distribution (I_{ramp} = 0), 3D Plot (left), Projected onto the ($v_\perp$, $v_\parallel$)-Plane (right).

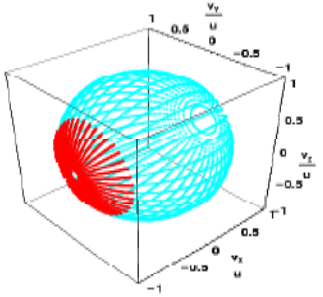

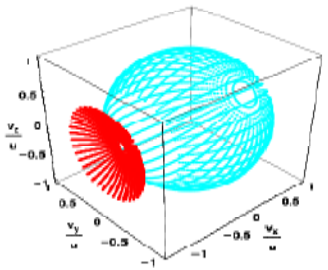

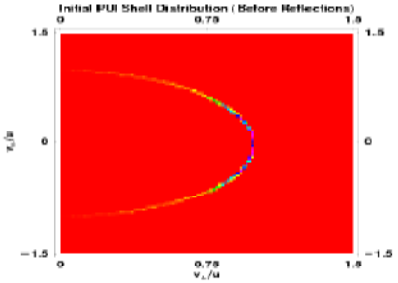

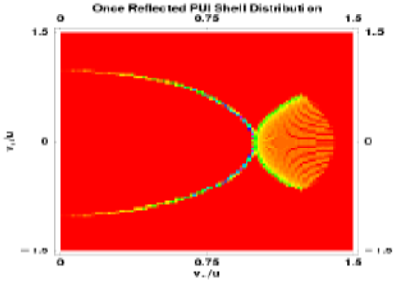

CSPAR-UAH

Percentage PUIs reflected

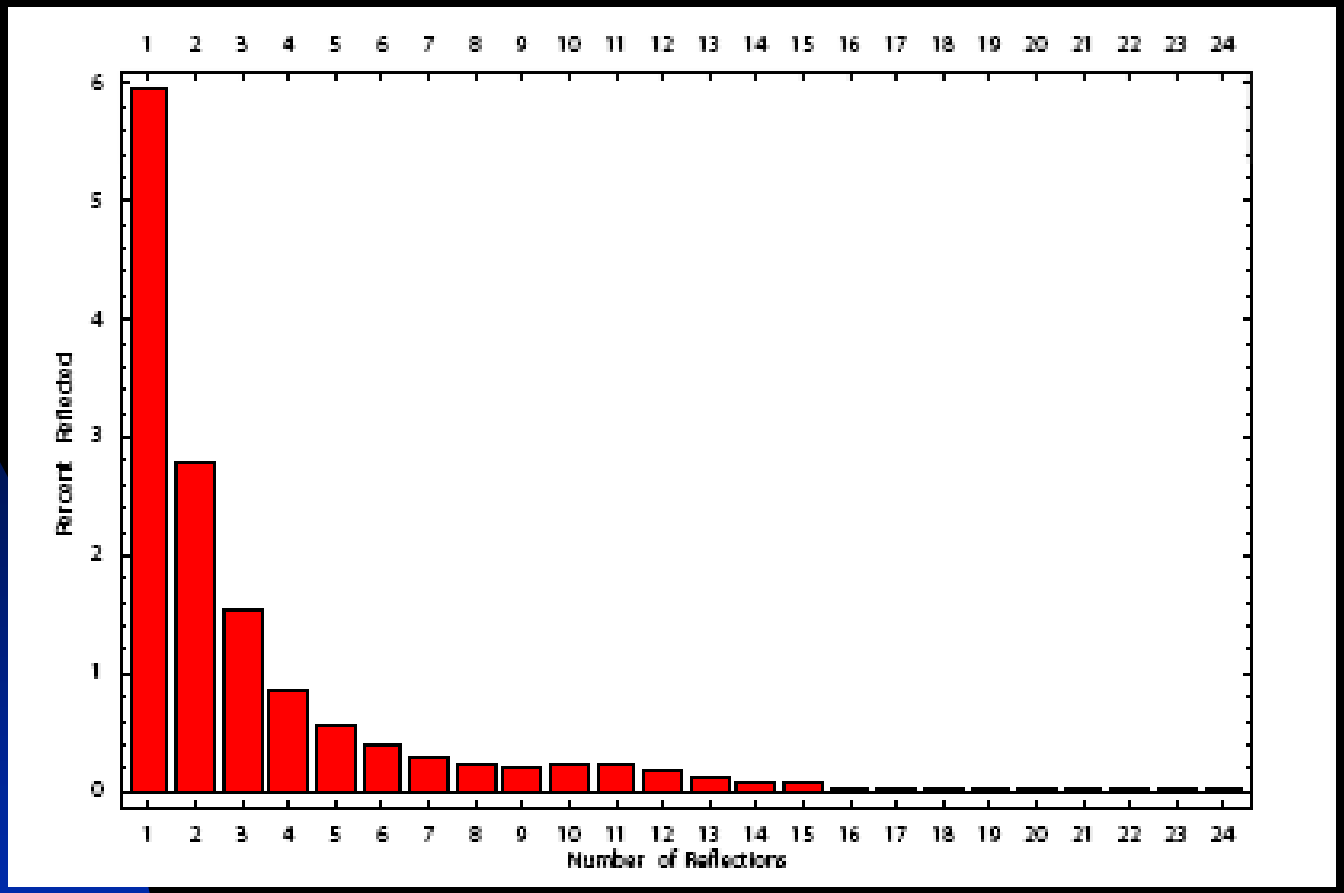

Number of reflections

- Approximately 14% to 16% of incoming PUIs experience at least one reflection at the TS – this example was run using the Voyager 2 TS3 observed magnetic field profile (courtesy of L. Burlaga)
- Corresponds to between 3 to 5% of total incoming ions

Construct theoretical model

- Incorporate basic physics and identify primary processes responsible for shock dissipation
- Understand shock structure and scalings
  - Assume 3-fluid model of electrons, solar wind protons, and pickup ions (PUIs)
  - Assume isotropic electron and SW pressure and that PUIs co-move with SW flow
  - Reflected PUIs make PUIs anisotropic in vicinity of shock

$$mn_{PUI}\left(\frac{\partial \mathbf{U}_s}{\partial t}+\mathbf{U}_s\bullet\nabla\mathbf{U}_s\right)=-\nabla P_{PUI}-\nabla\bullet\Pi^{PUI}+en_{PUI}\left(\mathbf{E}+\mathbf{U}_s\times\mathbf{B}\right)$$

Scalar Pressure P_{PUI}

1. Need to consider both reflected ion and transmitted PUI contribution: $P_{PUI} = P_P^{trans} + P_p^{ref}$.
2. Assume filled shell distribution incident on highly perpendicular TS i.e., V-Siscoe distribution.

$$f_p(c) = \frac{n_p}{4\pi U^{3/2}} \frac{3/2}{} c^{-3/2}$$

3. Particles whose normal component v_x satisfies $e\phi \geq \frac{1}{2} m v_x^2$ will be reflected at shock by cross-shock potential.
4. Reflected PUIs trapped in front of shock until particle Lorentz force exceeds force exerted by cross shock electrostatic potential – gives estimate of v_y
5. Can use moments of filled shell distribution to estimate P_{PUI}

Application of theory: partition of heliosheath energy

- Voyager 2 observes SW ions and not PUIs
- Upstream $T_{sw,1} = 2 \times 10^4$ K
- Downstream $T_{sw,2} \sim 2 \times 10^5$ K
- Inclusion of PUIs ➔ high beta plasma ~ 4
- Perpendicular shock
- Assume filled shell distribution for PUIs
- Can use theoretical model above to estimate N_{PUI} of reflected and transmitted PUIs, upstream temperature of PUIs, and downstream temperatures of transmitted SW ions, transmitted and reflected PUIs.

Application of theory: partition of heliosheath energy – cont.

- Use V2 TS3 data (U_1 ~ 300km/s, U_2 ~ 80km/s, N_1 ~ 0.001 cm-3, $T_{SW,1} = 2 \times 10^4$ K, $T_{PUI,1} = 3.6 \times 10^6$ K, r ~ 2.5 or less, B_{z1} = 0.05nT, $T_{SW,2} = 4 \times 10^5$ K
- Compute $T_{PUI,1} = 1.56 \times 10^6$ K
- Compute $T_{SW,2}$ ~ $(2.5)^2$ X 20,000K = 180,000K (observed!)
- Problem: Where is the heated plasma?

Application of theory: partition of heliosheath energy- cont

- Need to estimate temperatures of transmitted PUI population and reflected PUI population
- For ***transmitted*** ions: For 20% PUI population wrt N_{SW}, model ➔ transmitted $T_{PUI,2(trans)} \sim 9 \times 10^6 K$
- ***Reflected ions***: trapped at shock front by balance of Lorentz force ev_yB_z and cross-shock potential gradient
- $L_{ramp} = 1.5 min \times V_{sh} \sim 7000$ *km*
- $L_{foot} = 23$ *min* $\times V_{sh} \sim 110{,}000$ *km (Burlaga et al., 2008)*
- ➔ Reflected PUIs $T_{PUI,2(ref)} \sim 7.7 \times 10^7 K$

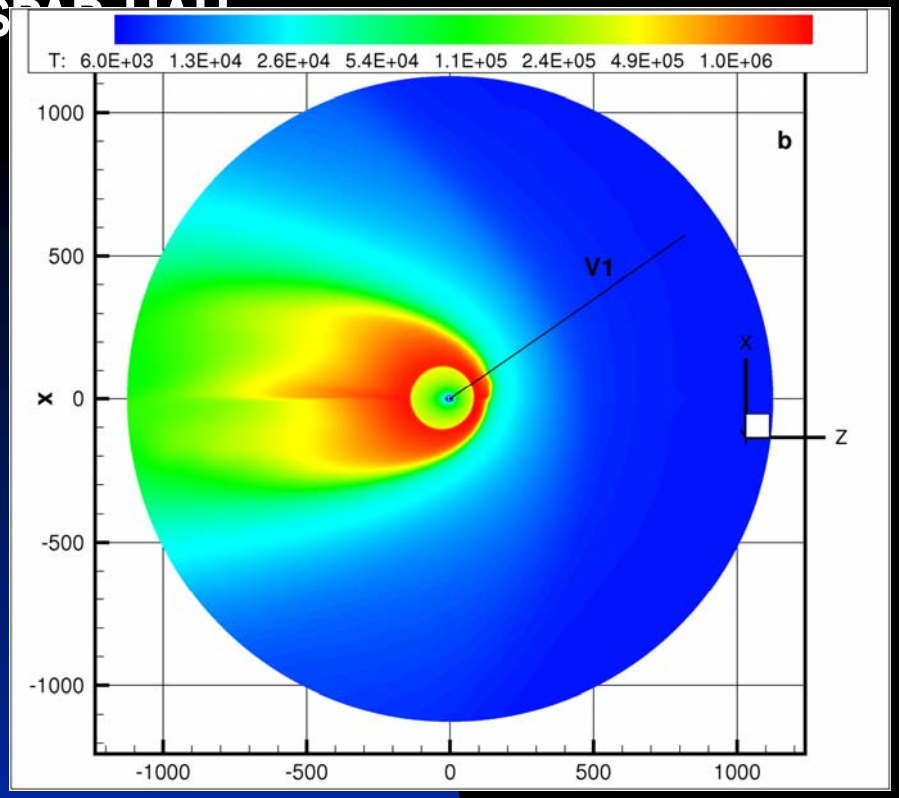

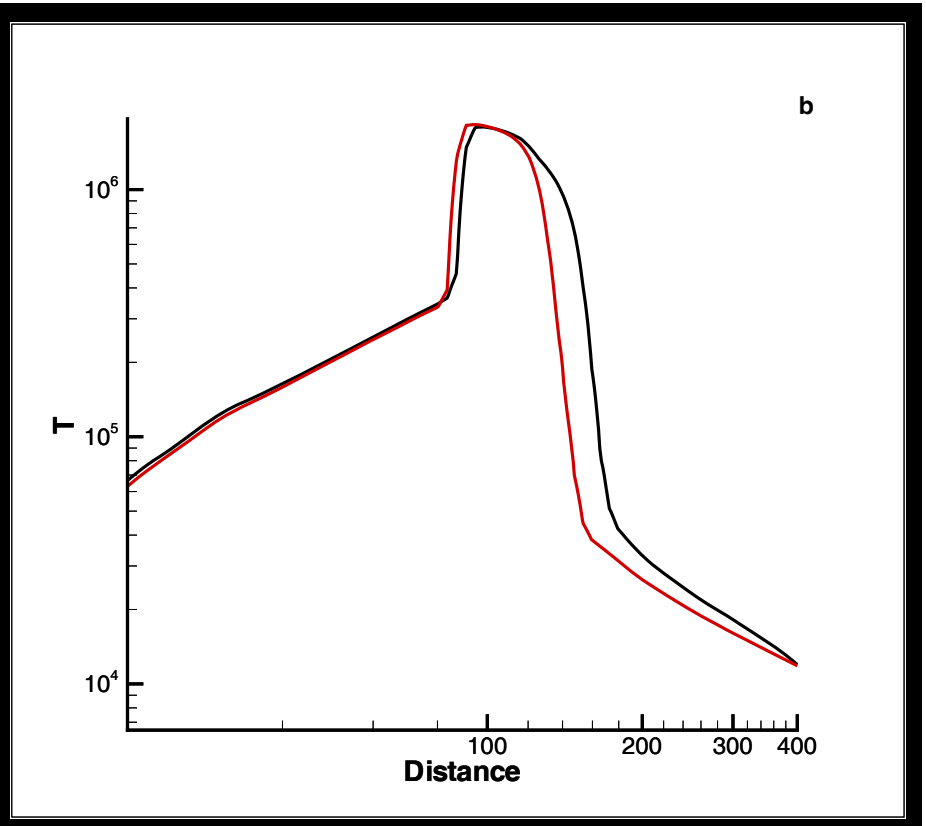

Pogorelov et al., 2008

- $T_2 = 0.8\ T_{SW,2} + N_{PUI,2(trans)}\ T_{PUI,2(trans)} + N_{PUI,2(ref)}\ T_{PUI,2(ref)} = 3.4 \times 10^6$ K

(consistent with global self-consistent MHD simulations)

REFLECTED AND TRANSMITTED PUIs PROVIDE DOWNSTREAM HEATING AND REFLECTED PUIs RESPONSIBLE FOR DISSIPATION AT HTS.

Can we test shock structure and properties using ENA observations?

- Can use model predictions for downstream density and temperature of solar wind ions, transmitted PUIs, and reflected PUIs to construct the inner heliosheath ions distribution function.

- The constructed ion distribution function can then be used as the background plasma distribution from which ENAs are created provided the temperature distribution is constrained by self-consistent global MHD simulations.

CSPAR-UAH

Downstream ion distribution

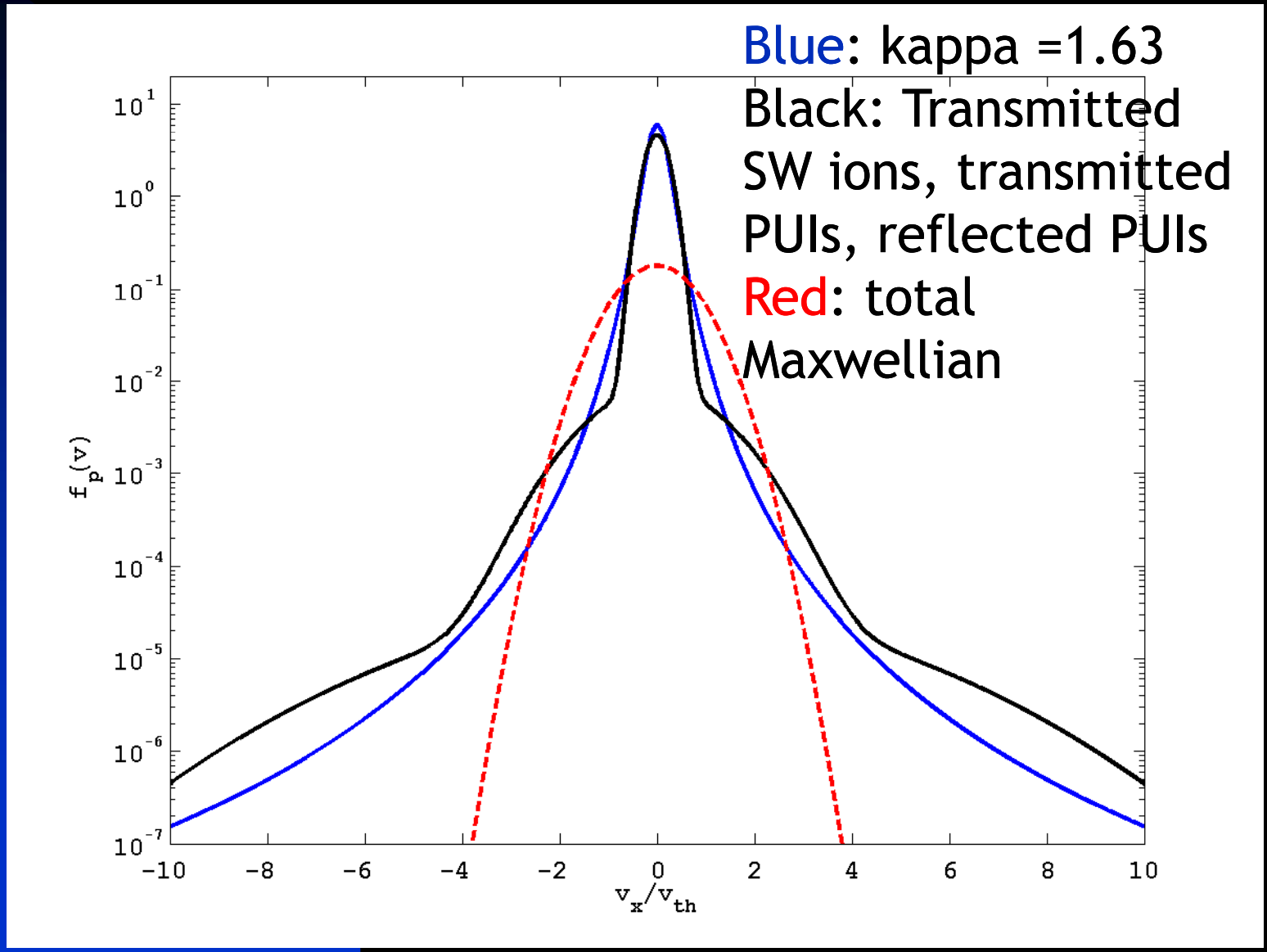

SUMMARY

Reflected PUIs represent the primary dissipation mechanism at the quasi-perpendicular termination shock, dominating both the scalar pressure and the stress tensor. Solar wind ions are largely irrelevant to TS dissipation.

- Derived the fully nonlinear model equations, including dissipation terms, for a 3-fluid description of the TS. Exploited the geometric form of the PUI distribution in the derivation.

- Model provides explanation for why a kappa distribution should be an adequate representation of the heliosheath plasma.

- Predicted skymaps can be tested against ENA observations and are consistent with kappa-based skymaps.